The role of AMPK and purinergic signaling in astrocytic hypoglycaemia detection

Submitted by **Julia Melanie Vlachaki Walker** to the **University of Exeter**

as a thesis for the degree of

Master of Philosophy in Medical Studies

In **June 2017**

I certify that all material in this thesis which is not my own work has been identified and that no material has previously been submitted and approved for the award of a degree by this or any other University.

Signature: ……..

Abstract

Following recurrent hypoglycaemia (RH) patients with type 1 diabetes (T1D) may develop an impaired counter-regulatory response (CRR) to future hypoglycaemic episodes. This is a result of maladaptive responses to hypoglycaemia, involving AMP-activated protein kinase (AMPK) activity in the ventromedial hypothalamus (VMH). Research has focused mainly on glucosensing neurones, with little emphasis on the potential role of astrocytes. This study aims to examine the response of astrocytes to a hypoglycaemic stimulus and changes to this following RH.

The U373 human astrocytoma cell line and mouse primary cortical astrocytes (CRTAS), as well as wild type (WT) and α1/α2 AMPK knockout (KO) mouse embryonic fibroblasts (MEF), were used. Astrocytes were maintained at 25mM glucose, and stepped down to physiological (2.5mM) glucose for the experiments. Western blotting was used to measure total and phosphorylated protein expression. Luminescence and absorbance plate-based assays were used to measure ATP and lactate levels, respectively. A plate-based assay was used to measure intracellular calcium ($[Ca^{2+}]_i$) using Fluo4.

Our study demonstrates that astrocytes intrinsically respond to a hypoglycaemic stimulus by increasing AMPK activation. Following RH there was a blunted AMPK activation, accompanied by a reduction in extracellular ATP (eATP). Using the AMPK activator, A-769662, we saw a concentration-dependent increase in AMPK activation and eATP. However, enhancing AMPK activation by co-application of A-769662 and 5-aminoimidazole-4-carboxamide riboside (AICAR), or by exposing astrocytes to a hypoglycaemic stimulus in the

presence of A-769662, did not enhance ATP release. A-769662 also caused an increase in $[Ca^{2+}]_i$. Both the A-769662-mediated increase in eATP and $[Ca^{2+}]_i$ persisted in MEF α1/α2 AMPK KO cells. The effect of A-769662 on eATP was not attenuated by pre-treating cells with the gap junction blocker carbenoxolone, or by removing extracellular Ca^{2+}, however there was a small attenuation following pre-treatment with the $[Ca^{2+}]_i$ chelator, BAPTA-AM.

In our study we show that astrocytes intrinsically respond to a hypoglycaemic stimulus by increasing phospho AMPK (pAMPK). Following RH, the AMPK response to hypoglycaemia is blunted, alongside a significant reduction to eATP. We also demonstrate that the changes in eATP observed are likely independent of changes in AMPK activity. Importantly, the AMPK activator, A-769662, has AMPK-independent effects on eATP and $[Ca^{2+}]_i$, and these changes in eATP are mediated by changes in $[Ca^{2+}]_i$.

Publications

Vlachaki Walker JM, Robb JL, Cruz AM, Malhi A, Weightman Potter PG, Ashford MLJ, McCrimmon RJ, Ellacott KL, Beall C (**2017**) AMP-activated protein kinase activator A-769662 increases intracellular calcium and ATP release from astrocytes in an AMPK-independent manner. *Diabetes, Obesity and Metabolism*

Dadak S, Beall C, **Vlachaki Walker JM**, Soutar MPM, McCrimmon RJ, Ashford MLJ (**2017**) Oleate induces KATP channel-dependent hyperpolarisation in mouse hypothalamic glucose-excited neurones without altering cellular energy charge. *Neuroscience*

Howie J, Reilly L, Fraser NJ, **Vlachaki Walker JM**, Wypijewski KJ, Ashford MLJ, Calaghan SC, McClafferty H, Tian L, Shipston MJ, et al (**2014**) Substrate recognition by the cell surface palmitoyl transferase DHHC5. *PNAS*

Manuscripts in preparation

Vlachaki Walker JM, Weightman Potter PG, Robb J, Ellacott KL, Beall C (2017) Exposure of Astrocytes to Recurrent Hypoglycemia *in vitro* Alters Gliotransmission and Purinergic Signalling

Weightman Potter PG, **Vlachaki Walker JM**, Cruz AM, Williamson R, Randall A, Beall C (2017) Human Primary Astrocyte (HPA) Metabolism is Altered Following Exposure to Recurrent Hypoglycemia *In Vitro*

Vlachaki Walker JM, Robb J, Weightman Potter PG, Ellacott KL, Beall C (2017) Physiological culture of neural cells

Acknowledgements

First, I would like to thank my supervisor Dr Craig Beall who gave me the opportunity to undertake this MPhil degree, and for his help, support and advice throughout. I would also like to thank my secondary supervisor, Dr Kate Ellacott for sharing her knowledge with me regarding the project. Thank you to my mentor Professor Lorna Harries for her advice and support. Thank you to all the Beallacotts past and present, official and honorary, Paul, Ana, Josie, Nicole, Alistair, Jade, Ash, Lydia, Ben and Nadia for making it fun to work in this lab, and for helping out when I'm drowning in work. I would also like to thank Professor Noel Morgan for giving me the opportunity to undertake this MPhil and Nikki for making the transition from Dundee and our integration in the new lab so smooth and easy. Thank you to Exeter Martial Arts and all the wonderful people there for giving me a place to vent my frustration and keep me sane. Thank you to my flatmate Matt for being there to support me through my little breakdowns, and to Shogo for making sure I eat and keeping me company during my non-stop writing days. Thank you to my mom for encouraging me to work hard for what I love, and for funding my journey to independence. Last but not least, thank you to Dr Will Fuller for giving me the opportunity to work in his lab and thus preventing my journey into academia from being cut short.

Candidate's Declaration

I hereby declare that all results described in this thesis, unless otherwise specified, are my own work. I further state that the composition of this thesis was performed by myself and none of the material has been submitted for any other degree. Lastly, I verify that all sources have been appropriately cited. Part of this work was carried out in the Cardiovascular and Diabetes Medicine Centre in the University of Dundee, and part in the Medical School in the University of Exeter, under the supervision of Dr Craig Beall.

Julia M. Vlachaki Walker

Table of contents

Abstract 1
Publications 3
Acknowledgements 4
Candidate's Declaration 5
Table of contents 6
List of figures 9
List of tables 11
Abbreviations 12
Chapter 1: Introduction 15
1.1 Diabetes and hypoglycaemia 15
1.1.1 Diabetes mellitus 15
1.1.2 Hypoglycaemia 17
1.1.3 Hypoglycaemia detection 18
1.2 Defective counter-regulation 20
1.2.1 The counter-regulatory response (CRR) 20
1.2.2 Impaired counter-regulation 21
1.3 AMP-activated protein kinase (AMPK) 23
1.3.1 Whole body energy homeostasis 23
1.3.2 AMPK and the counter-regulatory response 26
1.3.3 AMPK in glucosensing neurones 27
1.4 Glial cells 28
1.4.1 Glial cells support neuronal function 28
1.4.2 Astrocytes: More than a supporting role 32
1.5 Adenosine triphosphate (ATP) 33
1.5.1 ATP as a gliotransmitter 33
1.5.2 ATP release from astrocytes 37
1.5.3 Calcium signalling in astrocytes 39
1.5.4 The purinergic system in diabetes 41
1.6 Astrocytic lactate 43
1.6.1 The astrocyte-neurone lactate shuttle (ANLS) hypothesis 43
1.6.2 Brain glycogen supercompensation 46
Study aims 49
Chapter 2: Materials and Methods 50

2.1 Materials 50
2.1.1 Chemicals and equipment 50
2.1.2 Antibodies 53
2.2 Methods 54
2.2.1 Cell culture 54
2.2.1.1 Neonatal primary astrocyte isolation and culturing 54
2.2.1.2 Culturing of U373 MG cells 55
2.2.1.3 Plating cells for experiments 55
2.2.1.4 Collection of supernatants and protein extraction 55
2.2.1.5 Recurrent Hypoglycaemia 57
2.2.2 Determining protein concentration 59
2.2.3 Immunoblotting 59
2.2.4 ATP assay 61
2.2.4.1 Determining extracellular ATP concentration 61
2.2.4.2 Determining intracellular ATP concentration 62
2.2.4.3 Determining total ATP concentration 62
2.2.5 Determining extracellular lactate concentration 62
2.2.6 Intracellular Ca^{2+} assay 64
2.2.7 Quinacrine Imaging 64
2.3 Statistical analysis 65
Chapter 3: Results 66
3.1 Hypoglycaemia detection in astrocytes 66
Introduction 66
3.1.1 Acute hypoglycaemia increases AMPK and ACC phosphorylation and decreases extracellular lactate in astrocytes 70
3.1.2 Noradrenaline increased extracellular lactate in both euglycaemic and hypoglycaemic conditions 73
3.1.3 2-day antecedent hypoglycaemia blunts the AMPK response to further hypoglycaemia 75
3.2 Discussion 81
Chapter 4: Results 87
4.1 AMPK pharmacology 87
Introduction 87
4.1.1 Both A-769662 and AICAR cause an increase in AMPK activation, but only A-769662 increases ATP release 91

4.1.2 A-769662 causes a concentration-dependent increase in pAMPK and eATP in U373 cells and primary mouse astrocytes 94

4.1.3 AICAR enhances A-769662-mediated AMPK activation, but has no effect on eATP 97

4.1.4 A769662 enhances eATP and eLactate at both euglycaemic and hypoglycaemic conditions 100

4.1.5 Noradrenaline has an additive effect on A-769662-mediated increase in eLactate without affecting AMPK phosphorylation or eATP 102

4.2 Understanding the mechanism of A-769662-mediated ATP release 106

Introduction 106

4.2.1 Blocking gap junctions does not attenuate the A-769662-mediated increase in eATP 109

4.2.2 Imaging of acidic vesicles in astrocytes using quinacrine 111

4.2.3 A-769662 increases intracellular calcium in astrocytes 114

4.2.4 Extracellular calcium is not required for the A-769662-mediated increase in eATP 116

4.2.5 Chelating intracellular calcium causes a decrease in the A-769662-mediated increase in eATP in primary astrocytes 118

4.2.6 A-769662 causes an increase in eATP and intracellular calcium in AMPK knockout cells 121

4.3 Discussion 124

Chapter 5: Conclusions 136

Supplementary figures 142

References 149

List of figures

Chapter 1

Figure 1.1. AMPK structure and regulation

Figure 1.2. Schematic drawing of neuronal and glial interactions

Figure 1.3. Overview of purinergic signalling

Figure 1.4. Diagrammatic representation of the astrocytic calcium wave propagation

Figure 1.5. The ANLS hypothesis

Chapter 2

Figure 2.1. 2 day recurrent hypoglycaemia model

Chapter 3

Figure 3.1. Low glucose increases pAMPK, pACC and lactate production

Figure 3.2. NA enhances lactate production during hypoglycaemic stimulus

Figure 3.3.1. Recurrent hypoglycaemia blunts the pAMPK response to further hypoglycaemia at 15 min

Figure 3.3.2. Recurrent hypoglycaemia blunts the pAMPK response to further hypoglycaemia at 30 min

Figure 3.3.3. Recurrent hypoglycaemia blunts the pAMPK response to further hypoglycaemia at 180 min

Chapter 4

Figure 4.1. A-769662 potently activates AMPK and stimulates ATP release in U373 cells

Figure 4.2.1. A-769662 increases eATP in a concentration-dependent manner in U373 cells

Figure 4.2.2. A-769662 increases eATP in a concentration-dependent manner in CRTAS

Figure 4.3. Co-application of A-769662 and AICAR enhances pAMPK but not ATP release

Figure 4.4. A-769662 increases ATP and lactate release at both euglycaemic and hypoglycaemic conditions

Figure 4.5. NA enhances the A-769662-evoked increase in eLactate

Figure 4.6. Carbenoxolone did not attenuate the A-769662-evoked ATP release

Figure 4.7. No change in fluorescence was observed with A-769662 using Quinacrine

Figure 4.8. A-769662 causes an increase in intracellular calcium

Figure 4.9. Extracellular calcium is not required for the A-769662-mediated increase in eATP

Figure 4.10. Chelating intracellular calcium attenuates the A-769662-evoked ATP release in primary astrocytes

Figure 4.11. A-769662 increases ATP release and intracellular calcium in α1/α2 AMPK KO MEF cells

List of tables

Chapter 2

Table 1: Media compositions

Table 2: Plate seeding protocol

Table 3: Western blot buffer components

Table 4: Gel-making protocol

Table 5: Antibody dilutions and incubation conditions

Table 6: Plate setup for extracellular lactate assay

Abbreviations

$[Ca^{2+}]_i$	intracellular calcium
3V	third ventricle
ACC	acetyl co-A carboxylase
AICAR	5-aminoimidazole-4-carboxamide riboside
AMPK	AMP-activated protein kinase
AMPKK	AMPK kinase
ANLS	astrocyte-neurone lactate shuttle
ARC	arcuate nucleus
AUC	area under the curve
BAT	brown adipose tissue
CaMKK	calcium calmodulin-dependent protein kinase kinase
CFTR	cystic fibrosis transmembrane conductance regulators
CM	conditioned media
CRR	counter-regulatory response
CRTAS	cortical astrocytes
Cx	connexin
DID	dead-in-bed
eATP	extracellular ATP
eLactate	extracellular lactate
ENPP	ectonucleotide pyrophosphatase/phosphodiesterase
ENTPD	ectonucleoside triphosphate diphosphohydrolase
GABA	gamma aminobutyric-acid
GE	glucose-excited
GI	glucose-inhibited
GK	glucokinase

GP	glycogen phosphorylase
GS	glycogen synthase
GSIS	glucose-stimulated insulin secretion
HAAF	hypoglycaemia-associated autonomic failure
HTAS	hypothalamic astrocytes
iATP	intracellular ATP
K_{ATP}	ATP-sensitive K^+ channel
KO	knockout
LDH	lactate dehydrogenase
MBH	mediobasal hypothalamus
MCT	monocarboxylate transporter
MEF	mouse embryonic fibroblast
NA	noradrenaline
nAChR	nicotinic acetyl-choline receptor
NS	normal saline
OCT1	organic cation transporter 1
pACC	phospho ACC
pAMPK	phospho AMPK
PDH	pyruvate dehydrogenase
pGP	phospho GP
PI3K	phosphoinositide 3-kinase
PLL	poly-L-lysine
PMV	portal mesenteric vein
PrF	phenol red-free
RH	recurrent hypoglycaemia
SD	seeding density
SF	serum-free

STZ	streptozotocin
T1D	type 1 diabetes
T2D	type 2 diabetes
TAK1	TGF-β-activating kinase 1
tATP	total ATP
Thr172	threonine 172
VMH	ventromedial hypothalamus
VRAC	volume-regulated anion channels
WT	wild type
ZMP	5-aminoimidazole-4-carboxamide ribotide

Chapter 1: Introduction

1.1 Diabetes and hypoglycaemia

1.1.1 Diabetes mellitus

Diabetes is a metabolic disorder characterised by lack of effective glycaemic regulation. Cells are unable to take up sufficient glucose, resulting in elevated blood glucose (over 7 mM fasted or over 11 mM 2-hour post-prandial glucose). The kidneys are unable to reabsorption all the glucose back into the circulation, leading to loss of glucose through the urine, and rapid weight loss. Chronically elevated blood glucose levels can lead to micro- and macrovascular complications and substantially reduce life expectancy. There are two main types of diabetes mellitus, Type 1 (T1D) and Type 2 diabetes (T2D).

T1D often starts during childhood and is caused by the loss of β-cell function in the pancreas (Alberti and Zimmet, 1998). These cells are responsible for the production of insulin in response to elevated blood glucose concentrations. The cause for this cell loss is not yet fully understood, however it is now known that at least 1-2% of diabetes cases are due to monogenic diabetes, whereby inherited or sporadic mutations in a single gene linked to β-cell function cause the disease (Naylor *et al.*, 2011). Environmental factors, such as viral infection are also believed to be a trigger for the development of T1D; in fact, T1D is strongly associated with autoimmune activity (Richardson *et al.*, 2011; Willcox *et al.*, 2011). Most T1D patients, with the exception of some types of monogenic diabetes, rely on insulin injections to maintain euglycaemia.

T2D is characterised by the combination of a decrease in insulin secretion and decrease in insulin sensitivity. This is believed to be caused by a variety of genetic predispositions combined with the effect of lifestyle habits, such as overeating, lack of exercise and obesity (Unoki *et al.*, 2008; Voight *et al.*, 2010; Yasuda *et al.*, 2008). T2D usually develops later in life, although the age of onset has been decreasing over the past few years, potentially due to the increase in childhood obesity (Ogden *et al.*, 2007). T2D can often be managed by changes in lifestyle, such as diet and exercise, as well as using oral medication, such as the biguanide metformin, or sulphonylureas; However in advanced T2D, where significant β-cell loss has occurred, insulin injections may be necessary.

In both T1D and T2D it is crucial to maintain tight glycaemic control. High blood glucose levels can result in a number of long-term microvascular (retinopathy, nephropathy and neuropathy) as well as macrovascular complications. This can in turn result in sight loss, renal failure and gangrene, as well as an increased risk for arteriosclerosis which may lead to stroke, myocardial infarction and occlusive artery disease of the lower extremities. Hyperglycaemia can also result in a variety of acute complications such as ketoacidosis and hyperosmolar syndrome, which can lead to loss of consciousness, coma and, in extreme cases, death (Alberti and Zimmet, 1998). Whilst trying to achieve tight glycaemic control and avoid these side-effects of hyperglycaemia, people on insulin treatment might use a higher dose than necessary, which increases the risk of experiencing a hypoglycaemic episode (less than 4mM blood glucose).

1.1.2 Hypoglycaemia

Even though insulin has been used as a treatment for diabetes since 1922 (Banting *et al.*, 1922), insulin-induced hypoglycaemia (blood glucose below 4mM) remains a serious side effect and is the limiting factor in maintaining tight glycaemic control. Severe hypoglycaemia is defined as a hypoglycaemic episode where assistance from another individual is required (Donnelly *et al.*, 2005). The symptoms of hypoglycaemia can be separated into two categories, neurogenic and neuroglycopenic. Neurogenic symptoms result from the activation of the autonomic nervous system and normally precede the neuroglycopenic. The increase in cholinergic signalling can cause symptoms such as sweatiness, hunger and tingling, and the increase in adrenergic signalling can cause tremulousness, palpitations and anxiety. They function to alert the individual of hypoglycaemia. Neuroglycopenic symptoms are a result of glucose deprivation in the brain and include warmth, weakness, confusion and tiredness (Towler *et al.*, 1993). If no corrective action is taken they can lead to coma and even death. Hypoglycaemia therefore has the potential to be acutely life-threatening, making glycaemic control challenging in insulin-dependent diabetes patients.

One dangerous aspect of hypoglycaemia is what is referred to as the dead-in-bed (DID) syndrome (Tattersall and Gill, 1991), where the patients are found dead in their, usually, undisturbed bed. DID due to hypoglycaemia is responsible for 5-6% of deaths in patients suffering with T1D under 40 years old (Cryer, 2011; Koltin and Daneman, 2008; Tanenberg *et al.*, 2010). Through continuous glucose monitoring and other post-mortem examinations, DID

appears to be due to a nocturnal hypoglycaemic episode (Koltin and Daneman, 2008; Tanenberg *et al.*, 2010). T1D patients often have defective counter-regulatory (CRR) hormone release, accompanied by a defective awakening response to nocturnal hypoglycaemia (Banarer and Cryer, 2003; Schultes *et al.*, 2007). It is suggested that a nocturnal hypoglycaemic episode from which the patient does not wake up, may result in severe neuroglycopenia, brain damage and death. Another suggestion is that a nocturnal hypoglycaemic episode results in a fatal cardiac arrhythmia (Chow *et al.*, 2014; Clark *et al.*, 2014; Gill *et al.*, 2009; Tanenberg *et al.*, 2010). Apart from the dangers posed by hypoglycaemia itself, the fear of experiencing a hypoglycaemic episode can lead to complications as well, as it can result in patients maintaining a higher glycaemic level than recommended in order to avoid it (Bloomgarden, 2016; Cryer, 2002).

1.1.3 Hypoglycaemia detection

Hypoglycaemia is detected by glucosensing neurones both in the periphery and in the brain. Peripheral glucosensors have been identified in the hepatic portal-mesenteric vein (PMV) and the carotid body, as well as the gut and oral cavity. Glucosensing neurones in the PMV can detect changes in glucose and relay the message through the vagus nerve and spinal cord back to the central nervous system, to areas such as the hypothalamus, to elicit a response (Watts and Donovan, 2010). Central glucosensing neurones are spread throughout the brain, but are most highly expressed in specific loci associated with the regulation of food intake, energy metabolism, neuroendocrine function and energy homeostasis. These areas are the hypothalamus, specifically, the lateral

hypothalamus and ventromedial hypothalamus (VMH), and the hindbrain, especially the area postrema, the nucleus of the solitary tract and the dorsal motor nucleus of the vagus (Watts and Donovan, 2010). Thanks to its positioning adjacent to the third ventricle (3V) and median eminence, the hypothalamus can directly sample the blood glucose and circulating hormones such as insulin and leptin, to elicit a response (Beall *et al.*, 2012a).

Two main types of glucosensing neurones have been identified in the brain, glucose excited (GE) and glucose inhibited (GI) neurones (Oomura *et al.*, 1969). In these neurones, glucose does not only act as fuel, but also acts as a regulator to activate or inhibit neuronal activity in GE and GI neurones respectively. These neurones have been compared to α and β-cells in the pancreas, as they both share a number of characteristics in the mechanism in which they respond to changes in glucose (Ashford *et al.*, 1990; Dunn-Meynell *et al.*, 2002). Both glucosensing neurones and β-cells express the glucose transporter GLUT3 and GLUT2, as well as the glucokinase enzyme (GK). The majority of GE neurones also express the ATP-sensitive K^+ channel (K_{ATP}), which play a crucial part in glucosensing (Ashford *et al.*, 1990). The GLUT2 transporter, GK and the K_{ATP} channel are required in both these neuronal and pancreatic cells in order to respond to changes in glucose (Balfour *et al.*, 2006). AMP-activated protein kinase (AMPK) is also expressed in both cell types, and genetic ablation of its α2 subunit in GE neurones or pancreatic β cells abolishes their ability to respond to hypoglycaemia (Beall *et al.*, 2012b; Beall *et al.*, 2010).

1.2 Defective counter-regulation

1.2.1 The counter-regulatory response (CRR)

As blood glucose concentration falls in a healthy individual, a number of counter-regulatory mechanisms are initiated. Once blood glucose levels fall below approximately 4.44mM, endogenous insulin release is suppressed (Wendt *et al.*, 2004; Zhou *et al.*, 2007).This is followed by an increase in glucagon secretion from pancreatic α-cells at glucose levels of approximately 3.8mM, which acts to stimulate hepatic glucose production by increasing glycogenolysis and gluconeogenesis and therefore increases blood glucose levels (Ishihara *et al.*, 2003). This is accompanied by the activation of the sympathetic and parasympathetic autonomic nervous system, causing an increase in noradrenaline and adrenaline release. Noradrenaline acts on nerve terminals to produce some of the symptoms of hypoglycaemia. Adrenaline is released into the circulation and activates alpha and beta adrenergic receptors to sustain blood glucose concentrations. This effect is mediated by further inhibiting insulin release and promoting glucagon release from the pancreas, as well as reducing glucose uptake and utilisation in muscles, further increasing gluconeogenesis and glycogenolysis in the liver and increasing lipolysis in adipose tissue (Avogaro *et al.*, 1993). Further decreases in glucose result in the release of growth hormone (at 3.7mM blood glucose) and cortisol (at 3.2mM blood glucose). These have not been shown to directly improve blood glucose, but are believed to have more long-term effects. They induce gluconeogenesis and ketogenesis in the liver as well as lipolysis in adipose tissue (Fanelli *et al.*, 1994; Mitrakou *et al.*, 1991; Schwartz *et al.*, 1987).

In the brain, glucose concentration differs significantly from peripheral blood glucose; However, it still parallels that of the periphery. In the brain, euglycaemic glucose levels range between 0.7-2.5mM. During peripheral hypoglycaemia, brain glucose falls to 0.2-0.5mM and during hyperglycaemia it can go up to 5mM (Karnani and Burdakov, 2011; Silver and Erecinska, 1994). Inducing local hypoglycaemia in the VMH using 2-deoxyglucose has been shown to induce the CRR, resulting in increased peripheral glucose, glucagon, adrenaline and noradrenaline (Borg *et al.*, 1995). This indicates that glucosensors in the brain can induce the CRR independently during experimental central hypoglycaemia, even in the presence of peripheral euglycaemia.

1.2.2 Impaired counter-regulation

Patients with T1D do not release endogenous insulin, and thus inject exogenous insulin to regulate their blood glucose levels. This means that there is no mechanism to switch off or inhibit this insulin if glucose levels fall. After approximately 5 years the glucagon response in these individuals is often diminished, leaving them highly reliant on the adrenaline response to hypoglycaemia (Segel *et al.*, 2002). Following recurrent hypoglycaemia (RH) episodes however, patients can develop an impaired CRR to hypoglycaemia (also referred to as hypoglycaemia-associated autonomic failure (HAAF)) where the threshold for the adrenaline response to hypoglycaemia becomes higher, giving those patients less time from the appearance of symptoms to taking corrective action. Impaired hypoglycaemia awareness affects approximately

20% of people with T1D and increases the risk of experiencing a severe hypoglycaemic episode by over 2-fold (Geddes *et al.*, 2008).

Previous hypoglycaemia is a significant predictor of future hypoglycaemia (Donnelly *et al.*, 2005). Studies on T1D and T2D patients, as well as healthy controls, have demonstrated impaired CRR to hypoglycaemia following even a single recent hypoglycaemic episode (Arbelaez *et al.*, 2008; Joy *et al.*, 2015; Segel *et al.*, 2002). These studies have also been replicated in animal models (LaGamma *et al.*, 2014; McCrimmon *et al.*, 2006). The impaired CRR to hypoglycaemia has been shown to be reversible through avoidance of hypoglycaemia, with improvements seen following 2 weeks of hypoglycaemia prevention, and near complete normalisation of CRR following 3 months of hypoglycaemia avoidance (Fanelli *et al.*, 1993). This provides further evidence that hypoglycaemia itself, is responsible for impaired CRR and that this effect is reversible.

Even though the involvement of the central and peripheral nervous system in glucosensing and the development of impaired counter-regulation has been long established, the underlying mechanism is still unknown. Nicotinic acetylcholine (nACh) neurones in the chromaffin cells in the adrenal glands are activated during hypoglycaemia, promoting the biosynthesis and release of adrenaline. One theory behind the impaired CRR is that prolonged or repeated activation of these nAChR through full agonists, such as insulin, causes a maladaptive response to antecedent hypoglycaemia. Indeed, studies on rats showed that a partial activation of peripheral nAChR using the partial agonist,

cytisine, increases de novo catecholamine synthesis and greatly restores the hormonal response to hypoglycaemia (LaGamma *et al.*, 2014).

Basal gamma aminobutyric acid (GABAergic) tone in the VMH prevents adrenaline and glucagon secretion during euglycaemia and hyperglycaemia. This needs to be suppressed in order to initiate the hormonal response to hypoglycaemia (Zhou *et al.*, 2010). Rats exposed to RH or rat models of Type 1 diabetes have an increased GABA baseline, by 3-fold and 2-fold respectively, measured through brain microdialysis, meaning that inhibition of GABA release during hypoglycaemia is not sufficient to allow adrenaline and glucagon release (Chan *et al.*, 2008; Chan *et al.*, 2013). Lactate has been shown to raise GABA levels in the VMH, and has also been shown to inhibit the CRR. Since inhibiting lactate transport from astrocytes or preventing its uptake and utilisation by neurones prevents lactate-mediated impairment in CRR, it is possible that an increase in brain lactate drives the increase in basal GABA levels, and thus prevents counter-regulatory hormone release (Borg *et al.*, 2003; Zhou *et al.*, 2010).

1.3 AMP-activated protein kinase (AMPK)

1.3.1 Whole body energy homeostasis

AMP-activated protein kinase (AMPK) has also recently been shown to be involved in the CRR to hypoglycaemia. In the past decade, AMPK has been established as a cellular energy sensor involved in whole body energy homeostasis and has been shown to be involved in the response to

hypoglycaemia. It was first described in two different cellular processes by independent groups in 1973 (Beg *et al.*, 1973; Carlson and Kim, 1973). The same enzyme was discovered to be responsible for both processes (Carling *et al.*, 1987), and was later named AMPK (Sim and Hardie, 1988).

AMPK is composed of a catalytic α-subunit and regulatory β- and γ-subunits. In mammals, two α-subunits (α1, α2), two β subunits (β1, β2) and three γ-subunits (γ1, γ2, γ3) have been identified (Carling, 2004) (Figure 1.1). AMPK is activated through phosphorylation on the threonine 172 (Thr172) residue of the α-subunit by a variety of AMPK kinases (AMPKK) (Carling, 2004), such as the tumour suppressor kinase, LKB1, (Hawley *et al.*, 2003), TGF-β-activating kinase 1 (TAK1) (Herrero-Martin *et al.*, 2009) and the intracellular calcium sensor, calcium calmodulin-dependent protein kinase kinase β (CaMKKβ) (Gowans *et al.*, 2013; Hawley *et al.*, 2005; Hurley *et al.*, 2005; Woods *et al.*, 2005). AMPK is also regulated by changes in the intracellular AMP:ATP ratio (Corton *et al.*, 1994). AMP and ATP both bind to the γ-subunit of AMPK, the former of which binds at a much higher affinity than the latter, mediating opposing effects; ATP inhibits AMPK activation, whilst AMP increases AMPK activation through direct allosteric activation (Gowans *et al.*, 2013; Scott *et al.*, 2004). AMP as well as ADP also protect AMPK from dephosphorylation (Xiao *et al.*, 2011).

AMPK is involved in the regulation of a variety of cellular processes, such as proliferation, autophagy, phagocytosis and energy homeostasis. AMPK phosphorylation of the Thr172 residue on the α-subunit has been shown to decrease during hyperglycaemia and increase during hypoglycaemia or fasting

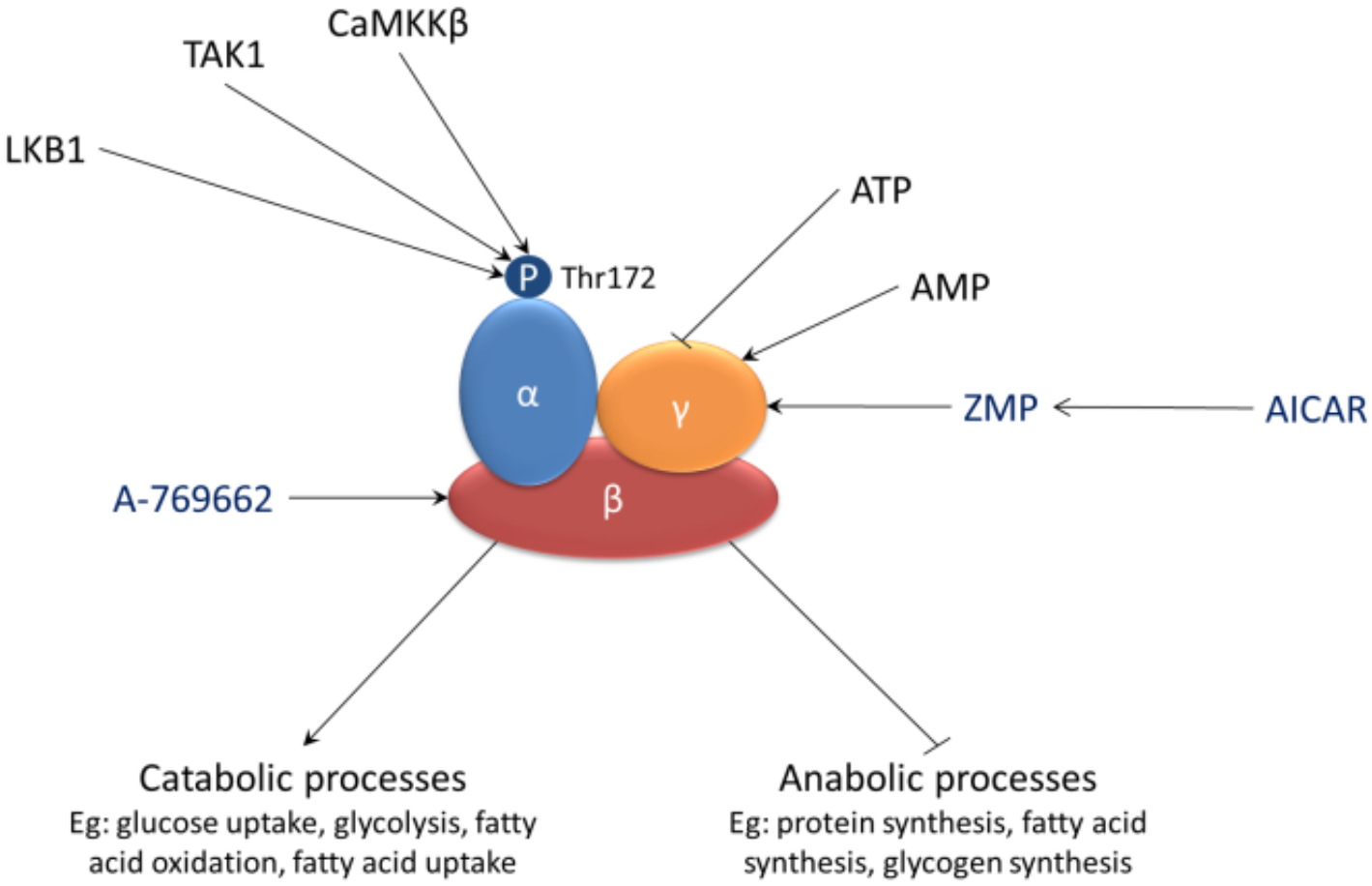

Figure 1.1. General AMPK structure and some of its modulators. AMPK is made up of a catalytic α subunit and regulatory β and γ subunits. The physiological regulators of AMPK, CaMKKβ, TAK1 and LKB1 phosphorylate AMPK on the α subunit, and ATP and AMP inhibit and activate AMPK respectively through the γ subunit. The AMPK activator AICAR gets converted to ZMP once inside the cell, which acts as AMP mimic through the γ subunit. The AMPK activator A-769662 binds to the βsubunit to mediate its effect.

(Taib *et al.*, 2013). It acts to increase catabolic processes such as glucose uptake, glycolysis and fatty acid oxidation and uptake, while simultaneously, decreasing anabolic processes, such as protein, glycogen and fatty acid synthesis, to promote energy production and increase ATP (Scott *et al.*, 2014). AMPK activation has been shown to decrease blood glucose and lipid levels by increasing glucose transport into the cells, and fatty acid oxidation, while inhibition has been shown to raise them (Bergeron *et al.*, 2001; Cool *et al.*, 2006), making it an important regulator of whole body energy homeostasis, and a potential therapeutic target for a variety of metabolic diseases.

AMPK has also been associated with diabetes. During both hyperglycaemia and hypoglycaemia, experienced in T1D and T2D, AMPK activity is altered, and evidence suggests AMPK activation may be beneficial for both. The AMPK activator A-769662 has been shown to be beneficial for both hepatic steatosis and insulin resistance in animal models, two characteristics of T2D, as well as for maintaining more physiological levels of blood glucose and lipids (Cool *et al.*, 2006). Studies in rats also suggest central AMPK activation may be beneficial for restoring the defective CRR to hypoglycaemia (McCrimmon *et al.*, 2006; McCrimmon *et al.*, 2004), suggesting AMPK may have potential as a therapeutic target for treatment of diabetes.

1.3.2 AMPK and the counter-regulatory response

The involvement of AMPK in peripheral glucose homeostasis has long-been established. It has been shown that knocking out AMPK in animals results in reduced glucose tolerance, insulin resistance and increased fatty acids (Viollet

et al., 2003), whereas overexpression in the liver causes a reduction in blood glucose, and increased fatty acid oxidation (Foretz *et al.*, 2010). AMPK is also essential for β-cell K_{ATP} channel opening during hypoglycaemia, which is required for β-cell glucosensing (Ashcroft and Rorsman, 1990; Beall *et al.*, 2013). Studies on mice with pancreatic AMPK α2 deletion showed impaired glucose homeostasis and glucose-stimulated insulin secretion (GSIS), which was exacerbated in mice also lacking α1 AMPK. Cultured islets from both genotypes of mice had a decreased GSIS as well as an attenuated ability to supress insulin secretion in low glucose (Beall *et al.*, 2010). This indicates that β-cells require AMPK in order to respond to both high and low glucose. Cultured islets have a decreased AMPK phosphorylation in response to high glucose, and pharmacologically activating AMPK supresses the GSIS. In agreement to this, introducing a constitutively active AMPK mutation in β-cells inhibits GSIS, whereas, a dominant negative mutation causes insulin release during hypoglycaemia (da Silva Xavier *et al.*, 2003). Taken together, this data suggests that AMPK regulation is necessary for glucosensing and controlled insulin secretion in β-cells.

1.3.3 AMPK in glucosensing neurones

AMPK is known to be essential for mediating the CRR to hypoglycaemia in the periphery; However, increasing evidence suggests that it is also essential for the central regulation of glucose. Both β-cells and glucosensing neurones have been shown to share multiple similarities in their response to changes in glucose. Both cell types require K_{ATP} activity (Ashcroft and Rorsman, 1990; Beall *et al.*, 2012b), as well as GK and GLUT2 (Balfour *et al.*, 2006) for

glucosensing. One of the main glucosensing areas in the brain is the hypothalamus, with the VMH playing an important role in glucosensing and responses to energy availability, as well as other homeostatic processes (Karnani and Burdakov, 2011; Routh *et al.*, 2014). Similarly, to the pancreas, hypothalamic AMPK activation increases during hypoglycaemia (Han *et al.*, 2005). Pharmacologically inhibiting this hypothalamic AMPK activation or genetically downregulating VMH AMPK expression, attenuates the CRR to hypoglycaemia (Han *et al.*, 2005; McCrimmon *et al.*, 2008). Inversely, activating VMH AMPK amplifies glucose production and the CRR during hypoglycaemia (McCrimmon *et al.*, 2006; McCrimmon *et al.*, 2004). Studies on a cell line of hypothalamic GE neurones, GT1-7 cells, showed a decrease in AMPK phosphorylation when exposed to high glucose (Taib *et al.*, 2013). Similarly to the observation made in β-cells, reducing AMPK α2 activity in GT1-7 cells, blunts their response to hypoglycaemia (Beall *et al.*, 2012b). This suggests that central, and more specifically, neuronal glucosensing requires AMPK for the detection of both high and low glucose. The involvement of AMPK in neuronal glucosensing has been studied extensively, however, glial AMPK involvement in this mechanism has been overlooked. A large body of evidence implicates the involvement of glia, especially astrocytes, in the response to both hyper- and hypoglycaemia (Lam *et al.*, 2005; Marty *et al.*, 2005; Taib *et al.*, 2013).

1.4 Glial cells

1.4.1 Glial cells support neuronal function

Glial cells were originally considered the “glue” of the brain; However, over the years, they have been shown to be involved in a multitude of processes. There

are three types of glial cells, oligodendrocytes, microglia and astrocytes. Oligodendrocytes form the myelin sheath around neuronal axons, microglia act as the innate immune system of the brain and astrocytes were initially thought of as the “housekeeping” cells in the brain. (Figure 1.2)

Astrocytes regulate neuronal activity, maintain ion balance in the extracellular space, remove neurotransmitters, and provide neurones with nutrients, such as lactate (refer to section 1.6). Astrocytes form what is referred to as the “tripartite synapse” by enveloping the post- and pre-synaptic nerve terminal of a synapse, with astrocytic processes (Araque *et al.*, 1999). This allows them to detect and modulate neuronal transmission. Each astrocyte is also in contact with a blood vessel through astrocytic end-feet (Kacem *et al.*, 1998). This allows astrocytes to monitor the synaptic environment and bloodstream simultaneously, and thus modulate synaptic activity, as well as the entry of substances through the blood-brain barrier. One essential function of astrocytes, is their ability to take up glutamate released into the synaptic cleft by neurones, convert it to glutamine, and export it back into the extracellular medium for neurones to take up and recycle back into glutamate stored in vesicles. This is referred to as the glutamate-glutamine cycle. Prolonged glutamate stimulation of neurones can have excitotoxic effects, meaning that glutamate uptake by astrocytes is a very important process in maintaining neuronal health, as well as replenishing neuronal glutamate stores (Broer and Brookes, 2001). For recent review on neuroglial signalling see (Gundersen *et al.*, 2015).

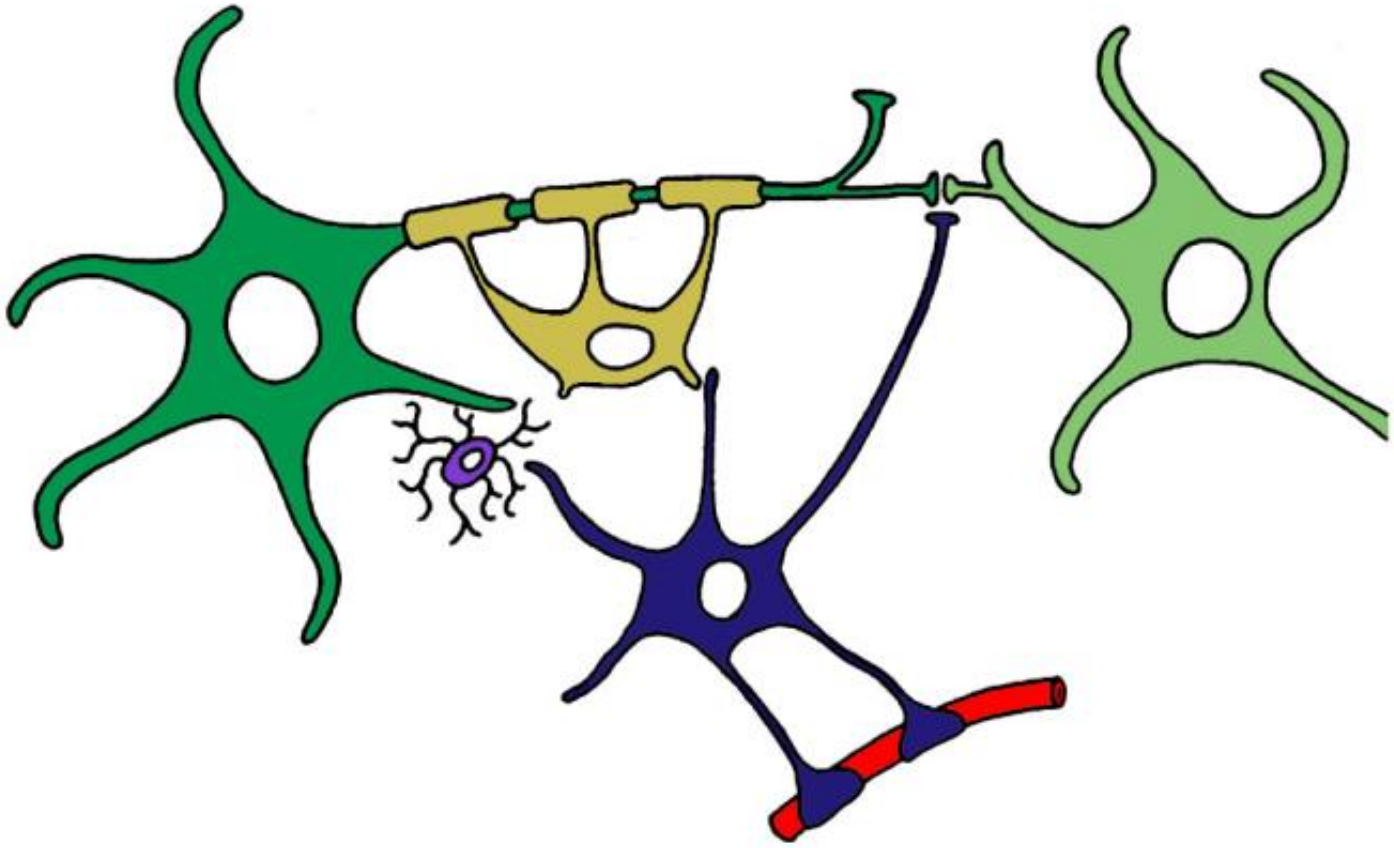

Figure 1.2. Schematic drawing of neuronal and glial interactions. Oligodendrocytes (yellow) make myelin and wrap neuronal (green) axons. Microglia (purple) make contact with neurones. Astrocytes (blue) envelop neuronal synapses and send processes to blood vessels (red).

One important function of astrocytes is the production and export of lactate. Even though glucose is thought of as the main energy substrate for neuronal metabolism, studies suggest that neurones may preferentially use lactate (Beall *et al.*, 2012b; Song and Routh, 2005). Astrocytes express glucose transporters, predominantly GLUT1 (Iwabuchi *et al.*, 2014), allowing glucose uptake; However, unlike neurones, astrocytes express low levels of pyruvate dehydrogenase (PDH), suggesting that they are geared towards glycolysis rather than oxidative metabolism of glucose (Laughton *et al.*, 2007). Astrocytes also express high levels of lactate dehydrogenase (LDH), especially LDH1 and LDH5, of which the latter is almost exclusively expressed in astrocytes and has a higher affinity for pyruvate than lactate, meaning it preferentially converts pyruvate to lactate (Laughton *et al.*, 2007). Lactate can then be exported through monocarboxylate transporters (MCT), of which MCT1, MCT2 and MCT4 are expressed in astrocytes (Pellerin *et al.*, 2005). Astrocytes can also produce lactate from glutamate taken up from the synaptic cleft. Astrocytes also express glycogen synthase (GS) which converts glucose to glycogen, and glycogen phosphorylase (GP), which breaks down glycogen stores. This suggests that astrocytes can use the glucose taken up from the extracellular medium and store it as glycogen, which can be broken down and exported as lactate during periods of energy stress to sustain neurone activity (Brown *et al.*, 2003; Suh *et al.*, 2007; Swanson and Choi, 1993; Walls *et al.*, 2008). Breakdown of astrocytic glycogen stores to release lactate has also been demonstrated in normoglycaemia during intense exercise in rats (Matsui *et al.*, 2015). This has also been shown in long-term potentiation and memory-formation (Newman *et al.*, 2011), suggesting that it is not only important in

pathophysiological conditions, but in physiological high energy demand activities.

1.4.2 Astrocytes: More than a supporting role

Even though astrocytes play an important role in supporting neuronal function through removal of potentially excitotoxic neurotransmitters from the extracellular space and providing neurones with energy, they have also been shown to be directly involved in the modulation of neurotransmission in a variety of physiological and pathophysiological processes. Astrocytes release a variety of gliotransmitters, such as GABA, D-serine, TNFα, ATP, glutamate and lactate, which can propagate a signal across astrocytic populations, mediate effects on other cells in the brain, such as microglia and oligodendrocytes, or modulate synaptic transmission and plasticity (Araque *et al.*, 2014; Araque *et al.*, 1999; Bezzi and Volterra, 2001; Gundersen *et al.*, 2015).

Hypothalamic astrocytes are glucosensing cells and act to modulate the response to both hypoglycaemia and hyperglycaemia. They respond to changes in glucose by changing AMPK activity (Taib *et al.*, 2013). A glucose injection in the carotid increases insulin release accompanied by an activation of astrocytes in the arcuate nucleus (ARC). Inhibiting this activation of astrocytes inhibits the insulin response to glucose (Guillod-Maximin *et al.*, 2004). A different group has showed that this activation of the hypothalamo-pancreatic axis by carotid glucose injection requires the conversion of glucose to lactate, as well as pyruvate metabolism, indicating the potential involvement of astrocytes (Allard *et al.*, 2013). The two major glucose transporters

expressed in astrocytes are GLUT1 and GLUT2. Astrocytes predominantly express GLUT1, although, hypothalamic astrocytes specifically, highly express GLUT2 (Iwabuchi *et al.*, 2014). GLUT2 KO mice have impaired sensitivity to both hyper- and hypoglycaemia, and fail to initiate a glucagon response and brainstem c-Fos activation following peripheral or central 2DG-mediated hypoglycaemia. This was rescued by re-expressing GLUT2 in astrocytes, but not neurones (Marty *et al.*, 2005). This indicates that astrocytic GLUT2 plays an important role in the detection and response to hypoglycaemia. In streptozotocin (STZ)-induced diabetic rats, GLUT1 expression was reduced in hypothalamic astrocytes. This was accompanied by defective hypothalamic glucosensing. Overexpressing GLUT1 in hypothalamic astrocytes was able to reverse this (Chari *et al.*, 2011). Another astrocyte-like type of cell found in the hypothalamus that has been shown to be glucosensing is tanycytes. These cells line the 3V in the hypothalamus, placing them in direct contact to glucose and hormones in the CSF, and send projections into the ARC and VMH, areas involved in energy homeostasis, and exhibit ATP-mediated responses to glucose (Frayling *et al.*, 2011). Taken together, this evidence suggests that astrocytes play an essential role in central glucosensing.

1.5 Adenosine triphosphate (ATP)

1.5.1 ATP as a gliotransmitter

ATP was originally viewed solely as the source of cellular energy; however, it is now accepted that extracellularly, ATP acts as a neurotransmitter acting on a large family of receptors, known as the purinergic P2 receptors, to modulate a

multitude of processes throughout the body. The action of ATP as a neurotransmitter was first proposed by Burnstock in 1972 (Burnstock, 1972).

Extracellular ATP is a universal “danger signal “, causing inflammatory responses, such as cytokine release and recruitment of immune cells (Idzko *et al.*, 2014). It acts as a fast excitatory neurotransmitter, mediating short-term effects, as well as long-term effects on proliferation, growth and development (Burnstock, 2006b; Idzko *et al.*, 2014). ATP can be released through a variety of regulated mechanisms such as vesicular release or through channels, or passively as a result of damage to the cell wall. Once released, ATP is hydrolysed by ectonucleotidases, into AMP, ADP and adenosine, from which, ADP and adenosine, can in turn activate other purinergic receptors (Idzko *et al.*, 2014) (Figure 1.3).

Most ectonucleotidases are membrane-bound, either by expressing membrane helices, or through anchorage to the membrane, although soluble forms have also been reported. There are four main families of ectonucleotidases in mammalian cells, ectonucleotiside triphosphate diphosphohydrolase (ENTPD), ectonucleotide pyrophosphatase/phosphodiesterase (ENPP), alkaline phosphatase, and ecto-5’-nucleotidase (also known as CD73). Each of these preferentially hydrolyses different nucleotides with different affinities. Seven ectonucleotidases have been discovered in the ENTPD family (ENTPD1-6 and 8), of which only four hydrolyse nucleotides (ENTPD1-3 and 8). These ENTPDases hydrolyse ATP and ADP to AMP. In the ENPP family, three have been characterised (ENPP1-3), which hydrolyse ATP to AMP and pyrophosphate. Alkaline phosphatase hydrolyses ATP, ADP and AMP to

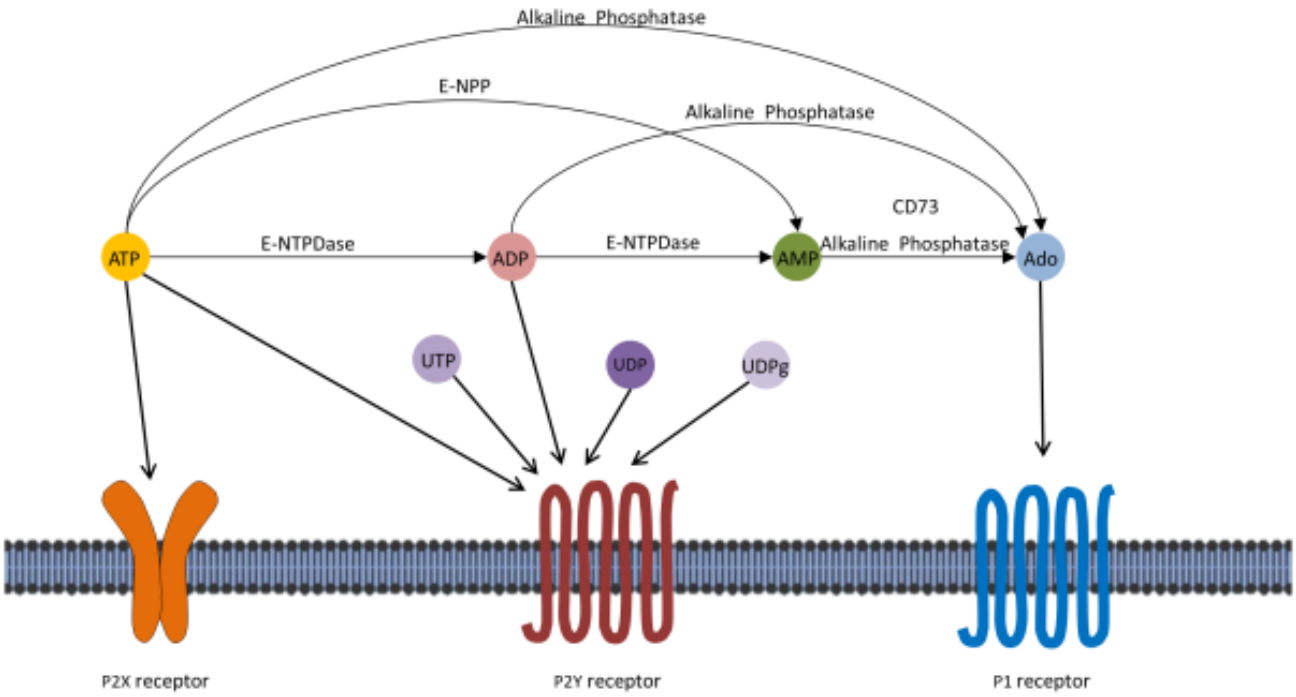

Figure 1. 3. Overview of purinergic signalling. ATP is broken down to ADP and AMP by ectonucleoside triphosphate diphosphohydrolase (E-NTPDase), to AMP by ectonucleotide pyrophosphatase/phosphodiesterase (E-NPP) and to adenosine (Ado) by alkaline phosphatase. Alkaline phosphatase also breaks ADP or AMP down to adenosine. CD73 breaks AMP down to adenosine. ATP activates P2X and P2Y receptors. UTP, ADP, UDP and UDP-glucose (UDPg) activate P2Y receptors. Adenosine activates adenosine (P1) receptors

adenosine, and CD73 hydrolyses AMP to adenosine. For recent reviews: (Yegutkin, 2008; Zimmermann *et al.*, 2012). These nucleotides, and the nucleoside, adenosine, as well as UTP, UDP and UDP-sugars, act on purinergic receptors to elicit a wide variety of responses.

Purinergic receptors are split into two categories, P2X and P2Y receptors. In the P2X receptor family, 7 subunits have been cloned, P2X1-7. P2X receptors are plasma membrane channels that can form heterotrimers or larger heteromeric complexes. They are activated by ATP and are permeable to small monovalent and divalent cations, such as Na^+, K^+ and Ca^{2+}. This entry of Ca^{2+} upon channel activation initiates the Ca^{2+} signalling cascade. The P2X7 receptor acts in a biphasic mode, where upon initial activation, it acts as a cation channel, however, following prolonged activation, forms a pore, which is permeable to small molecules, including ATP, glutamate and GABA (Suadicani *et al.*, 2006). This receptor has been linked to a variety of pathologies, such as temporal lobe epilepsy, neurodegenerative disorders, neuropathic pain, diabetes, and cancer (Burnstock, 2006a). The P2Y receptor family is composed of 8 subtypes, P2Y1, 2, 4, 6, 11-14. These are G-protein-coupled receptors and upon activation either activate PLC-β, raising intracellular calcium, or activate or inhibit adenylate cyclase, depending on the G protein coupled to each receptor. ATP binds to all P2Y receptors except for P2Y6 and 14. P2Y11 binds ATP exclusively. P2Y1, 12 and 13 also bind ADP, and P2Y2, 4 and, to a lesser extent, P2Y6 bind UTP. P2Y6 mainly binds UDP and P2Y14 binds UDP-glucose and other UDP-sugars. Adenosine activates a separate type of receptors, adenosine (also known as P1) receptors, of which there are four subunits, ADORA1, ADORA2A, ADORA2B and ADORA3 (Burnstock, 2006a, b; Idzko *et al.*, 2014).

1.5.2 ATP release from astrocytes

Astrocytic ATP release is important in modulating neuronal and astrocytic activation in several, if not all, brain regions (Bowser and Khakh, 2004; Gourine *et al.*, 2010; Koizumi *et al.*, 2003). There is some disagreement regarding the method of ATP release from astrocytes (Hamilton and Attwell, 2010), with studies suggesting it is through connexin (Cx) or pannexin (Px) hemichannels, P2X7 receptors, vesicles, volume regulated anion channels (VRAC) or cystic fibrosis transmembrane conductance regulators (CFTR).

Astrocytic vesicular ATP release is believed by some to be the main mechanism behind astrocytic ATP release (Bowser and Khakh, 2007; Lalo *et al.*, 2014). Astrocytes can store ATP in vesicles, mainly lysosomal vesicles, although some ATP appears to also be stored in smaller vesicles. The lysosomal-associated vesicular nucleotide transporter (VNUT) is expressed in astrocytes, and is believed to be responsible for astrocytic ATP release (Oya *et al.*, 2013). Activation of purinergic currents in pyramidal neurones by astrocytic ATP release is abolished in astrocytes expressing dominant negative soluble N-ethylmaleimide-sensitive-factor attachment protein receptor (DN-SNARE), indicating that vesicle fusion is necessary for astrocytic purinergic stimulation of neurones (Lalo *et al.*, 2014).

ATP can also be released by the P2X7 receptor. This receptor has been associated with a variety of pathologies (Burnstock, 2006a), as well as with ATP-induced cell lysis and apoptosis, and the mediation of immune responses (Arulkumaran *et al.*, 2011). This receptor has been shown to be permeable to a

variety of small molecules of up to 1KDa, including ATP, glutamate and GABA. This only occurs after prolonged activation, when the channel changes conformation into a pore (Surprenant *et al.*, 1996). Studies have suggested that this receptor, is responsible for ATP-induced ATP release, and thus Ca^{2+} propagation (Suadicani *et al.*, 2006).

Hemichannels are another mechanism through which ATP can be released. These are channels organised in a hexamer, formed by connexins or pannexins, and are referred to as connexons or pannexons, respectively. Pannexins can only form hemichannels, whereas, connexins from adjacent cells can join to form gap junctions allowing direct intracellular exchange between astrocytes (Bennett *et al.*, 2003; Giaume *et al.*, 2010; Lazarowski *et al.*, 2011). When activated, hemichannels are permeable to small molecules, up to 1-1.2kDa, such as ATP. These channels are also permeable to small dyes, which are often used to examine the function of these channels. Astrocytes mainly express Cx43 and Cx30 (Dermietzel *et al.*, 1991; Giaume *et al.*, 1991), although mRNA receptor expression of other Cx subunits has been reported (Blomstrand *et al.*, 2004). The ATP secretion from poorly coupled cell lines, such as C6, U373 and HeLa can be increased by inducing the expression of Cxs. This increase in ATP release involved the mobilisation of Ca^{2+} stores in astrocytes and the action of Cl^- channels (Cotrina *et al.*, 1998).

ATP release has also been shown to be mediated by other channels, often overlooked when studying astrocytic ATP release, the VRAC. According to a study by Anderson et al, ATP-induced ATP release in primary cortical astrocytes did not involve changes in $[Ca^{2+}]_i$, and was not inhibited by blocking

vesicular release, or hemichannels. However, it was blocked by anion channel blockers. It was suggested that ATP release may be through VRAC (Anderson *et al.*, 2004a).

1.5.3 Calcium signalling in astrocytes

Unlike neurones, astrocytes do not exhibit action potentials, but instead communicate through gliotransmission and Ca^{2+} waves. ATP-induced ATP release is crucial for Ca^{2+} wave propagation (Bowser and Khakh, 2007; Cotrina *et al.*, 1998) (Figure 1.4). Mechanical stimulation of astrocytes initiates Ca^{2+} wave propagation and inhibits excitatory glutamatergic neurotransmission through a process involving astrocytic ATP release and P2 receptor activation (Koizumi *et al.*, 2003). The same group showed that unstimulated astrocytes exhibit spontaneous Ca^{2+} waves which exert a tonic inhibition on glutamatergic neuronal transmission. This tonic inhibition was abolished by inhibiting astrocytic ATP release (Koizumi *et al.*, 2003). The adaptive increase of breathing following pH changes in the brain is also mediated by Ca^{2+} wave propagation. Small pH changes in the brainstem causes an increase in $[Ca^{2+}]_I$ and ATP release. This results in Ca^{2+} wave propagation across populations of astrocytes, and subsequent activation of chemoreceptor neurones (Gourine *et al.*, 2010).

As with general astrocytic ATP release, views regarding the mechanism behind Ca^{2+} wave propagation are opposing. Cotrina et al showed that Ca^{2+} wave propagation through stimulation of P2 receptors was a result of ATP release through hemichannels, acting on P2Y receptors. This was shown to also involve

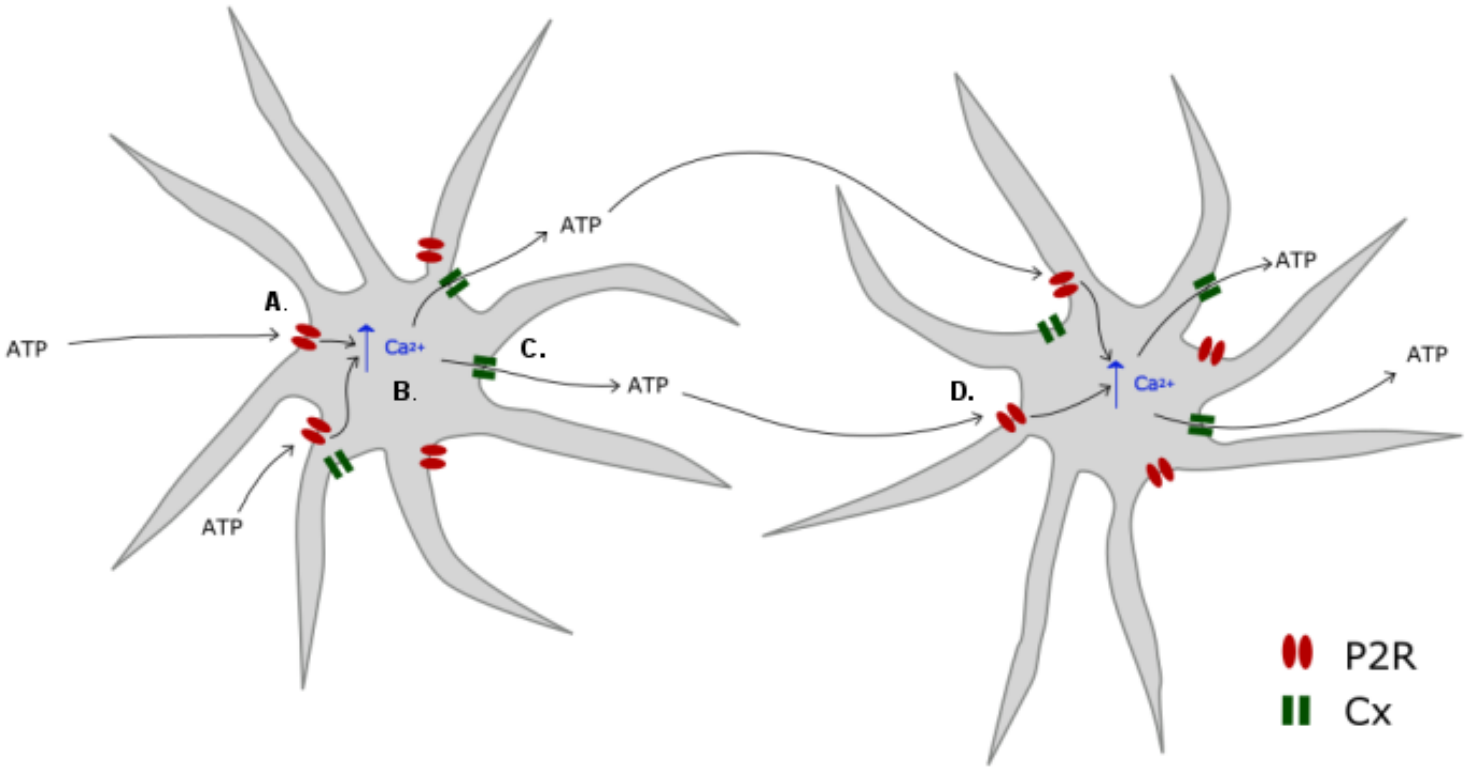

Figure 1.4. Diagrammatic representation of the astrocytic calcium wave propagation. A. Extracellular ATP acts on purinergic receptors (P2R) on astrocytes. **B.** This causes an increase in intracellular calcium, which opens connexin hemmichanels (Cx), releasing ATP (**C.**). **D.** This ATP acts on neighbouring astrocytes to in turn increase intracellular calcium and cause further ATP release, thus propagating the signal.

the activity of Cl^- channels, and was not blocked by inhibiting P2X receptors or gap junctions (Cotrina *et al.*, 1998). Another study showed that Ca^{2+} wave propagation was not through Cx43 hemichannels, but through the activation of P2X7 receptors, causing ATP-induced ATP release (Suadicani *et al.*, 2006). Bowser and Khakh on the other hand showed that Ca^{2+} wave propagation caused by mechanical stimulation was mediated through vesicular ATP release acting on P2Y1 receptors (Bowser and Khakh, 2007). Even though the evidence on the ATP release mechanism is contradicting, most studies seem to agree that this eATP acts in P2Y receptors to propagate the signal.

1.5.4 The purinergic system in diabetes

Numerous studies have suggested alterations in the purinergic system in T1D and T2D patients as well as animal models of diabetes. These have been shown in a variety of tissues, and in most cases are believed to be a result of prolonged hyperglycaemia. For review see (Burnstock and Novak, 2013).

ATP sensitivity was shown to increase in skin fibroblasts exposed to high glucose concentrations, and P2X7 receptors exhibited aggregation into ring-like structures in the periphery of the cells (Solini *et al.*, 2000). In fibroblasts from T2D patients, there was an increase in P2X7 receptor-mediated responses and a large increase in extracellular ATP (Solini *et al.*, 2004). P2X7 receptors were also upregulated in islets of obese patients, but downregulated in islets of T2D patients. This was thought to be due to the hyperglycaemia-protective release of interleukin-1 receptor agonist (IL-1Ra) by P2X7 receptors (Glas *et al.*, 2009). P2X2 and 3 have also been shown to be altered in STZ-induced diabetic rats

and mice in the periphery, as have nucleotide release, uptake and sensitivity (Burnstock and Novak, 2013).

In the brain, and more specifically in the hippocampus of STZ-induced diabetic rats, decreased ADORA1 and increased ADORA2A receptor expression has been reported. Duarte et al also observed a decrease in ATP metabolism and decrease in P2X3, 5, 7 and P2Y2, 6 and 11 receptor expression in nerve terminals of the hypothalamus of STZ rats. This was accompanied by an increase in P2X1, 2, 5, 6, 7 and P2Y6 receptors in whole hippocampal membranes and a decrease in cerebrospinal fluid ATP (Duarte *et al.*, 2007). In microglia, exposure to high glucose concentrations resulted in an enhanced Ca^{2+} response to P2 receptor activation. Glucose starvation in astrocytes also showed mediations in the purinergic system, where an increase in P2Y4 was observed, coupled to a decrease in NMDAR1 (Cavaliere *et al.*, 2004).

High glucose also resulted in defective gap junctional communication and reduced expression of Cx36 and Cx30 in astrocytes in culture. The same effects were seen in brain slices of STZ diabetic rats, and this was shown to be through oxidative stress (Gandhi *et al.*, 2010). Allard et al also showed changes in Cx43 expression in the mediobasal hypothalamus (MBH). Cx43 is highly expressed in the ARC and ventromedial hypothalamus (VMN), especially around capillaries and the edge of the medial part of 3V. Hyperglycaemia caused an increase in the expression in the MBH, and Cx43 inhibition in the MBH was shown to reduce the insulin response observed during central hyperglycaemia. On the other hand, fasting was shown to reduce Cx43 expression which persisted following refeeding (Allard *et al.*, 2014). These

studies suggest that connexin expression is dynamic, adapting to changes in metabolic demands, and that they might play an important role in the response to these metabolic challenges, potentially through changes in ATP release and thus purinergic signalling.

The purinergic system is altered following high or low glucose exposure, as well as in diabetes and obesity. These changes in purinergic signalling are tissue specific and may underlie some of the pathologies in diabetes.

1.6 Astrocytic lactate

1.6.1 The astrocyte-neurone lactate shuttle (ANLS) hypothesis

Glucose is thought of as the main energy source in the brain; however, neurones are also capable of metabolising lactate and ketones for energy. Both can be produced by astrocytes during periods of energy stress, such as hypoglycaemia (Pellerin and Magistretti, 2012; Taib *et al.*, 2013). Some studies suggest that GE neurones might even preferentially use lactate over glucose (Beall *et al.*, 2012b; Song and Routh, 2005).

Lactate in the brain can either be transported across the blood-brain barrier via MCT or can be produced by astrocytes. Some studies have shown an increase in MCT expression at the blood-brain barrier and an increase in lactate import into the brain during hypoglycaemia following antecedent hypoglycaemia and in T1D patients (Herzog *et al.*, 2013; Mason *et al.*, 2006). This change in lactate transport, however, is not enough to support normal neuronal function, suggesting that another mechanism, such as locally derived lactate, may be

essential to maintain neuronal activity. Changes in neuronal metabolism have also been reported; indicating neurones may become more efficient at metabolising glucose. However, the increase in brain lactate appears to be necessary for the maintenance of normal neuronal function during hypoglycaemia (Herzog *et al.*, 2013).

A prevalent hypothesis is that during hypoglycaemia, astrocytes increase the production and export of lactate, providing neurones with energy during energy stress (Pellerin and Magistretti, 2012) (Figure 1.5). During energy demand, astrocytic lactate is essential for maintenance of neuronal activity and survival (Brown *et al.*, 2003; Suh *et al.*, 2007; Swanson and Choi, 1993; Walls *et al.*, 2008). Astrocytes are highly glycolytic cells, with most glucose being metabolised anaerobically. Astrocytes express glucose transporters, predominantly GLUT1 (Iwabuchi *et al.*, 2014), allowing glucose uptake. They also express hexokinase I, which phosphorylates glucose into glucose-6-phosphate in the first step of glycolysis (Wiesinger *et al.*, 1997). As mentioned previously (Chapter 1.4), astrocytes possess the necessary equipment for highly efficient lactate production and export. Both astrocytes and neurones express GS, which allows glycogen synthesis, however, only astrocytes express GP which allows its subsequent breakdown. This is in agreement with the notion that astrocytes are the major glycogen stores in the brain (Wiesinger *et al.*, 1997). The lactate produced, either by breakdown of blood-derived glucose, or breakdown of glycogen stores, can then be transported out of the astrocytes, into the extracellular space, and then into the neurones through MCT transporters, which are highly expressed in both astrocytes and neurones. This process, by which glucose or glycogen is metabolised into lactate and

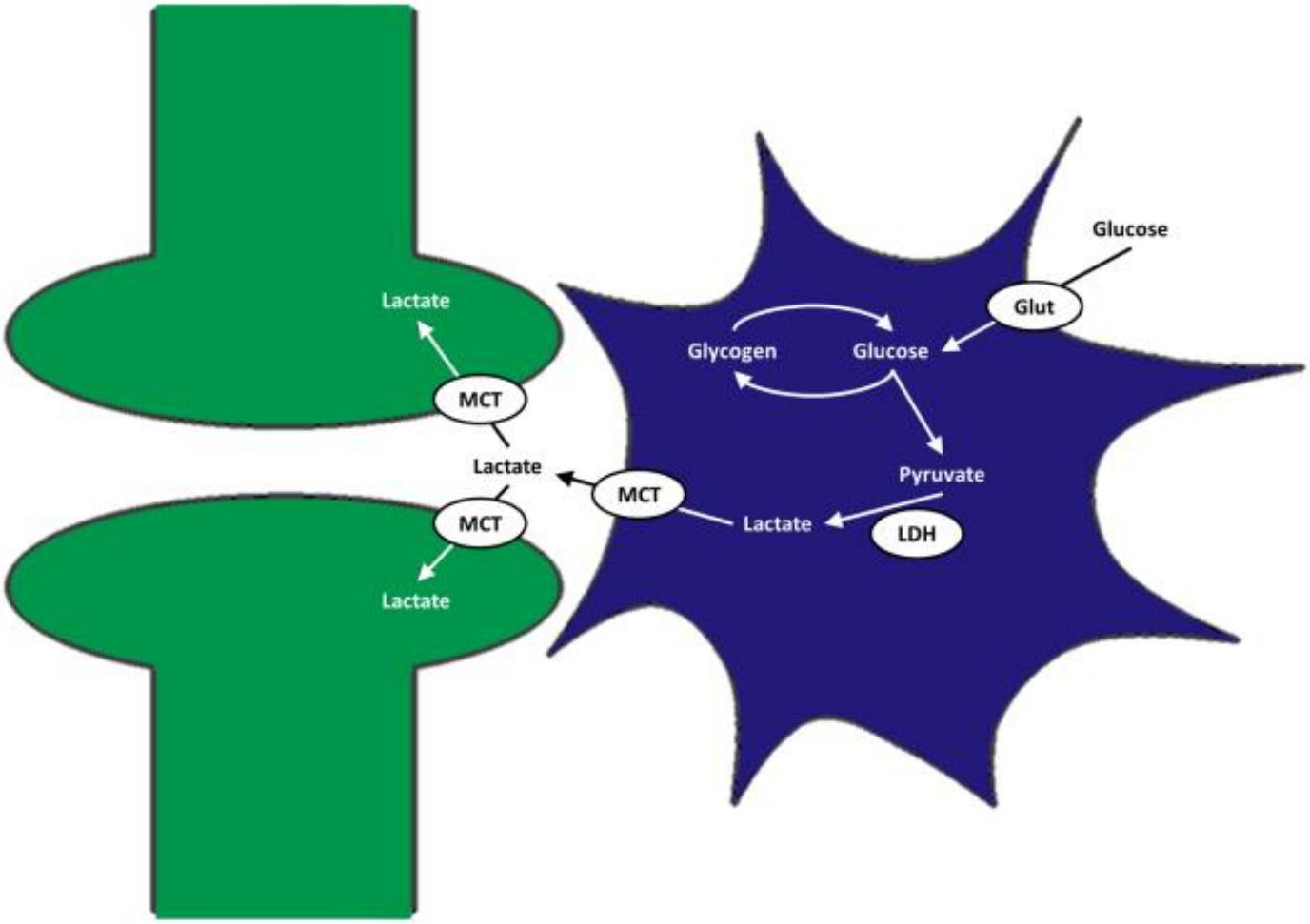

Figure 1.5. The ANLS hypothesis. According to the ANLS hypothesis, glucose is taken up by astrocytes (blue) through Glut transporters. There it can be stored as glycogen or broken down to pyruvate. Pyruvate can then be converted to lactate through the action of LDH, and exported through MCT transporters. Lactate can then be taken up into neurones (green) through MCT transporters, and used as fuel.

exported out of astrocytes to provide neurones with energy is referred to as the astrocyte-neurone lactate shuttle (ANLS) hypothesis (Pellerin and Magistretti, 1994).

1.6.2 Brain glycogen supercompensation

One adaptation of astrocytes to hypoglycaemia and ischemia which has been reported by multiple studies is glycogen supercompensation. Iwabuchi et al showed a decrease in astrocytic glycogen during mild ischemia, *in vitro*, followed by an increase to levels above basal during re-perfusion. They interpret this as one of the mechanisms behind ischemia pre-conditioning. The increase in glycogen storage following a mild ischemic insult would increase the capacity of astrocytes to produce lactate and thus prolong fuelling of neurones during a future, severe ischemic insult (Iwabuchi *et al.*, 2014). This mechanism is thought to also be responsible for maladaptive responses of antecedent hypoglycaemia, leading to impaired CRR and hypoglycaemia unawareness. An adaptive increase in glycogen storage in astrocytes could support neuronal function during hypoglycaemia for prolonged periods, preventing neurones from detecting and responding to the hypoglycaemic episode. Studies have shown increases in brain lactate during hypoglycaemia, which cannot be explained by increases in lactate transport across the blood-brain barrier alone, and thus it is speculated that glycogen supercompensation in astrocytes may be resulting in increased lactate production and export during hypoglycaemia (Herzog *et al.*, 2013). Glycogen supercompensation has been demonstrated by multiple groups in a variety of models. In mice, glycogen supercompensation was shown following acute or recurrent hypoglycaemia, demonstrating that even a single

bout of hypoglycaemia may be enough to induce changes in brain glycogen storage (Canada *et al.*, 2011). In healthy human volunteers, an increase in glycogen mobilisation was reported during hyperinsulimic-hypoglycaemic clamp, compared to hyperinsulimic-euglycaemic clamp. This group further showed an increase in brain glycogen following hypoglycaemia that persisted for at least 80 hours (Oz *et al.*, 2009).

These studies would suggest that following antecedent hypoglycaemic episodes glycogen storage in astrocytes increases. This allows for prolonged lactate release following future hypoglycaemic events, which would prolong neuronal activity. In fact, studies have shown that an increased brain glycogen content prior to hypoglycaemia, preserves neuronal activity for longer during hypoglycaemia (Suh *et al.*, 2007). This increase in lactate release by astrocytes however, may be preventing neurones from responding to hypoglycaemia and thus resulting in defective or delayed CRR. Neurones are able to use lactate as fuel, and some studies even suggest that neurones may have a preference in lactate metabolism. Lactate has a greater capacity to depolarise GE neurones in culture and in slices than glucose (Beall *et al.*, 2012b; Song and Routh, 2005). Furthermore, both GE and GI neurones have been shown to respond to lactate, which reverses low-glucose-induced K_{ATP} channel activation (Song and Routh, 2005).

These studies all support the hypothesis that glycogen supercompensation may occur following RH. However there have been other studies which have failed to show changes in brain glycogen following RH. A study on rats by Herzog et al observed no changes in brain glycogen following acute or RH (Herzog *et al.*,

2008). In a later study in humans by Oz et al, no glycogen supercompensation was seen in T1D and hypoglycaemia unawareness (Oz *et al.*, 2012). Accurately measuring glycogen stores in the brain is difficult, as glycogen storage can be affected by a variety of conditions and drugs such as phenobarbital anaesthesia, which could explain the contradicting results in this case (Nelson *et al.*, 1968).

Study aims

This study aims to investigate the potential involvement of astrocytes in the central detection of hypoglycaemia. Provided that astrocytes respond to a hypoglycaemic stimulus, this study further aims to investigate whether astrocytes undergo adaptive responses following RH, which may underlie or contribute to the impaired CRR observed in diabetes. We hypothesise that in response to a hypoglycaemic stimulus, astrocytes will have an increase in AMPK activity. We further hypothesise that this AMPK activation may lead to changes in eATP. This would lead to changes in purinergic activation in neurones and astrocytes, as well as changes in astrocytic calcium wave propagation. Extracellular lactate would be expected to decrease during a hypoglycaemic stimulus, as less glucose would be available for glycolysis. We speculate that following RH, the AMPK, and as a result, the eATP response to a hypoglycaemic stimulus will be blunted, reflecting the blunted CRR response observed in diabetes following RH. Based on the glycogen supercompensation hypothesis (Canada *et al.*, 2011; Iwabuchi *et al.*, 2014), we speculate that extracellular lactate (eLactate) may not drop to the same extent during a hypoglycaemic stimulus following RH compared to control.

Chapter 2: Materials and Methods

2.1 Materials

2.1.1 Chemicals and equipment

2-mercaptoethanol – Sigma Aldrich

A769662 – Tocris

AICAR – Tocris

Ammonium persulfate (APS) – Sigma Aldrich

ATPLite Luminescence assay system – Perkin Elmer

BAPTA-AM – Abcam

Benzamidine – Sigma Aldrich

Bio-Rad Protein Assay Dye Reagent – BioRad

BioTrace™ Nitrocellulose – VWR

Bovine Serum Albumin (BSA) – Sigma Aldrich

Bovine Serum Albumin Standard (2mg/ml) – Life Technologies

Bromophenol Blue sodium salt (BPB) – Sigma Aldrich

Carbenoxolone disodium – Tocris

D-(+)-Glucose – Sigma Aldrich

Dithiothreitol (DTT) – Melford

DMEM, no glucose – Thermo Fisher

DMEM, no glucose, no phenol red – Thermo Fisher

Dulbecco's Modified Eagle's Medium (DMEM), high glucose, without L-glutamine, without Sodium Pyruvate – Sigma Aldrich

Ethylene glycol-bis(2-aminoethylether)-N,N,N′,N′-tetraacetic acid (EGTA) – Melford

Ethylenediaminetetraacetic acid disodium salt dihydrate (EDTA) – Sigma Aldrich

Fluo-4 Direct Calcium Assay reagent – Thermo Fisher

Glycerol – Sigma Aldrich

Glycine – Melford

Grade 3MM Chr blotting paper – Fisher Scientific

HBSS, without calcium-magnesium-phenol red – Thermo Fisher

HEPES (1M) – Sigma Aldrich

Hyclone Serum – GE Healthcare Bio

Lactic acid (Lactate) – Sigma Aldrich

L-Glutamine (200mM) – Thermo Fisher

L-Lactic Dehydrogenase (LDH) from rabbit muscle – Sigma Aldrich

Metformin – Abcam

Methanol – Sigma Aldrich

N,N,N′,N′-Tetramethylethylenediamine (TEMED) – Sigma Aldrich

Noradrenaline – Abcam

Penicillin-Streptomycin (5,000 U/ml) – Thermo Fisher

Phenylmethanesulfonyl fluoride (PMSF) – Sigma Aldrich

Phosphate Buffered Saline tablets (PBS) – Thermo Fisher

Poly-L-lysine Hydrobromide – Sigma Aldrich

Ponceau S solution – Sigma Aldrich

ProtoGel (30%) Acrylamide – Fisher Scientific

Quinacrine dihydrochloride – Sigma Aldrich

SeeBlue Plus2 Pre-stained Protein Standard – Thermo Fisher

Semicarbazide – Sigma Aldrich

Sodium Chloride (NaCl) – Sigma Aldrich

Sodium Dodecyl sulphate (SDS) – Melford

Sodium Fluoride (NaF) – Sigma Aldrich

Sodium Hydroxide – Sigma Aldrich

Sodium Orthovanadate – Sigma Aldrich

Sodium Pyrophosphate Tetrabasic Decahydrate (NaPPi) – Sigma Aldrich

Sucrose – Melford

Sulfuric Acid H_2SO_4 – Sigma Aldrich

Tris(hydroxymethyl) aminomethane (TRIS) – Melford

TritonX-100 – VWR

Trypsin (2.5%), no phenol red – Thermo Fisher

Trypsin-EDTA (0.05%), phenol red – Thermo Fisher

TWEEN 20 – Sigma Aldrich

β-Nicotinamide adenine dinucleotide sodium salt (NAD) – Sigma Aldrich

2.1.2 Antibodies

ACTB Mouse Monoclonal – Protein Tech (60008-1-Ig)

Goat Polyclonal anti-rabbit – Rockland (ROCK611-132-122)

Donkey anti-sheep – Life Technologies (A21102)

Goat anti-mouse – Life Technologies (A21057)

pT172 AMPK – Cell Signalling (2535L)

pS15 Glycogen phosphorylase – DSTT

pS79 Acetyl CoA carboxylase (ACC) – Cell Signalling (3661S)

2.2 Methods

2.2.1 Cell culture

Table 1: Media compositions

Media	Components
Stock media	High glucose (25 mM) DMEM, 10% (v/v) Hyclone serum, 2% (v/v) Pen/Strep, 4% (v/v) L-glutamine
Experimental media	Glucose-free DMEM (11966), 10% (v/v) Hyclone serum, 2% (v/v) Pen/Strep, 2% (v/v) L-glutamine, 2.5-7.5 mM glucose
Serum free (SF) media	Glucose-free DMEM (11966), 0.1-10 mM glucose
Phenol red-free serum-free (PrF/SF) media	Glucose-free, phenol red free DMEM, 2.5 mM Glucose, 25 mM HEPES
Normal saline	135 mM NaCl, 5 mM KCl, 1 mM $MgCl_2$, 1 mM $CaCl_2$, 10 mM HEPES, 2.5 mM glucose
Calcium-free saline	135 mM NaCl, 5 mM KCl, 1 mM $MgCl_2$, 3 mM Mannitol, 10 mM HEPES, 2.5 mM glucose

2.2.1.1 Neonatal primary astrocyte isolation and culturing

T75 flasks were coated with 10 µg/ml Poly-L-lysine (PLL) and incubated for 1 hour before washing with PBS. Primary astrocyte cultures were prepared from mice at P1-5. The mice were decapitated, and the skull opened using a scalpel. The meninges were removed and the cortices and hypothalamus were dissected from the brain tissue and minced separately in HBSS. The cortices and hypothalamus were then transferred to 5ml trypsin-EDTA (0.5% w/v) and incubated at 37^{o}C for 20min, shaking every 5min. The tissue was then centrifuged at 1,000rpm for 5min. Excess trypsin was removed and the tissue re-dissolved in 25mM glucose stock media, with 10% (v/v) serum before transferring through a cell strainer into the PLL-coated flasks. The cells were

cultured in 25mM stock media, replacing the media every 2-3 days until ready to plate for experiments.

2.2.1.2 Culturing of U373 MG cells

Cells were cultured in T75 or T175 flasks in 15 or 25ml of 25mM glucose stock media respectively, passaging them every 3-4 days up to no more than p35.

2.2.1.3 Plating cells for experiments

For experiments, cells were plated in 2.5-7.5mM glucose DMEM 1-2 days before experimentation. For primary astrocyte cultures, the dishes or plates were coated with PLL prior to plating. To delay cell attachment and promote a more even cell distribution, the cells were left in the hood for 30-60 minutes before placing in the incubator. Before experiments, the cells were serum starved using 2.5mM glucose serum free (SF) media for 2hr.

2.2.1.4 Collection of supernatants and protein extraction

At the end of treatment, media samples were collected from each dish, transferred to microtubes and kept on ice. These samples were used for extracellular assays or stored at -20^{o}C for further analysis. The cells were lysed using lysis buffer and scraped on ice. The cell lysates were collected into

microtubes and centrifuged at 14,000rpm at 4^{o}C for 15min. Protein concentration was determined by the method of Bradford (Bradford, 1976) and retained for Western blotting analysis.

5 x Lysis Buffer:

125 mM Tris HCl (pH 7.5)

250 mM NaF

0.5 M NaCl

5 mM EDTA

25 mM EGTA

5% (v/v) Triton X 100

50 mM NaPPi

Added fresh on the day to 1 x Lysis buffer:

92 mg/mL Sucrose

1 mM PMSF

1 mM Benzamidine

1 mM Sodium Orthovanadate

0.1% (v/v) 2-Mercaptoethanol

Table 2: Plate seeding protocol

	Plated one day before experiment		Plated two days before experiment	
	U373	Primary astrocytes	U373	Primary astrocytes
96-well plate	20,000 cells	20,000 cells	N/A	N/A
4cm dish (glass-bottomed)	N/A	N/A	80,000 cells	80,000 cells
6-well plate	150,000 cells	150,000 cells	N/A	N/A
6cm dish	450,000 cells	450,000 cells	300,000 cells	450,000 cells
10cm dish	1,000,000 cells	N/A	N/A	N/A

2.2.1.5 Recurrent Hypoglycaemia

U373 cells were plated at 200,000 cells per dish in twelve 6cm dishes the day before experimentation in 7.5mM glucose media with serum. On day one, the cells were serum starved in 3ml 2.5 mM glucose serum free media for 2 hours followed by 2 hours of 0.1mM or 2.5mM glucose in 3ml serum free media for the hypoglycemic vs euglycemic stimulus. The cells were then recovered in 3ml 5mM glucose serum free media for 2 hours before repeating the hypoglycemic vs euglycaemic stimulation for two hours. The cells were then recovered overnight in 5ml 5mM glucose serum free media. The same procedure was repeated on day two, omitting the first 2 hour serum starving step. After the first recovery, the cells were split into three sets of four containing two dishes that had been exposed to RH and two that had not. Each pair from these was

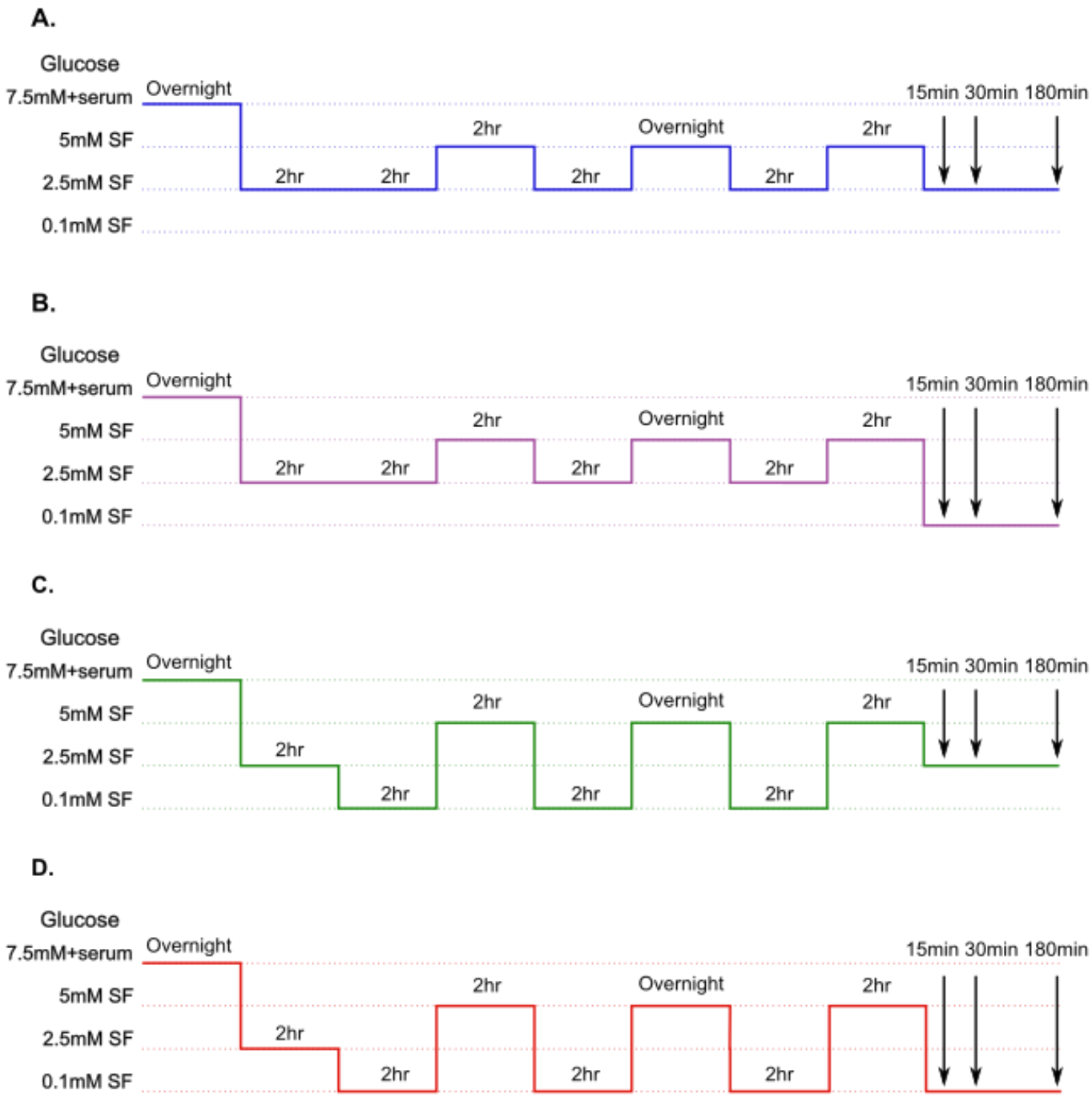

Figure 2.1. 2 day recurrent hypoglycaemia model. A. Diagrammatic representation of the 2-day model in U373 cells for the control, acute hypoglycaemia (**B.**), antecedent hypoglycaemia (**C.**), and recurrent hypoglycaemia (**D.**) groups.

exposed to 2.5 or 0.1mM glucose for 15, 30, or 180 minutes before collecting the media and lysate samples (see Figure 2.1).

2.2.2 Determining protein concentration

0-5µl of 1mg/mL BSA standard was used in triplicates in a clear 96-well plate for the protein standards, adding 1µl of the lysis buffer to each. 1µl of the sample lysates was added/well in triplicates and 200µl of Bradford reagent was added to each well. The plate was shaken for 5 minutes before reading at 595nm.

2.2.3 Immunoblotting

The cell lysates were prepared in sample buffer (see table 3) containing DTT (100mM) or β-Mercaptoethanol (0.1% v/v). 10µg of lysate was loaded per well and run initially at 90-100mV for 15-20 minutes to ensure optimal protein migration, and then at 150mV for a further ~90 minutes to separate the proteins. The proteins were transferred onto Nitrocellulose membranes using a wet transfer, and transferred at 100mV for 75min. The membranes were then blocked in 5-10% (w/v) dried skimmed milk, or 1-2.5% (w/v) BSA (made up in 1-2.5% w/v BSA in TBS/TWEEN) for 1 hour and placed in primary antibody (made up in 1-2.5% w/v BSA in TBS/TWEEN) overnight (see table 5). The primary antibody was then removed and the membranes washed 6 times in TBS/TWEEN changing the wash every 5-10 minutes before placing in the secondary antibody (made up in 1-2.5% w/v BSA in TBS/TWEEN) for 60min.

The membranes were then washed 6 times in TBS/TWEEN changing the wash every 10 minutes and scanned using the Licor Odyssey CLx.

Table 3: Western blot buffer components

Buffer	Recipe
4x Sample Buffer	125 mM Tris/HCl (pH 6.8), 4% (w/v) SDS, 20% (v/v) Glycerol, BPB, made up in dH_2O
Transfer buffer	20% (v/v) Methanol, 0.048 M Tris, 0.039 M Glycine, made up in dH_2O
10x Running buffer	0.25 M Tris, 1.92M Glycine, 1% (w/v) SDS
TBS/TWEEN	152 mM NaCl, 20 mM TRIS/HCl (pH 7.4), 0.05% (v/v) TWEEN 20 made up in dH_2O

Table 4: Gel-making protocol

2 x Gels	Stacking (4%)	7%	10%
d.H2O	2.8 ml	5.28 ml	4.15 ml
1.5 M Tris (pH 8.8)		3.15 ml	3.15 ml
0.5 M Tris (pH 6.8)	1.25 ml		
30% Acrylamide	850 µl	2.63 ml	3.75 ml
10% (w/v) SDS	50 µl	110 µl	110 µl
20% (w/v) APS	50 µl	55.4 µl	55.4 µl
TEMED	5.35 µl	11 µl	11 µl

Table 5: Antibody dilutions and incubation conditions

Antibody	Dilution	Incubation	2^{ary} antibody	Dilution	Incubation
pT172 AMPK	1:1,000	Overnight Cold room	Anti-Rabbit	1:10,000	1hr RT
pS79 ACC	1:1,000	Overnight Cold room			
β-Actin	1:5,000	Overnight Cold room			
pS15 Glycogen phosphorylase	1 µg/ml	Overnight Cold room	Anti-Sheep	1:5,000	1hr RT
ACTB Mouse Monoclonal	1:10,000	1hr RT	Anti-Mouse	1:10,000	1hr RT

2.2.4 ATP assay

For determining extracellular, intracellular or total ATP concentration, the ATPlite assay kit was used as described below.

2.2.4.1 Determining extracellular ATP concentration

For determining extracellular ATP concentration 80µl of conditioned media (CM), 40µl Mammalian Cell Lysis Solution, and 40µl reconstituted ATP Substrate Solution were used in triplicates in a black 96-well plate. The standard curve was prepared in triplicates in 80µl of the media used during the treatment.

2.2.4.2 Determining intracellular ATP concentration

For determining intracellular ATP concentration, cells were plated in a black 96-well plate and treated in triplicates. At the end of the treatment the media was aspirated and 40µl Mammalian Cell Lysis Solution and 80µl of the media used to treat the cells was added to the wells. 40µl reconstituted ATP Substrate Solution was used for this reaction.

2.2.4.3 Determining total ATP concentration

For determining total ATP concentration, cells were plated in a black 96-well plate and treated in 100µl of the treatment media in triplicates. At the end of treatment 50µl Mammalian Cell Lysis Solution was added to the wells. 50µl of reconstituted Substrate Solution was used for this procedure.

2.2.5 Determining extracellular lactate concentration

For determining extracellular lactate concentration an assay based on the reaction below was used, measuring changes in absorbance from the production of NADH:

$$\text{Lactate} + \text{NAD}^{+} \xrightarrow{\text{LDH}} \text{Pyruvate} + \text{NADH}$$

The lactate assay reaction buffer was prepared as shown below:

Reaction Buffer pH 10 (100ml in dH_2O):

1.5g Glycine

2.23g Semicarbazide

Added fresh on the day (for 10ml):

0.02152mg NAD

50µl LDH

The following reaction was prepared in a clear 96-well plate (see table 6), incubated at 37^{o}C for 1 hour shaking every 10 minutes for 5 minutes and the absorbance read at 350/450:

Table 6: Plate setup for extracellular lactate assay

	Lactate	Media	CM	Reaction Buffer
0 nmol Standard	10µl of 0mM	90µl	-	100µl
10 nmol Standard	10µl of 1mM	90µl	-	100µl
20 nmol Standard	10µl of 2mM	90µl	-	100µl
30 nmol Standard	10µl of 3mM	90µl	-	100µl
40 nmol Standard	10µl of 4mM	90µl	-	100µl
50 nmol Standard	10µl of 5mM	90µl	-	100µl
Samples	-	-	100µl	100µl

2.2.6 Intracellular Ca^{2+} assay

Cells were plated in a quarter of a clear 96-well plate in 7.5mM glucose experimental media as described above. After serum starving for 2hr, the media was replaced with Fluo 4 direct calcium dye made up in phenol red-free DMEM (25mMHEPES, 2.5mM glucose) and incubated for 1 hour at 37^{o}C before reading in the PheraStar. Treatment was injected at t=30s. Each treatment group was done in triplicate or quadruplicate. Relative fluorescence was calculating by dividing each value by the baseline reading (t=0s) of the corresponding well and then calculating the mean of the triplicates or quadruplicates for each treatment group at each time point measured. The total area under the curve for each treatment group was calculated setting the baseline to 1.

2.2.7 Quinacrine Imaging

Protocol 1

80,000 cells or 100,000 cells of U373 or mouse primary astrocytes respectively were plated per 4cm glass-bottomed dishes two days before imaging in 25mM glucose stock media. The day before the experiment the media was replaced with 7.5mM glucose experimental media. The cells were serum starved in 2.5mM SF media for 2hr, before loading with 1µM Quinacrine made up in 2.5mM glucose 25mM HEPES buffered PrF/SF media for 15 minutes at room temperature. The dye was washed off and the cells incubated at 37^{o}C in 750µl 2.5mM glucose 25mM HEPES buffered PrF/SF media for 15min. The cells were

imaged using a confocal microscope, capturing one image per minute. At t=10min, 750µl of treatment were added.

Protocol 2

The procedure above was used, using 1.4ml media after washing off the quinacrine, and 100µl for treatment instead, to minimise shear stress on the cells.

2.3 Statistical analysis

All data-sets are shown as mean with standard error unless otherwise stated. Values for western blots were normalised to actin and then to control, and were analysed using a one sample t-test unless otherwise stated. All other data-sets were analysed using a 1-way ANOVA or 2-way ANOVA with Bonferroni's Multiple Comparison test. Significance is measured against control, unless stated otherwise, and is indicated as follows:

* $p \leq 0.05$, ** $p \leq 0.01$, *** $p \leq 0.001$

Chapter 3: Results

3.1 Hypoglycaemia detection in astrocytes

Introduction

Hypoglycaemia has been a known side-effect of insulin treatment for nearly a century (Banting *et al.*, 1923); however, no effective preventative medication has yet been developed. There has been a multitude of studies showing the involvement of the central nervous system in glucosensing and the CRR to hypoglycaemia (Beall *et al.*, 2012a) but the exact mechanism behind impaired CRR is still not fully understood. One enzyme that has been shown to play an important part in the response to hypoglycaemia and glucose regulation is AMP-activated protein kinase (AMPK).

Activation of AMPK in the VMH was found to result in an increase in glucose production during hypoglycaemia (McCrimmon *et al.*, 2006). The hypothalamus is a key regulator of whole body homeostasis, and is largely involved in the central response to changes in glucose (Allard *et al.*, 2013; Guillod-Maximin *et al.*, 2004). Specialised glucosensing neurons, found both peripherally and centrally, are highly expressed in the hypothalamus. Both glucose-excited and glucose-inhibited neurones are expressed, which respond to changes in glucose (Oomura *et al.*, 1969). Increasing amounts of evidence implicate astrocytes in central glucosensing and the response to both hyper and hypoglycaemia (Lam *et al.*, 2005; Marty *et al.*, 2005; Taib *et al.*, 2013).

Guillod-Maximin et al showed that carotid artery glucose injection increases astrocyte activation in both the paraventricular nucleus (PVN) and ARC of the

hypothalamus. They further showed that inhibiting astrocytes in the ARC supressed the glucose-induced insulin secretion (Guillod-Maximin *et al.*, 2004). Similarly, Allard et al showed that injection of glucose into the carotid artery stimulated the hypothalamo-pancreatic axis through a process requiring the conversion of glucose to lactate as well as pyruvate metabolism, suggesting the involvement of astrocytes (Allard *et al.*, 2013). Astrocytes also play a crucial role in the response to hypoglycaemia. For example, Marty et al showed that inactivating the GLUT2 gene impaired the glucagon response to hypoglycaemia, which was restored when GLUT2 was re-expressed specifically in astrocytes (Marty *et al.*, 2005).

Astrocytes release a variety of gliotransmitters that can modulate neuronal activity. One of the gliotransmitters that has been implicated in diabetes is ATP. ATP is the universal “danger signal” and acts as a pro-inflammatory mediator (Idzko *et al.*, 2014). It also acts as a fast excitatory neurotransmitter, mediating short-term as well as long-term effects. Changes in the purinergic system in the hippocampus of STZ rats have been observed, including changes in purinergic receptor expression, ATP metabolism and levels of extracellular ATP (Duarte *et al.*, 2007). Fasting or hyperglycaemia also result in changes in astrocytic connexin expression (Allard *et al.*, 2014; Gandhi *et al.*, 2010) which is a membrane channel permeable to small molecules such as ATP. Based on these observations, we hypothesised that changes in extracellular ATP could play a part in the central regulation of glucose homeostasis and the adaptations following repeated episodes of hypoglycaemia.

Another astrocyte-derived gliotransmitter that plays an important part in a variety of neuronal pathways is lactate. Astrocytes can produce lactate from glucose taken up from the blood, or from glycogen stores, and provide it to neurones during energy stress as described by the astrocyte-neuron lactate hypothesis (Pellerin and Magistretti, 1994). There is strong evidence that lactate plays an important role in ischaemia pre-conditioning and the counter-regulatory response to hypoglycaemia. For example, during ischemia pre-conditioning, Iwabuchi et al showed that brain glycogen content fell, followed by a further increase after re-perfusion, referred to as glycogen supercompensation (Iwabuchi *et al.*, 2014). This increase in glycogen storage in astrocytes may be part of the mechanism behind the protective ability of ischemia pre-conditioning to further ischemic insult. Increasing glycogen stores enables astrocytes to provide neurones with lactate for a longer period of time and improve viability during glucose depletion. An increase in brain glycogen content in mice (Canada *et al.*, 2011), rats (Choi *et al.*, 2003) and humans (Oz *et al.*, 2009) following acute or recurrent hypoglycaemia has also been shown, suggesting an adaptive mechanism to protect against future hypoglycaemic insults. In support of this, Suh et al showed a prolonged maintenance in neuronal activity during hypoglycaemia in rats with higher brain glycogen content at the start of hypoglycaemia (Suh *et al.*, 2007). Lactate administration in the hypothalamus blunts the response to hypoglycaemia in rats (Borg *et al.*, 2003). Taken together, these data suggest that an adaptive increased lactate release during hypoglycaemia may be responsible for the blunted counter regulatory response following recurrent hypoglycaemia.

The aim of this study was to characterise astrocytic response to a hypoglycaemic stimulus, and any potential adaptations following repeated hypoglycaemic stimuli.

3.1.1 Acute hypoglycaemia increases AMPK and ACC phosphorylation and decreases extracellular lactate in astrocytes

To determine whether astrocytes detect and respond to hypoglycaemia, U373 cells were exposed to physiological (2.5mM) or low (0.1mM) glucose levels for 30 minutes. *In vivo* astrocytes remain in distinctly separate areas from each other, with very little overlap of processes (Bushong *et al.*, 2002), however, they would also be receiving input from other cell types in their surrounding environment (Gundersen *et al.*, 2015). To ensure we observe any significant differences caused by too much or too little interaction between our cells, this experiment was carried out at three different seeding densities (SD); low (150,000 cells/dish), medium (450,000 cells/dish) and high (1,000,000 cells/dish), plated in round, 6 cm dishes the day before the experiment. AMPK phosphorylation was measured through densitometric analysis of Western blots as an indicator of AMPK activation. Acetyl co-A carboxylase (ACC) phosphorylation was also measured using the same method. ACC is a downstream target of AMPK, and thus changes in its phosphorylation serve as indications of changes in AMPK activity. Extracellular ATP (eATP) from the CM was measured using a luminescence, plate-based assay, and eLactate was measured using an enzymatic, absorbance, plate-based assay, to determine whether astrocytic function was altered during an acute hypoglycaemic stimulus.

A significant increase in pAMPK was observed following low glucose in all SD groups (1.6, 2.4 and 2.9-fold in the low, medium and high respectively; Figure 3.1A, B; n=5; $p<0.01$). A significant increase in phospho ACC (pACC) was also observed (2.4, 2.9 and 3.3-fold in the low, medium and high SD groups

respectively; Figure 3.1A, C; n=5; p<0.001). There was no significant change in absolute eATP during low glucose in any of the groups; However, when normalised to protein content, there was a significant decrease in eATP between the three SD groups at euglycaemic glucose, with eATP being 2 and 6 times lower in the medium and high SD groups, respectively, when compared to the low SD group (Figure 3.1D, E; n=5; p<0.001). A 1.6-fold decrease in eLactate from 153.4 ± 18.28 to 95.78 ± 15.39 nmol/mg was measured in the high SD group following low glucose (Figure 3.1F; p<0.05; unpaired t test). In order to observe whether the decrease in eLactate was a direct result of decreased glucose availability for lactate production, eLactate, in this instance, was normalised to glucose availability. After normalising eLactate to glucose availability we see a 29.2, 21.2 and 15.6-fold increase in eLactate/mol of glucose available during a hypoglycaemic stimulus (Figure 3.1G; n=5; p<0.001; unpaired t test).

These data indicate that the U373 cells detect and respond to a hypoglycaemic stimulus, seen through changes in AMPK activity. The hypoglycaemic stimulus also caused a decrease in eLactate, which was not proportional to the decrease in glucose availability, and thus indicates an increased efficiency in lactate production and export per mol of glucose available. Increasing cell SD was shown to result in an unexpected decrease in eATP, which may be a result of increased eATPase activity. This means astrocytic eATP cannot be normalised to protein content in the rest of this work.

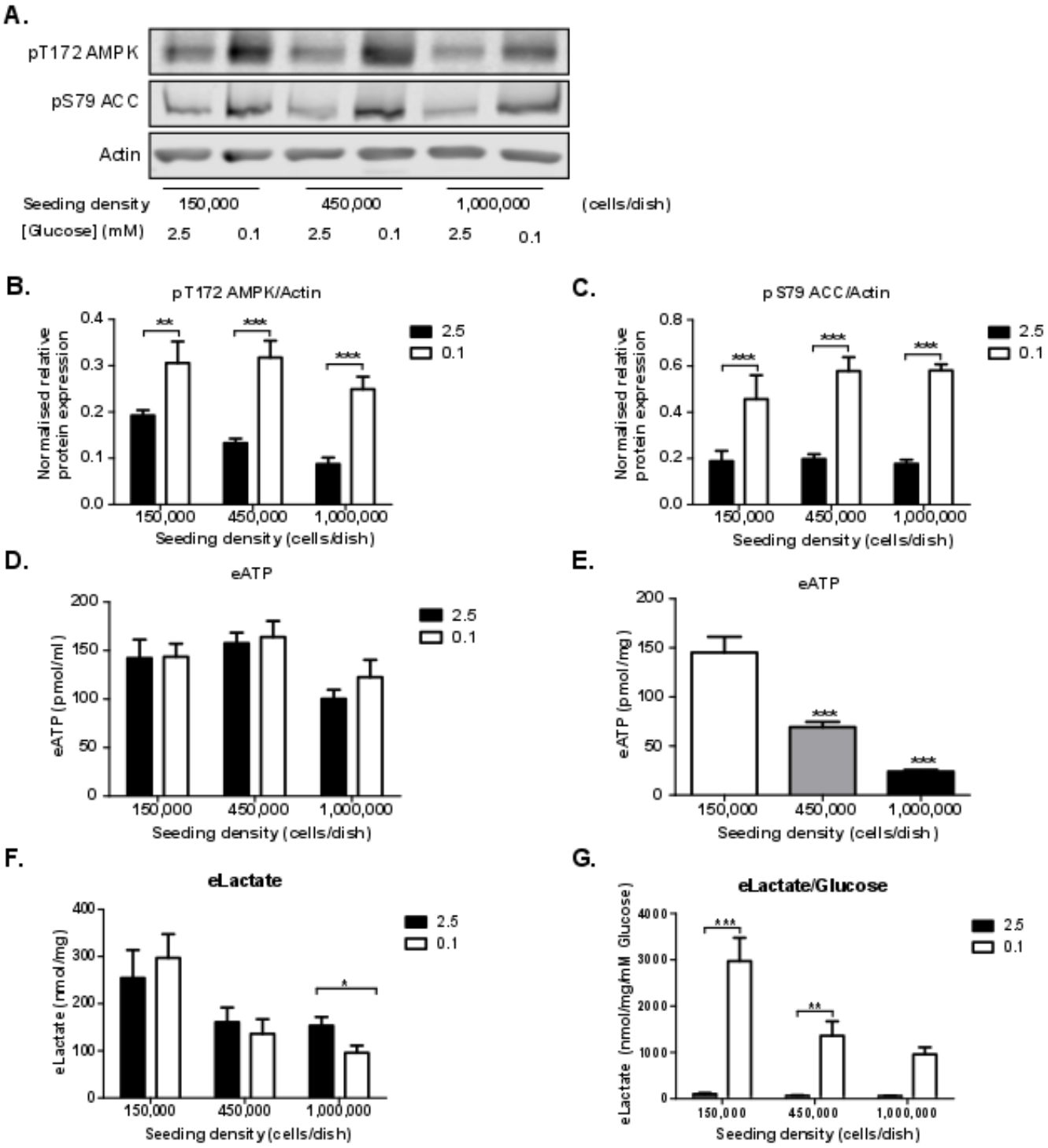

Figure 3.1. Low glucose increases pAMPK, pACC and lactate production. A. Representative Western blots of U373 lysates of phospho-AMPK and phospho-ACC following 30min of a euglucaemic (2.5mM) or hypoglycaemic (0.1mM) stimulus. **B.** Fold change in AMPK phosphorylation in U373 lysates (n=5). **C.** Fold change in ACC phosphorylation in U373 lysates (n=5). **D.** Extracellular ATP following treatment in U373 cells (n=5). **E.** Extracellular ATP normalised to protein content (n=5). **F.** Extracellular lactate following treatment in U373 cells (n=5). **G.** Extracellular lactate normalised to glucose concentration (n=5). **B-D.** & **F-G.** 2-way ANOVA with Bonferroni's multiple comparison test. **E.** 1-way ANOVA with Boneferroni's multiple comparison test. ***** p≤0.05, ****** p≤0.01, ******* p≤0.001

3.1.2 Noradrenaline increased extracellular lactate in both euglycaemic and hypoglycaemic conditions

During hypoglycaemia, noradrenaline (NA) is released into hypothalamic areas by the hindbrain (Palkovits *et al.*, 1980). To test whether the U373 response to low glucose is enhanced by NA, cells were plated at 450,000 cells/dish in round, 6 cm dishes the day before the experiment, and were exposed to a 30 minute hypoglycaemic stimulus with or without the addition of NA (50µM). There was a significant increase in pAMPK in cells exposed to low glucose (2.0-fold ± 0.2) when compared to the euglycaemic group ($p<0.01$). An increase in AMPK phosphorylation was also observed in U373 cells exposed to a hypoglycaemic stimulus +NA compared to euglycaemic conditions +NA, but did not reach significance. There was no significant change in pAMPK when comparing the vehicle-treated or NA-treated groups in either euglycaemic or hypoglycaemic conditions (Figure 3.2B; n=5). As observed previously (Figure 3.1A), there was also a significant increase in pACC in the vehicle-treated group in low glucose when compared to the control group (2.8-fold ± 0.4; $p<0.01$). A similar increase was observed in the NA-treated group when comparing the low glucose group to the euglycaemic group (2.1-fold ± 0.2; $p<0.05$). There was no significant difference in pACC between the vehicle-treated and NA-treated groups in either euglycaemic or hypoglycaemic conditions (Figure 3.2C; n=5). There was no significant difference in phospho-GP (pGP) or eATP between any of the groups (Figure 3.2D&E). There was a significant increase in eLactate from 178.8 ± 21.09 nmol/mg in the vehicle-treated group, to 342.4 ± 32.09 nmol/mg in the NA-treated group in euglycaemic conditions and from 107.2 ± 11.85 nmol/mg in the control group, to 308.2 ± 49.87 nmol/mg in the NA-treated group in hypoglycaemic conditions (Figure 3.2F; n=6; $p<0.01$).

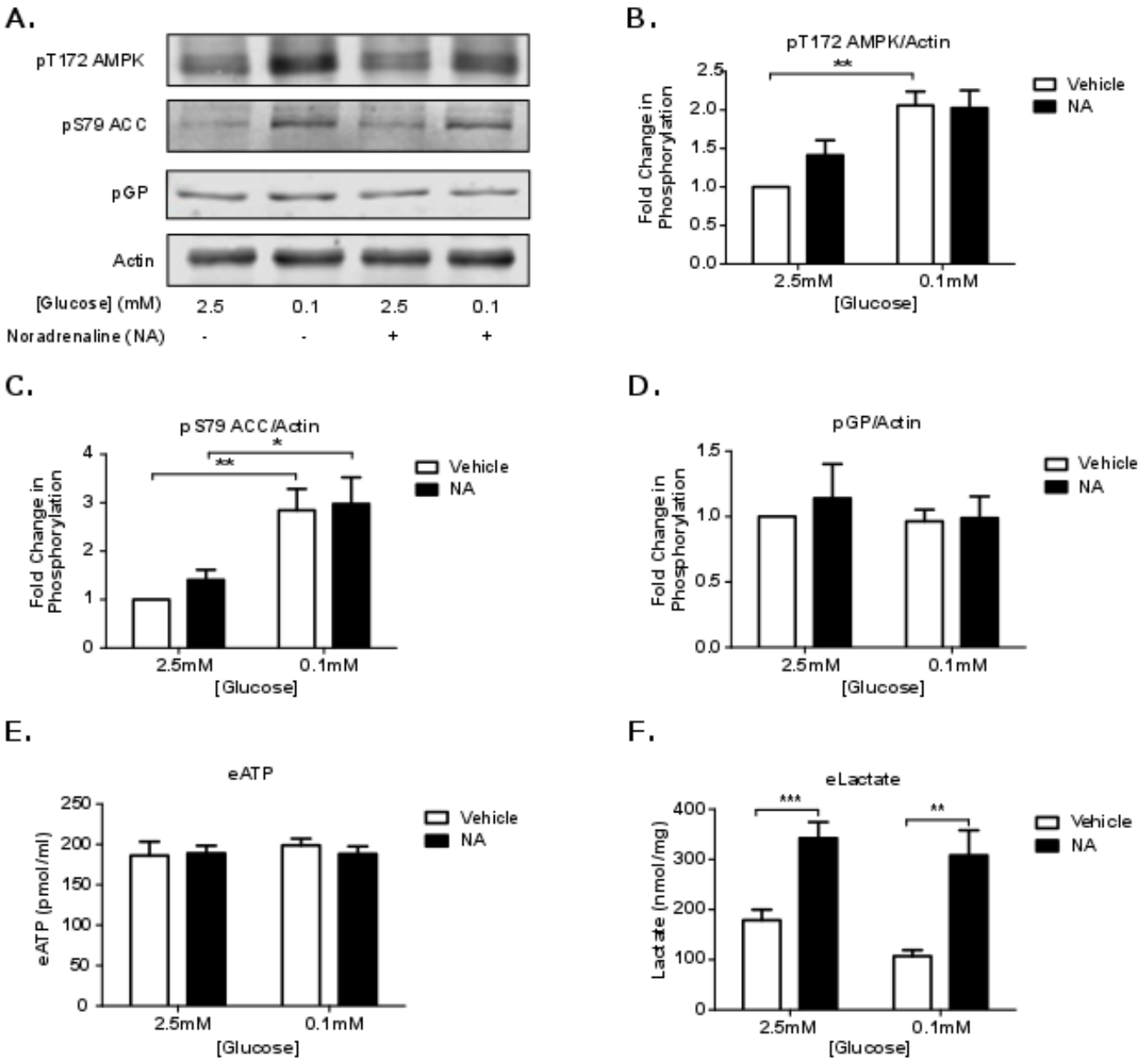

Figure 3.2. NA enhances lactate production during hypoglycaemic stimulus. A. Representative Western blots of pAMPK, pACC, pGP and Actin of lysates of U373 cells treated with noradrenaline (50µM) for 30min at 2.5 or 0.1mM glucose. **B.** Fold change in AMPK phosphorylation at the end of the 30min treatment (n=5). **C.** Fold change in ACC phosphorylation at the end of the 30min treatment (n=5). **D.** Fold change in GP phosphorylation at the end of the 30min treatment (n=5). **E.** Extracellular ATP at the end of the 30min treatment (n=6). **F.** Extracellular lactate at the end of the 30min treatment (n=6). **B-F.** 2-way ANOVA with Bonferroni's multiple comparison test. ***** p≤0.05, ****** p≤0.01, ******* p≤0.001

NA had no effect on AMPK, ACC or GP phosphorylation or eATP on either euglycaemic or hypoglycaemic conditions. However, there was a nearly 2-fold increase in eLactate in normal glucose, and nearly 3-fold increase in low glucose when the cells were treated with NA. This increase in eLactate suggests that even though glycogenolysis appears to be increased during hypoglycaemia, it retains capacity to be further activated by NA.

3.1.3 2-day antecedent hypoglycaemia blunts the AMPK response to further hypoglycaemia

To investigate potential adaptive changes in astrocytes following recurrent episodes of hypoglycaemia, astrocytes were exposed to a 2-day recurrent hypoglycaemia model (Figure 2.1). U373 cells were plated the day before the start of the experiment at 250,000 cells/dish, in round 6 cm dishes. In this study, changes in AMPK and ACC phosphorylation were measured as well as changes in eATP. Changes in pGP and eLactate were also measured to investigate any changes in glycogenolysis. The results are shown as fold change from the 2.5mM glucose control for each group with standard error. The acute hypoglycaemia group (H) was normalised to the control group (C), and the recurrent hypoglycaemia group (RH) to the antecedent hypoglycaemia group (AH).

In lysates of U373 cells exposed to the 2-day recurrent hypoglycaemia model, pAMPK after a 15 minute hypoglycaemic stimulus (0.1mM glucose) increased 2.0-fold ± 0.3 in the H group and 1.4-fold (± 0.1) in the RH group compared to their corresponding control (2.5mM glucose; $p<0.01$). This was significantly

different between the two groups (0.6-fold ± 0.3; Figure 3.3.1B; n=7; $p<0.05$). ACC phosphorylation increased 1.9-fold ± 0.2 in the H group and 1.6-fold ± 0.1 in the RH, which was not significant between groups (Figure 3.3.1C; n=9; $p<0.01$). Glycogen phosphorylase phosphorylation did not significantly change (Figure 3.3.1D), neither did eATP (Figure 3.3.1E) or eLactate (Figure 3.3.1F).

Following a 30 minute hypoglycaemic stimulus, pAMPK remained elevated at 1.9-fold ± 0.2 in the H group and 1.5-fold ± 0.2 in the RH group which was not significantly different between groups (Figure 3.3.2B; n=7; $p<0.05$). ACC phosphorylation was significantly increased to 2.9 ± 0.4 in the H group, and 3.5 ± 0.4 in the RH group which was not significant between groups (Figure 3.3.2C; n=9; $p<0.01$). There was no significant change in pGP for either group (Figure 3.3.2D). eATP did not change significantly when comparing H or RH to their respective controls (C and AH). However, the response in the H group was significantly higher than in the RH (0.4 ± 0.2; Figure 3.3.2E; n=8; $p<0.05$). Extracellular lactate was significantly reduced in the RH group to 0.8-fold ± 0.03 compared to its control (Figure 3.3.2F; n=7; $p<0.001$).

Following a 180 minute hypoglycaemic stimulus, pAMPK was significantly increased to 2.6-fold ± 0.3 and 2.1-fold ± 0.1 in the H and RH groups respectively (Figure 3.3.3B; n=6; $p<0.01$). ACC phosphorylation was significantly increased to 6.7-fold ± 1.0 and 6.8-fold ± 1.0 in the H and RH groups respectively (Figure 3.3.3C; n=9; $p<0.01$). GP phosphorylation was also significantly increased to 1.6-fold ± 0.1 and 1.6-fold ± 0.2 in the H and RH groups (Figure 3.3.3D; n=6; $p<0.05$). Extracellular ATP did not significantly

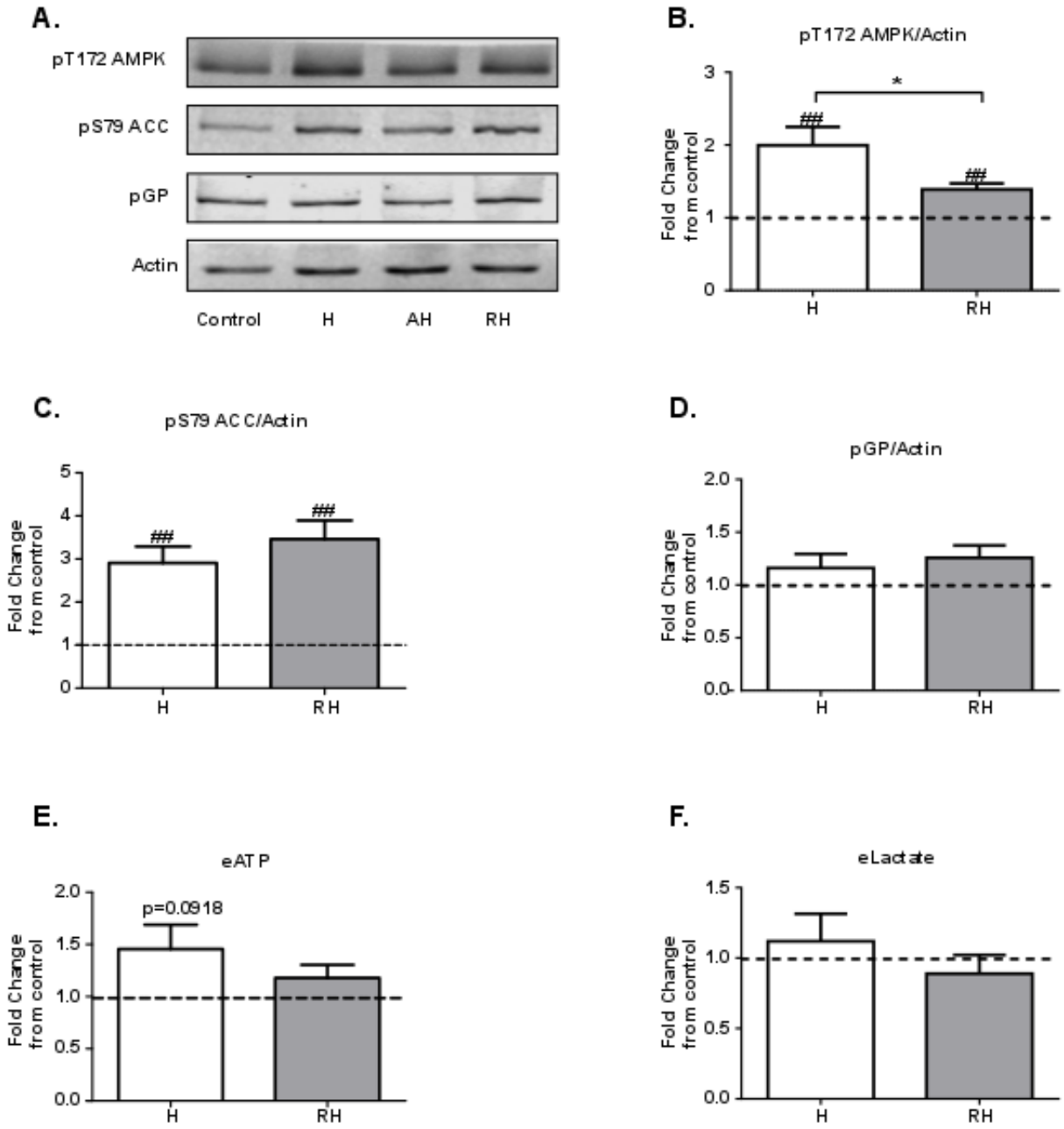

Figure 3.3.1. Recurrent hypoglycaemia blunts the pAMPK response to further hypoglycaemia at 15min. A. Representative Western blots of pAMPK, pACC, pGP and Actin of lysates of U373 cells exposed to three 2hr bouts of euglycaemia or hypoglycaemia over two days, followed by 15min of euglycaemia (2.5mM glucose) or hypoglycaemia (0.1mM glucose). **B.** Fold change in AMPK phosphorylation (n=7). **C.** Fold change in ACC phosphorylation (n=9). **D.** Fold change in GP phosphorylation (n=7). **E.** Extracellular ATP at the end of the final 15min hypoglycaemic stimulus (n=8). **F.** Extracellular lactate at the end of the final 15min hypoglycaemic stimulus (n=8). **B-F. *** p≤0.05 Comparing H to RH using an unpaired t test. ## p≤0.01, ### p≤0.001 Comparing each group to their corresponding control to which they have been normalised, using a one sample t test (hypothetical value of 1).

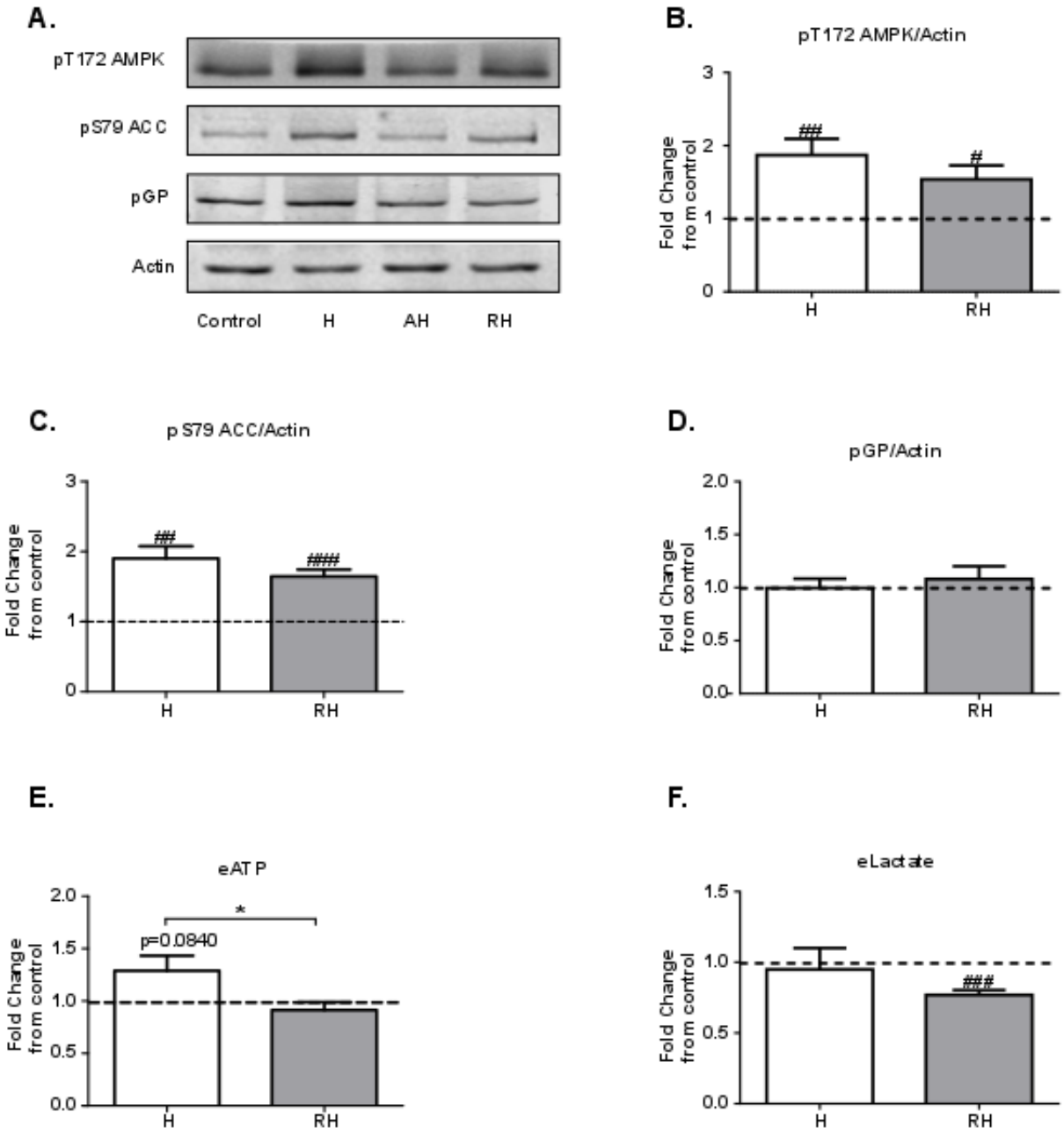

Figure 3.3.2. Recurrent hypoglycaemia blunts the pAMPK response to further hypoglycaemia at 30min. A. Representative Western blots of pAMPK, pACC, pGP and Actin of lysates of U373 cells exposed to three 2hr bouts of euglycaemia or hypoglycaemia over two days, followed by 30min of euglycaemia (2.5mM glucose) or hypoglycaemia (0.1mM glucose). **B.** Fold change in AMPK phosphorylation (n=7). **C.** Fold change in ACC phosphorylation (n=9). **D.** Fold change in GP phosphorylation (n=7). **E.** Extracellular ATP at the end of the final 30min hypoglycaemic stimulus (n=8). **F.** Extracellular lactate at the end of the final 30min hypoglycaemic stimulus (n=7). **B-F. *** p≤0.05 Comparing H to RH using an unpaired t test. # p≤0.05, ## p≤0.01, ### p≤0.001 Comparing each group to their corresponding control to which they have been normalised, using a one sample t test (hypothetical value of 1).

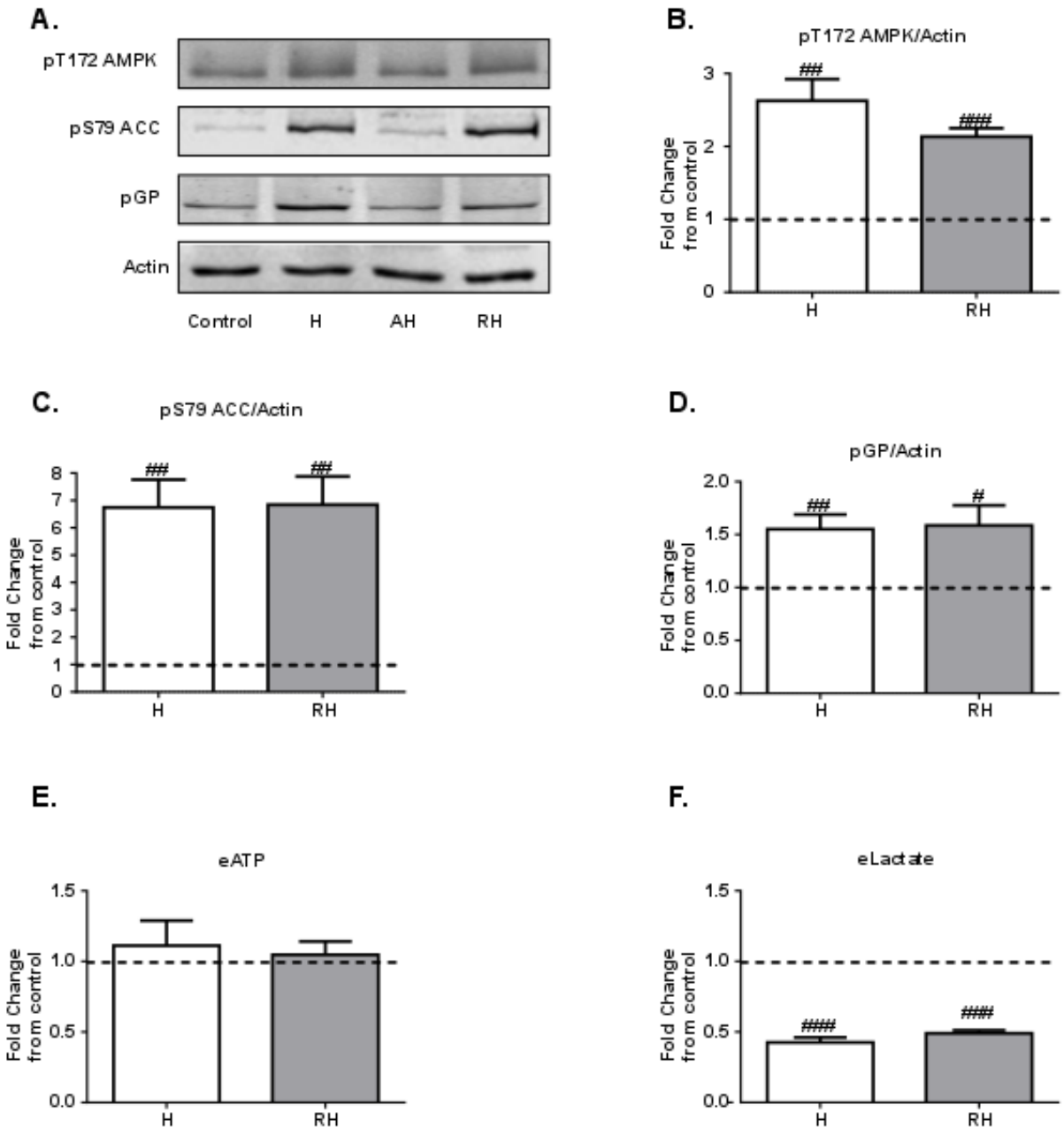

Figure 3.3.3. Recurrent hypoglycaemia blunts the pAMPK response to further hypoglycaemia at 180min. A. Representative Western blots of pAMPK, pACC, pGP and Actin of lysates of U373 cells exposed to three 2hr bouts of euglycaemia or hypoglycaemia over two days, followed by 180min of euglycaemia (2.5mM glucose) or hypoglycaemia (0.1mM glucose). **B.** Fold change in AMPK phosphorylation (n=6). **C.** Fold change in ACC phosphorylation (n=9). **D.** Fold change GP phosphorylation (n=6). **E.** Extracellular ATP at the end of the final 180min hypoglycaemic stimulus (n=7). **F.** Extracellular lactate at the end of the final 180min hypoglycaemic stimulus (n=8). **B-F.** # p≤0.05, ## p≤0.01, ### p≤0.001 Comparing each group to their corresponding control to which they have been normalised, using a one sample t test (hypothetical value of 1).

change in either group (Figure 3.3.3E). Extracellular lactate was significantly decreased to 0.4-fold ± 0.03 in the H group and 0.5-fold ± 0.02 in the RH group (Figure 3.3.3F; n=8; $p<0.001$).

No significant difference in basal (C vs AH) pAMPK, pACC, pGP, eATP or eLactate was observed (see Supplementary figures S2-S3 for a representation of the data from Figure 3.3.1-3.3.3 before normalising the H and RH groups to their respective controls).

In the U373 cells there was a blunted AMPK activation at the earlier time points following RH, demonstrated by the attenuated increase in AMPK phosphorylation in the RH group compared to the H at 15 min, which stayed persistently although not significantly lower in the 30 and 180 min timepoints. This, however, did not translate to reduced ACC phosphorylation, as there was no significant difference between the two groups. There was a lowered eATP response in the RH group compared to H which was only significant at 30min. The reduction in eLactate appeared to occur more rapidly following RH, which would suggest a faster activation of glycogenolysis in these cells.

3.2 Discussion

In our study, a hypoglycaemic stimulus induced an increase in pAMPK in U373 cells plated at different seeding densities (Supplementary figure S1). This increase in AMPK activation indicates that U373 astrocytoma cells detect and respond to a hypoglycaemic stimulus. It has previously been demonstrated that stressful stimuli, including hypoglycaemia, cause an increase in AMPK activity through changes in cytosolic AMP/ATP ratio in a variety tissues and cell-types. Hypoglycaemia in our study also resulted in an increase in ACC phosphorylation, a downstream target of AMPK, indicating an increase in AMPK activity (Figure 3.1A-D).

No change in eATP was observed during acute hypoglycaemic stimulus. However, there was a significant decrease in eATP as seeding density increased (Figure 3.1E). This effect of cell density on eATP may be due to increased ATP breakdown by eATPases. As seeding density increases, cells are at closer proximity to each other, which is likely to increase ATP breakdown by eATPases. Astrocytes, as well as most cell types express eATPases, especially NTPDase2, which preferentially hydrolyses ATP (Wink *et al.*, 2006). These act to break down ATP to its constituents, such as AMP, ADP and adenosine. This is an important step in purinergic signalling, terminating transmission and allowing the uptake and recycling of nucleotides (Zimmermann *et al.*, 2012).

The acute hypoglycaemic stimulus also caused an increase in lactate production compared to glucose availability. This suggests that during energy

stress, astrocytes may be working to maintain energy supply to adjacent neurones. This is in agreement with studies showing that astrocytes are able to prolong neuronal viability and activity during energy starvation by producing and exporting lactate (Brown *et al.*, 2003; Suh *et al.*, 2007; Swanson and Choi, 1993). Astrocytes are highly glycolytic cells, optimised for lactate production and export (Walz and Mukerji, 1988). They express high levels of LDH1 and 5, of which LDH5 has a higher affinity for pyruvate than lactate, thus favouring lactate production (Laughton *et al.*, 2007). Astrocytes also express MCT, particularly MCT1 and 4, which allow the export of lactate from the cells (Pellerin *et al.*, 2005). Lactate can be produced through two main processes in astrocytes, glycolysis where blood-derived glucose is hydrolysed to lactate or glycogenolysis, where glycogen stores are broken down. Astrocytes express GS and GP which allows them to readily produce and store glycogen, or break it down if needed. Astrocytes also express very low levels of PDH compared to neurones, (Laughton *et al.*, 2007), suggesting that astrocytes are more geared towards glycolysis than oxidative metabolism of glucose. During acute hypoglycaemic stimulus, the U373 cells may be maintaining lactate production by either increasing their capacity for glucose uptake, or by increasing glycogen breakdown.

Noradrenaline further stimulated lactate production and release, suggesting that astrocytes have not yet reached their maximal glycogenolytic capacity during hypoglycaemia, but can be further stimulated to increase glycogenolysis. Other studies have shown that NA-mediated increase in glycogenolysis is glucose-dependent, however these studies looked at hyperglycaemic levels of glucose and glucose analogues (5mM) (Cummins *et al.*, 1983). From our studies we see

that euglycaemic and hypoglycaemic levels of glucose do not affect NA-mediated lactate production. Previous studies have also shown NA causes an increase in pAMPK in brown adipose tissue (BAT) through UCP1 (Inokuma *et al.*, 2005). This was not observed in our study. However this could be because, unlike BAT, where the main UCP isoform expressed in UCP1, this isoform is expressed at low levels in astrocytes (Lengacher *et al.*, 2004; Perreten Lambert *et al.*, 2014). During hypoglycaemia in humans a variety of hormones and neurotransmitters, such as adrenaline, noradrenaline and growth hormone are released. Our results indicate that following a reduction in glucose availability alone, astrocytes will work to maintain fuel provision to neurones by increasing lactate production efficiency. However, the input from hormones accompanying a hypoglycaemic episode may be able to stimulate this further.

Following exposure to a 2-day recurrent hypoglycaemic stimulus, we observed a blunted pAMPK response to further hypoglycaemic stimulus, with the biggest difference observed at the 15 minute time point. This suggests a delayed activation of AMPK and could result in a delayed response to hypoglycaemia following recurrent hypoglycaemia, which may explain the reduced or delayed counter-regulatory response seen in people with T1D (Geddes *et al.*, 2008). AMPK activity has previously been associated with impaired CRR, as AMPK activators can recover the CRR which is lost following RH in rats (McCrimmon *et al.*, 2006). Even though AMPK phosphorylation was blunted following recurrent hypoglycaemic stimulus, pACC did not differ between cells exposed to a single or recurrent hypoglycaemic stimulus. This suggests that even though AMPK phosphorylation may be slightly blunted, its effect on its downstream target, ACC, is not affected. AMPK can be modulated through phosphorylation

by AMPKK, such as CaMKK and LKB1, or through allosteric activation by AMP, following changes in intracellular AMP:ATP ratio. This allosteric activation does not require phosphorylation of AMPK (Gowans *et al.*, 2013). It is possible that in in our study we are observing a decreased phosphorylation of AMPK in response to a hypoglycaemic stimulus following RH, with, however, no change in AMPK activity. For a more definitive answer we could perform an AMPK activity assay rather than examining changes in protein phosphorylation alone.

Following an acute hypoglycaemic stimulus, there was a non-significant trend for an increase in eATP at 15 and 30 minutes, which, at 30 min, was significantly larger than the response seen following a RH (Figure 3.3.1 & Figure 3.3.2). ATP release from astrocytes mediates the propagation of calcium waves, recruits microglia and modulates neuronal synaptic activity (Bowser and Khakh, 2004; Gourine *et al.*, 2010; Idzko *et al.*, 2014; Koizumi *et al.*, 2003). The blunted ATP release following RH in astrocytes could affect the modulation of any or all of these, and thus may in part mediate the impaired CRR to hypoglycaemia. We showed that astrocytes intrinsically respond to hypoglycaemia. However, in the brain, they would also receive signals such as hormones, cytokines and ATP from other cell types, such as microglia, which are likely to alter or enhance the astrocytic response. Microglial ATP release has been shown to stimulate astrocytes, which in turn amplifies this response (Pascual *et al.*, 2012).

No significant changes in GP phosphorylation were observed at 15 or 30 minutes of hypoglycaemia, however there was a significant increase following 180 minutes of the hypoglycaemic stimulus. It could be that at those earlier time

points, either astrocytic lactate production is maintained by increased glucose uptake for glycolysis rather than glycogenolysis, or that any changes in glycogen phosphorylase activation may be too small to be detectable. Another explanation is that glycogenolysis is being allosterically activated by AMPK. Evidence suggests that increases in AMPK activity can directly regulate glycogenolysis without changes in GP activity (Longnus *et al.*, 2003; Polekhina *et al.*, 2003). Following prolonged hypoglycaemic stimulus (180min) there was a ~50% increase in phosphorylation of glycogen phosphorylase, indicating a large increase in the activity of this enzyme, and thus suggesting an increase in glycogenolysis. Our data suggests that during prolonged (180min) hypoglycaemia astrocytic glycogenolysis increases to produce and export more lactate, which is seen as an increase in pGP and an increase in lactate released per mol of glucose available. This is in agreement with multiple studies, suggesting that during periods of glucoprivation, such as hypoglycaemia or ischaemia, or high energy demand, such as exercise or learning, astrocytes produce and export lactate to support neuronal function (Brown *et al.*, 2003; Matsui *et al.*, 2015; Newman *et al.*, 2011; Suh *et al.*, 2007; Swanson and Choi, 1993).

Following the 2-day RH model, lactate falls faster in the RH group compared to H when compared to their respective controls. At 15 minutes there was no significant change in eLactate, and at 180 minutes both were significantly reduced, however at 30 minutes eLactate was only significantly reduced in the RH group. It is possible that in the H group glycolysis and/or glycogenolysis is initially increased to maintain extracellular lactate, which in a physiological setting, would supply fuel to neurones. This response could be delayed in the

RH group as a result of or in conjunction with the delay in AMPK activation. As discussed previously, AMPK activation in the VMH can reverse RH-induced impairment in the CRR (McCrimmon *et al.*, 2006), and AMPK can allosterically modulate glycogenolysis (Longnus *et al.*, 2003; Polekhina *et al.*, 2003), suggesting that a blunted or delayed AMPK response following RH may be resulting in a decrease or delay in glycogenolysis, and thus, decrease in lactate production and export. In our model we did not observe any changes in basal eLactate levels, suggesting no changes in glycogen content. However, glycogen levels were not directly measured. To investigate whether glycogen supercompensation occurs in our model, a glycogen assay on cell lysates from C and RH cells, or a glucose uptake assay would need to be carried out. Another explanation would be that, in our model, we have astrocytes in isolation. *In vivo* or in a co-culture setting, neuronal signals may work to enhance astrocytic response to hypoglycaemia, or a hypoglycaemic stimulus.

Our data shows that astrocytes intrinsically respond to low glucose. There is a moderate attenuation in the pAMPK, eATP and eLactate responses following RH. These small changes might be enhanced if astrocytes were exposed to CM from neuronal or microglial cultures exposed to RH. Neurones release a variety of neurotransmitters, such as glutamate, GABA and NA. Microglia also release a variety of gliotransmitters, such as ATP, which have been shown to modulate astrocytic signalling (Pascual *et al.*, 2012), and cytokines. Small changes in the release of messengers from neurones and microglia may enhance or alter the intrinsic responses we observe in astrocytes following RH.

Chapter 4: Results

4.1 AMPK pharmacology

Introduction

AMPK is a central regulator of whole body energy homeostasis, and has been shown to play an important role in the response to hypoglycaemia. Downregulation of AMPK in the VMH of rats causes a defective CRR to hypoglycaemia (McCrimmon *et al.*, 2008). Similarly, intracerebroventricular administration of the AMPK inhibitor Compound C, or expression of dominant negative AMPK in the hypothalamus blunts the CRR to hypoglycaemia (Han *et al.*, 2005). These findings, combined with the observation that antecedent hypoglycaemia causes a decrease in the hormonal CRR to further hypoglycaemia (McCrimmon *et al.*, 2006) suggests that the blunted CRR observed in individuals with T1D with a history of frequent hypoglycaemic episodes may be mediated by changes in AMPK expression or activity. None of these studies showed that the relationship between AMPK and the CRR was specific to neurones; therefore, it is not unreasonable to speculate that this effect may also be mediated by astrocytes or microglia, or a combination of any or all of these three.

Astrocytes play an important part in the CRR to hypoglycaemia. Inactivation of the *glut2* gene results in an impaired glucagon response to hypoglycaemia which can be restored by re-expressing the gene in astrocytes alone (Marty *et al.*, 2005). This is evidence that astrocytic GLUT2 expression is necessary for the glucagon response to hypoglycaemia without the need of neuronal GLUT2. Astrocytes also respond to RH by increasing glycogen storage (Alquier *et al.*,

2007), known as glycogen supercompensation, which is thought to contribute to hypoglycaemia unawareness.

Our studies showed that exposing astrocytes in culture to a hypoglycaemic stimulus for 15-180 minutes results in a robust increase in AMPK activation. This was blunted following exposure to antecedent hypoglycaemia (Figure 3.3), providing further evidence that astrocytic AMPK might be involved in the defective CRR seen in T1D. To investigate the effect of AMPK activation in astrocytes, AMPK activators with different mechanisms of action were used and the functional outcomes measured. Three common AMPK activators that were used in this study are A-769662, AICAR and dimethylbiguanide, more commonly known as metformin.

A-769662 was developed by Cool et al (Cool *et al.*, 2006) as a potential treatment for T2D. Thousands of compounds were screened until A-592107 was identified to directly activate AMPK (Anderson *et al.*, 2004b). Based on this compound the drug was further optimised to create A-769662. A-769662 reversibly binds to AMPK, with specificity for β1 subunit-containing heterotrimers, to directly activate the enzyme. It also prevents AMPK dephosphorylation, making it a potent activator. It was screened for cross-reactivity against at least 67 other receptors and ion channels, and was not shown to significantly cross-react with any at 10 μM. In this paper, it was used to concentrations up to 100 μM and was shown to have no cytotoxic effects in rat hepatocytes (Cool *et al.*, 2006).

AICAR is a cell-permeable compound that due to its structural similarity to adenosine can enter most cells by competing for the adenosine transporter (Gadalla *et al.*, 2004), where it is phosphorylated by adenosine kinase into 5-Aminoimidazole-4-carboxamide ribotide (ZMP) (Vincent *et al.*, 1996). ZMP is an analogue of AMP and can thus activate AMPK directly by binding to the γ subunit (Day *et al.*, 2007). AICAR has been used extensively in research both *in vivo* and *in vitro*. Activating AMPK using AICAR in the VMH of rats was shown to amplify the CRR to hypoglycaemia (McCrimmon *et al.*, 2004), and improve the counter-regulatory hormonal response to hypoglycaemia in rats previously exposed to RH (McCrimmon *et al.*, 2006). This further supports the suggestion that AMPK may play an important part in the CRR to hypoglycaemia.

Metformin is part of the biguanide family and is the first line of therapy for T2D; However its mechanism of action is still not fully understood (Rena *et al.*, 2013). Although metformin was originally thought to mediate these effects through AMPK activation, more recent evidence has shown that AMPK is not essential for metformin's anti-hyperglycaemic action (Foretz *et al.*, 2010), suggesting its primary mode of action is through a still unknown mechanism. Metformin-mediated AMPK activation may still be involved in some of its long-term effects, such as improved lipid metabolism. One potential mechanism of action that has received attention recently is metformin's effect on mitochondrial Complex I (El-Mir *et al.*, 2000; Owen *et al.*, 2000). Metformin has been shown to inhibit mitochondrial ATP production and oxygen uptake which results in an altered cellular AMP:ATP ratio (Hawley *et al.*, 2010). The effects of metformin on AMPK activity are thus most likely the result of the changes in mitochondrial respiration and AMP concentration in the cell.

In this study we aim to characterise the response of astrocytes to an AMPK activator, in order to mimic the AMPK activation observed during a hypoglycaemic stimulus.

4.1.1 Both A-769662 and AICAR cause an increase in AMPK activation, but only A-769662 increases ATP release

To investigate whether AMPK phosphorylation alters eATP and eLactate in astrocytes, three different AMPK activators, A-769662, AICAR and metformin were used at high concentrations, to ensure sufficient AMPK activation. U373 cells were plated at 1,000,000 cells/dish in round, 10 cm dishes the day before the experiment. AMPK and ACC phosphorylation were measured to examine changes in AMPK activity, and eATP and eLactate were measured to establish whether they are regulated by AMPK activation in astrocytes.

A-769662 (100µM) caused a 6.6±1.7-fold increase in AMPK phosphorylation after 30 minutes of treatment (Figure 4.1C; n=8; $p<0.05$) and 10.3 ± 2.0-fold increase after 3 hours of treatment (Figure 4.1D; n=7; $p<0.01$). AICAR (1mM) caused a small but significant increase in AMPK phosphorylation at both 30 minutes (1.5 ± 0.1-fold) and 3 hours (1.9 ± 0.4-fold; Figure 4.1C; n=8; $p<0.05$; Figure 4.1D; n=7; $p<0.05$). There was a trend for a small increase in pAMPK when U373 cells were treated with metformin (1mM), but this did not reach significance (Figure 4.1C; n=8; $p=0.0819$; Figure 4.1D; n=7; $p=0.0696$).

To determine whether altered AMPK phosphorylation resulted in increased activity, ACC phosphorylation was also measured. A-769662 induced a large, 10.1 ± 2.1-fold increase in pACC at 30 minutes and 18.1 ± 5.2-fold at 3 hours (Figure 4.1E; n=9; $p<0.01$; Figure 4.1F; n=8; $p<0.05$). A more modest but significant increase in pACC was also observed following stimulation with AICAR for 30 minutes (2.3 ± 0.5-fold) and 3 hours (7.1 ± 2.0-fold; Figure 4.1E; n=9; $p<0.05$; Figure 4.1F; n=8; $p<0.05$). Metformin did not affect pACC.

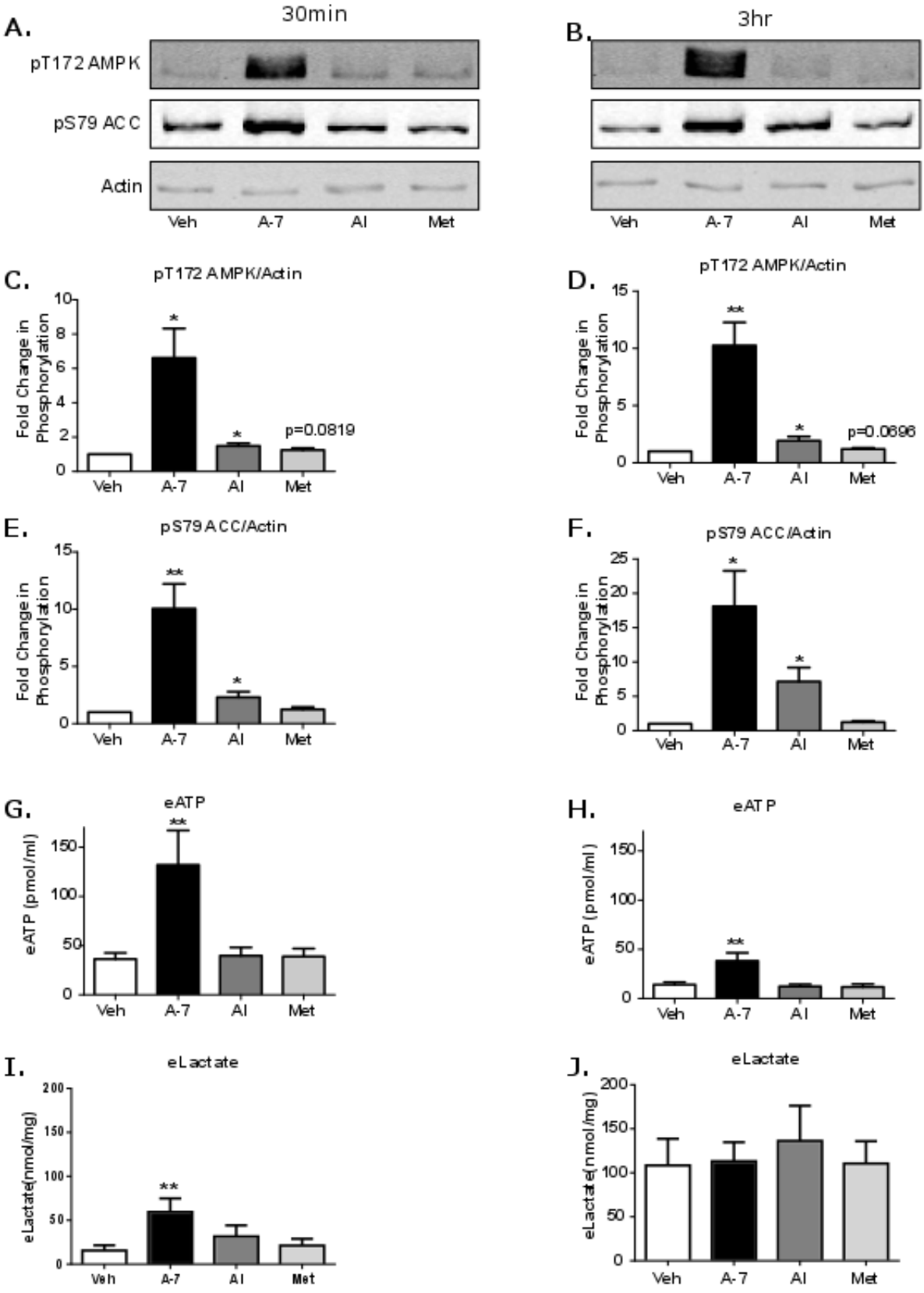

Figure 4.1. A-769662 potently activates AMPK and stimulates ATP release in U373 cells. Representative Western blots of lysates of U373 cells treated with vehicle (0.1% DMSO), A-769662 (100µM), AICAR (1mM) or Metformin (1mM) for 30min (**A.**) or 3hr (**B.**). Fold change in AMPK phosphorylation at 30min (**C.**; n=8) and at 3hr (**D.**; n=7). Fold change in phosphorylation of ACC at 30min (**E.**; n=9) and 3hr (**F.**;n=8). Extracellular ATP 30min (**G.**; n=9) and 3hr (**H.**; n=8) after treatment. Extracellular lactate 30min (**I.**; n=5) and 3hr (**J.**; n=7) after treatment. **C-F.** One sample t test. **G-J.** 1-way ANOVA with Bonferroni's multiple comparison test. * p≤0.05, ** p≤0.01

Extracellular ATP (eATP) was also measured from CM collected at the end of the 30 minute and 3 hour treatments. At 30 minutes, treatment with A-769662, a 3.6-fold increase in eATP (from 36.3 ± 6.3 to 132.0 ± 35.0 pmol/ml) was observed (Figure 4.1G; n=9; $p<0.01$). At 3 hours a 2.7-fold increase (from 14.2 ± 2.4 to 38.2 ± 8.3 pmol/ml) in eATP was measured (Figure 4.1H; n=8; $p<0.01$). No change in eATP was observed with AICAR or metformin.

Extracellular lactate was also measured in the CM. There was an increase in eLactate (3.8-fold increase from 15.53 ± 6.08 to 59.42 ± 15.55 nmol/mg) in the CM from A-769662-treated cells (30min; Figure 4.1I; n=5; $p<0.01$). Neither AICAR nor metformin altered eLactate at 30 minutes (Figure 4.1I), and none of the treatments had a significant effect at 3 hours (Figure 4.1J), suggesting that the A-769662-induced lactate release is a transient response. There was a much higher concentration of eLactate in the vehicle-treated group 3 hr after the treatment, compared to 30 min after treatment (Figure 4.1I&J). This is possibly due to lactate accumulation in the media.

We showed that, in U373 cells, both A-769662 and AICAR significantly increased AMPK activity at 30min, whereas metformin had no effect even by 3hr. Importantly, we also found that A-769662 caused a significant increase in eATP and eLactate within 30min, which is an effect that was not observed in any of the other AMPK activators used.

4.1.2 A-769662 causes a concentration-dependent increase in pAMPK and eATP in U373 cells and primary mouse astrocytes

To determine whether the response of astrocytes to A-769662 was concentration-dependent, cells were treated with increasing concentrations of A-769662 for 30 minutes and the CM and lysates were collected for analysis. U373 cells and CRTAS were plated at 300,000 cells/well in 6-well a plate the day before the experiment.

Western blotting analysis of U373 cells showed that A-769662 causes a concentration-dependent increase in pAMPK at concentrations above 50μM. AMPK phosphorylation was increased by 3.0 ± 0.8, 3.4 ± 0.9 and 4.7 ± 1.3-fold at A-769662 concentrations of 50, 75 and 100μM (Figure 4.2.1B; n=9; $p<0.05$). This corresponded to a concentration-dependent increase in pACC which was significantly increased by 2.6 ± 0.3-fold, 3.6 ± 0.6-fold, 4.7 ± 0.8-fold, 4.8 ± 0.8-fold, and 6.3 ± 1.2-fold at A-769662 concentrations of 10, 25, 50, 75 and 100μM (Figure 4.2.1C; n=9; $p<0.01$). Analysis of eATP levels in CM showed there was a significant increase in eATP at 75μM and 100μM A-769662 from 130.4 ± 16.6 to 232.1 ± 17.7 and 278.1 ± 34.3 pmol/ml respectively (Figure 4.2.1D; n=6; $p<0.05$). There was a modest, non-significant increase in eLactate levels between 10-75 μM, which did not reach significance, potentially due to being underpowered (Figure 4.2.1E; n=4).

We then performed the same study in CRTAS to determine whether the A-769662-induced ATP release occurred in non-transformed cells. A trend for a concentration-dependent increase in pAMPK was observed which was not significant (Figure 4.2.2B), and a 1.7-fold, 1.9-fold and 1.9-fold increase in

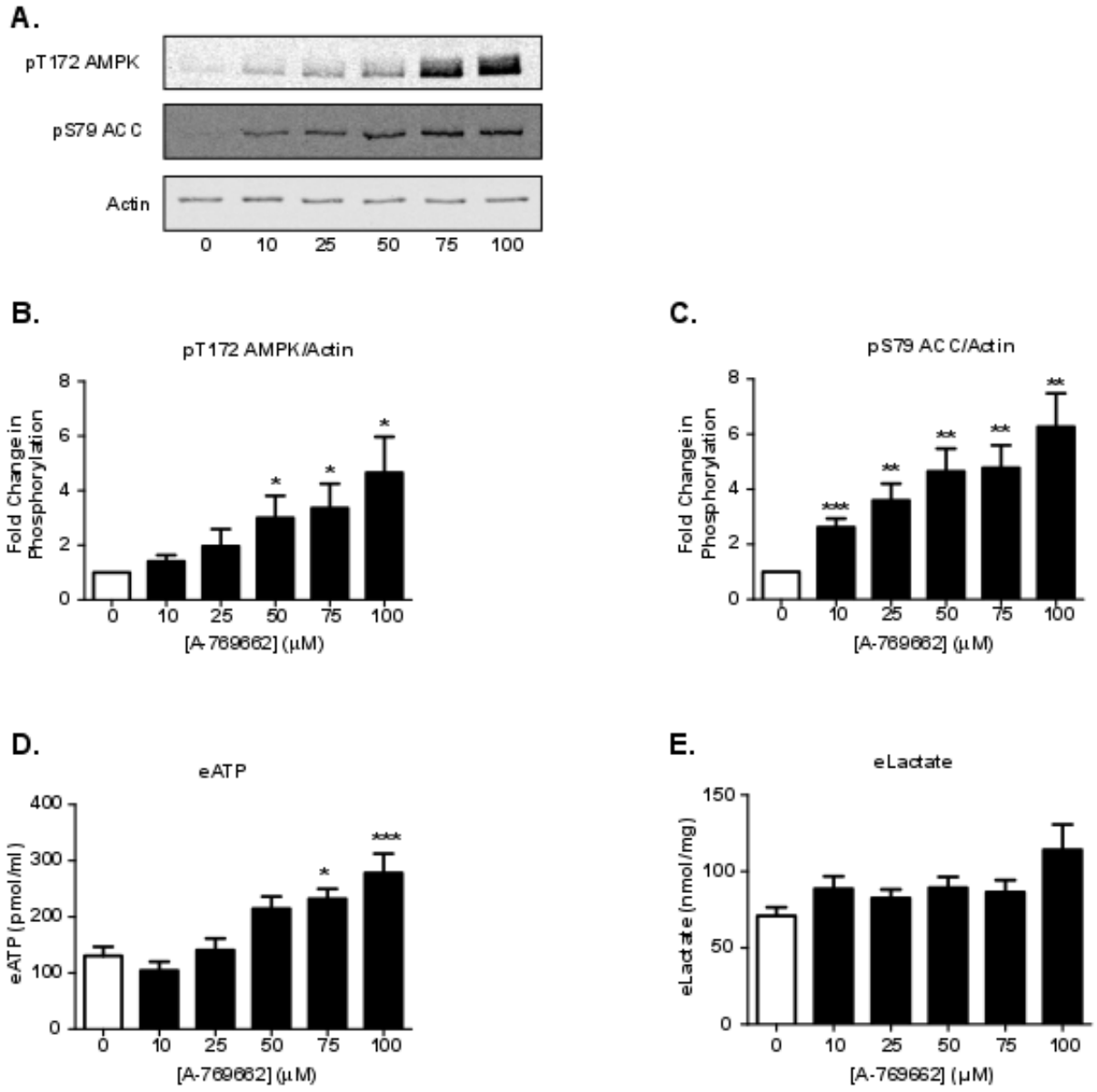

Figure 4.2.1. A-769662 increases pAMPK, pACC, eATP and eLactate in a concentration-dependent manner in U373 cells. A. Representative Western blots of U373 lysates of pAMPK and pACC following a 30min A-769662 concentration response (0-100µM). **B.** Fold change in AMPK phosphorylation (n=9). **C.** Fold change in ACC phosphorylation (n=9). **D.** Extracellular ATP following treatment (n=6). **E.** Extracellular lactate following treatment (n=4). **B-E.** 1-way ANOVA with Bonferroni's multiple comparison test. * p≤0.05, ** p≤0.01, *** p≤0.001

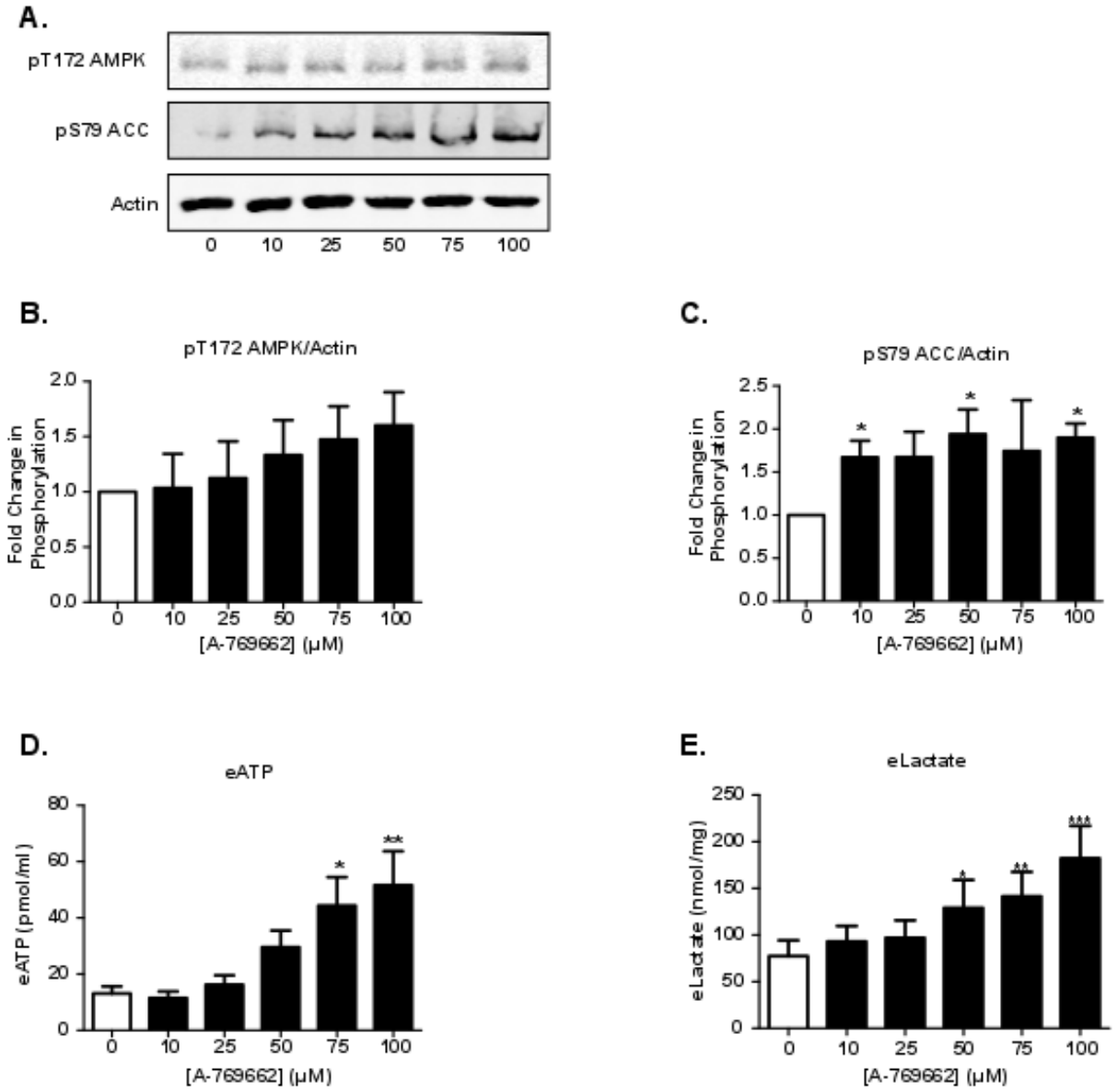

Figure 4.2.2. A-769662 increases pAMPK, pACC, eATP and eLactate in a concentration-dependent manner in CRTAS. A. Representative Western blots of CRTAS lysates of pAMPK and pACC following a 30min A-769662 concentration response (0-100μM). **B.** Fold change in AMPK phosphorylation (n=4). **C.** Fold change in ACC phosphorylation (n=4). **D.** Extracellular ATP following treatment (n=9). **E.** Extracellular lactate following treatment (n=9). **B-E.** 1-way ANOVA with Bonferroni's multiple comparison test. * p≤0.05, ** p≤0.01, *** p≤0.001

pACC at 10, 50 and 100μM A-769662 (Figure 4.2.2C; n=4; $p<0.05$). A significant, 3.4-fold and 3.9-fold increase in eATP was observed at 75 and 100μM A-769662 (Figure 4.2.2D; n=9; $p<0.05$). A significant, 1.7, 1.8 and 2.4-fold increase in eLactate was observed at 50, 75 and 100 μM A-769662 (from 77.45 ± 16.84 to 129.1 ± 29.99, 141.3 ± 26.32 and 182.2 ± 34.81 nmol/mg respectively; Figure 4.2.2E; n=9; $p<0.05$).

This experiment showed a concentration-dependent increase in AMPK activity, as well as eATP and eLactate when using increasing concentrations of A-769662 from 0-100μM in U373 cells. Extracellular ATP also increased in CRTAS at 75 and 100μM A-769662.

4.1.3 AICAR enhances A-769662-mediated AMPK activation, but has no effect on eATP

AICAR can enhance A-769662-mediated AMPK activation in primary hepatocytes (Ducommun *et al.*, 2014). This prompted us to investigate whether it had a similar effect on astrocytes and the A-769662-mediated increase in eATP. U373 cells and CRTAS were plated at 450,000 cells/dish in round, 6 cm dishes the day before the experiment, and treated with A-769662 (50μM) ± AICAR (1mM) for 30 minutes before collecting the CM and lysates for analysis. This A-769662 concentration was selected as it caused a small but non-significant increase in eATP after a 30 minute treatment in U373 cells, thus allowing us to see any potential increase in eATP (Figure 4.2).

Western blot analysis of U373 cell lysates treated with A-769662 or AICAR showed a 1.5 ± 0.1 or 1.6 ± 0.2-fold increase in pAMPK respectively ($p<0.05$). AMPK phosphorylation in lysates of cells treated with both A-769662 and AICAR was increased by 3.7 ± 0.6-fold compared to control and 2.5 and 2.4-fold compared to A-769662 or AICAR treatment alone (Figure 4.3B; n=6; $p<0.01$). A-769662 treatment alone also caused a significant, 1.9-fold increase in eATP from 208.8 ± 19.4 to 404.4 ± 44.6 pmol/ml ($p<0.001$). As observed previously (Figure 4.1), AICAR treatment alone did not cause any changes in eATP. Extracellular ATP from U373 cells co-treated with A-769662 and AICAR (370.7 ± 15.4 pmol/ml) did not significantly differ from that of A-769662-treated (404.4 ± 44.6 pmol/ml) and was significantly higher than both vehicle-treated (208.8 ± 19.4 pmol/ml) and AICAR-treated (216.6 ± 27.7 pmol/ml) (Figure 4.3C; n=7; $p<0.01$). No significant changes in eLactate were observed with any of the above treatments (Figure 4.3D). The study was repeated in CRTAS, where similarly, A-769662 caused a significant, 2.9-fold increase in eATP from 22.8 ± 5.2 to 65.3 ± 6.8 pmol/ml (n=3; $p<0.05$). No effect of AICAR on eATP was observed when used alone, or with the addition of A-769662. (Figure 4.3E). This study is in agreement with the study conducted by Ducommun et al, where they showed that A-769662 enhances AICAR-induced AMPK phosphorylation (Ducommun *et al.*, 2014). Co-treating the cells with A-769662 and AICAR, however, had no effect on the A-769662-mediated increase in eATP.

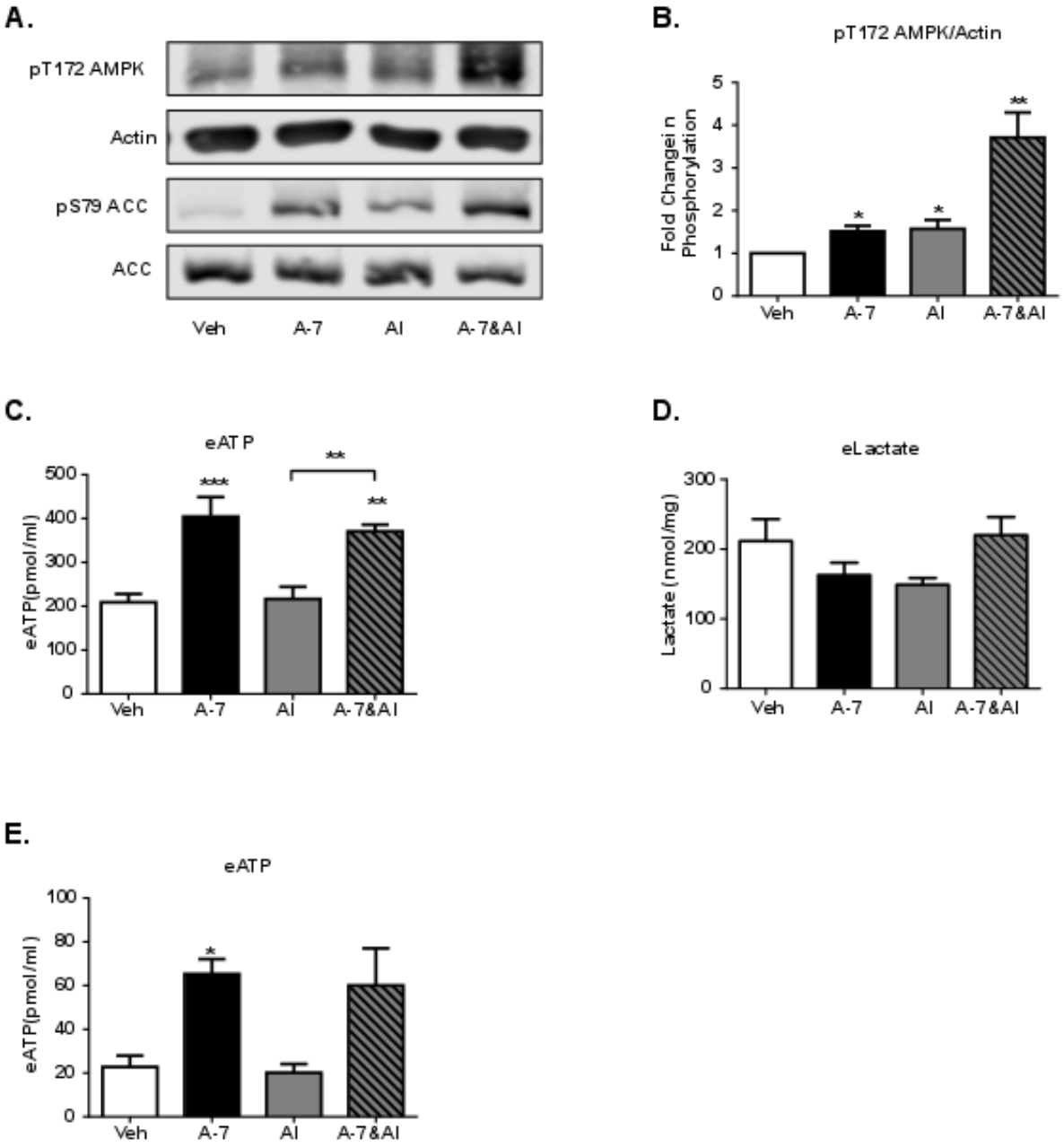

Figure 4.3. Co-application of A-769662 and AICAR enhances pAMPK but not ATP release. A. Representative Western blots of pAMPK, Actin, pACC and total ACC of lysates of U373 cells treated with A-769662 (50µM) +/- AICAR (2mM) for 30min. **B.** Fold change in phosphorylation of AMPK in lysates of U373 cells at the end of the 30min treatment (n=6). **C.** Extracellular ATP at the end of the 30min treatment of U373 cells (n=7). **D.** Extracellular lactate at the end of the 30min treatment of U373 cells (n=7). **E.** Extracellular ATP at the end of the 30min treatment of CRTAS (n=3). **B-E.** 1-way ANOVA with Bonferroni's multiple comparison test. * p≤0.05, ** p≤0.01, *** p≤0.001

4.1.4 A769662 enhances eATP and eLactate at both euglycaemic and hypoglycaemic conditions

We previously observed that both hypoglycaemia and A-769662 treatment causes an increase in AMPK phosphorylation. A-769662 was also shown to cause an increase in eATP and lactate, whereas hypoglycaemia had a less consistent effect on eATP and caused a decrease in eLactate at the high SD (Figures 3.1G & 4.1). To study whether A-769662 affects the astrocytic response to hypoglycaemia, we treated cells with A-769662 (100µM) in euglycaemic (2.5mM glucose) or hypoglycaemic (0.1mM glucose) conditions for 30 minutes before collecting CM and lysates for analysis. U373 cells and CRTAS were plated at 450,000 cells/dish in round, 6 cm dishes the day before the experiment.

In the U373 cells treated with A-769662 in euglycaemic conditions, there was a 1.8-fold increase in eATP from 234.3 ± 24.4 to 417.7 ± 40.6 pmol/ml ($p<0.01$)). A similar response was observed when cells were treated with A-769662 in hypoglycaemic conditions, with a 2-fold increase in eATP to 433.1 ± 37.4 pmol/ml (Figure 4.4A; n=5; $p<0.001$). There was a 1.7-fold decrease in eLactate when comparing CM from 2.5 vs 0.1 mM glucose-treated cells from 159.4 ± 6.0 nmol/mg to 95.81 ± 5.3 nmol/mg ($p<0.001$). This is comparable to the eLactate changes previously observed at the highest SD (1,000,000 cells/dish), but not to those observed at the medium SD (450,000 cells/dish; Figure 3.1F). This could be due to small differences in growth rate between experiments, due to passage number differences or unexpected variables during handling (eg. Room temperature or delays during plating). A-769662 increased eLactate levels in both euglycaemic (197.2 ± 14.7 nmol/mg) and hypoglycaemic (160.4 ±

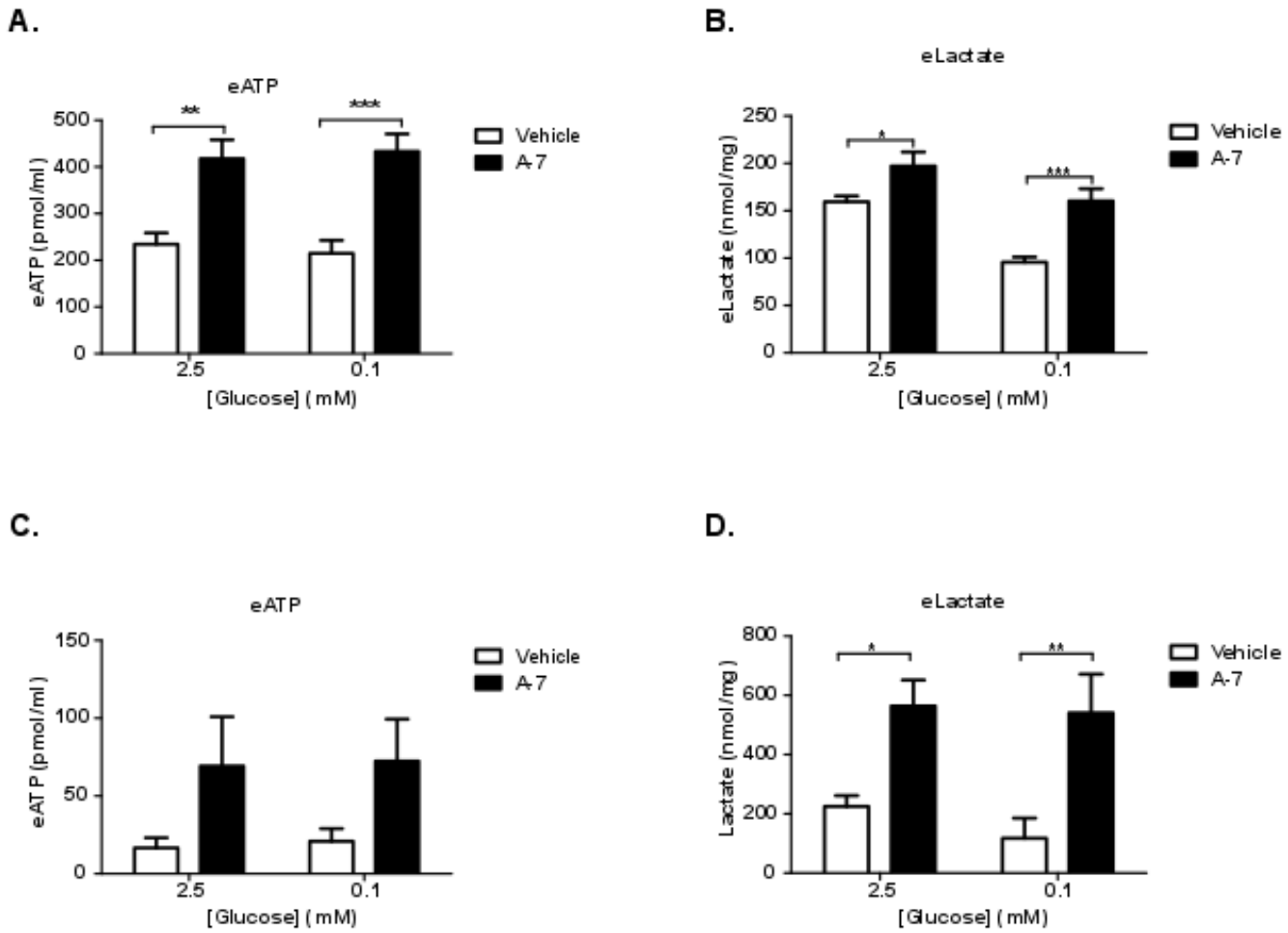

Figure 4.4. A-769662 increases ATP and lactate release at both euglycaemic and hypoglycaemic conditions. A. Extracellular ATP at the end of a 30min treatment of U373 cells with vehicle (0.1% DMSO) or A-769662 (100µM) in euglycaemic (2.5mM glucose) or hypoglycaemic (0.1mM glucose) (n=5). **B.** Extracellular lactate at the end of the 30min treatment of U373 cells (n=6). **C.** Extracellular ATP at the end of the 30min treatment of CRTAS (n=5). **D.** Extracellular lactate at the end of the 30min treatment from CRTAS (n=5). 2-way ANOVA with Bonferroni's multiple comparison test. * p≤0.05, ** p≤0.01, *** p≤0.001

12.8 nmol/mg) conditions by 1.2 and 1.7-fold respectively (Figure 4.4B; n=8; $p<0.05$).

The study was repeated in CRTAS and a trend for an increase in eATP in A-769662-treated cells was observed, but did not reach significance (Figure 4.4C; n=5). A-769662 caused a 2.5-fold increase in eLactate at euglycaemic (from 225.3 ± 36.3 to 564.3 ± 87.6 nmol/mg) and 4.6-fold increase in hypoglycaemic conditions (from 117.9 ± 67.8 to 541.1 ± 130.8 nmol/mg; Figure 4.4D).

This study shows that A-769662 increases eATP and eLactate in astrocytes independent of glucose availability. We can speculate that A-769662 may be having a direct effect on eATP and eLactate independent of low glucose-induced AMPK phosphorylation. However a broader range of A-769662 concentrations should be tested, to ensure submaximal activation by A-769662, and make any potential effects of hypoglycaemic stimulus apparent.

4.1.5 Noradrenaline has an additive effect on A-769662-mediated increase in eLactate without affecting AMPK phosphorylation or eATP

To investigate whether NA enhances any of the effects of A-769662 on eATP, and whether it has an additive effect on the A-769662-mediated increase of eLactate, U373 cells and CRTAS were exposed to A-769662 (100µM) ± NA (50µM) for 30min. The CM and lysates were collected at the end of the treatment for analysis. U373 cells and CRTAS were plated at 450,000 cells/dishes, in round, 6 cm dishes the day before the experiment.

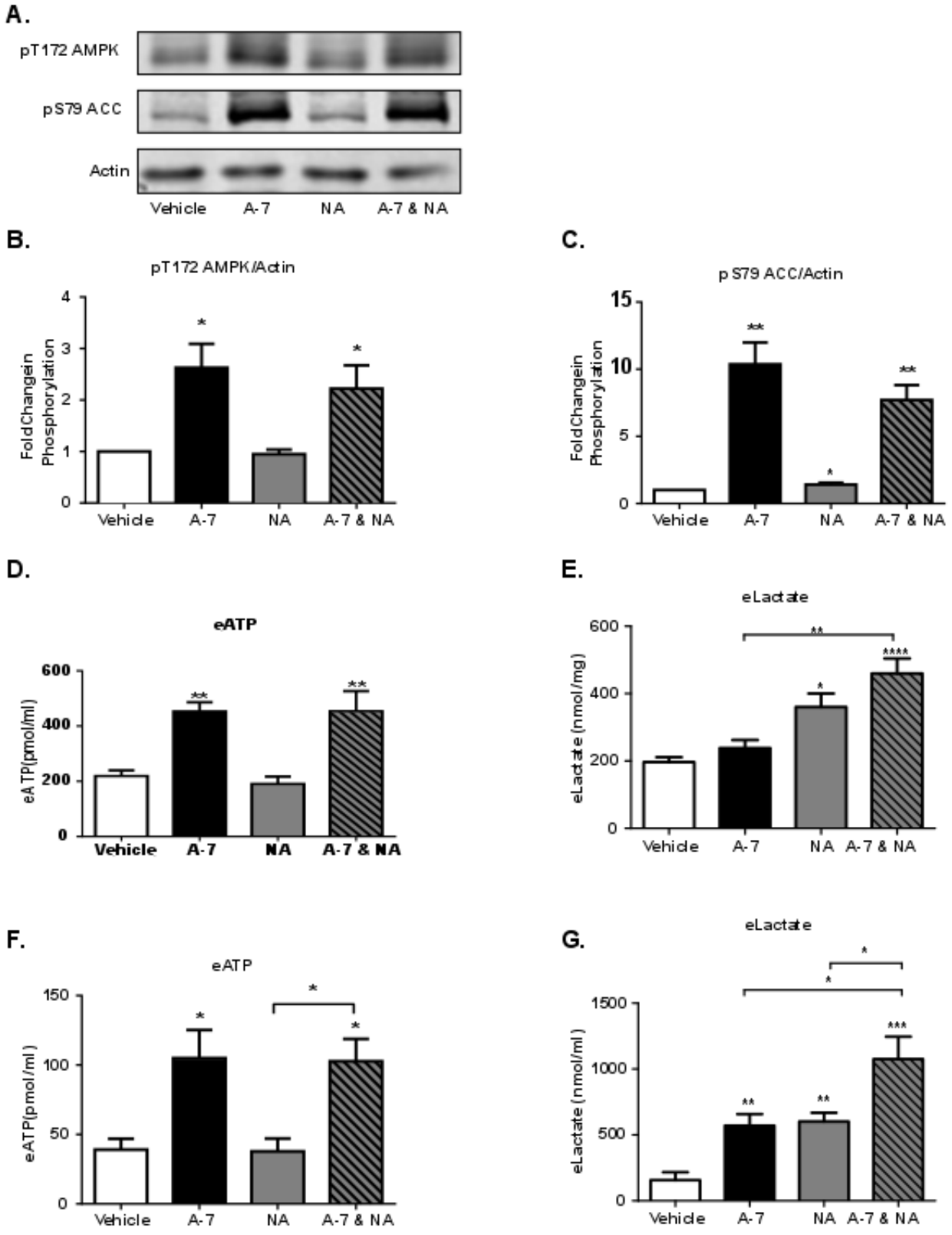

Figure 4.5. NA enhances the A-769662-mediated increase in eLactate. A. Representative Western blots of pAMPK, pACC, pGP and actin of lysates of U373 cells treated with A-769662 (100µM) +/- NA (50µM) for 30min. **B.** U373: Fold change in AMPK phosphorylation (n=5). **C.** U373: Fold change of ACC phosphorylation (n=5). **D.** U373: Extracellular ATP at the end of the 30min treatment (n=9). **E.** U373: Extracellular lactate at the end of the 30min treatment (n=6). **F.** CRTAS: Extracellular ATP at the end of the 30min treatment (n=6). **G.** CRTAS: Extracellular lactate at the end of the 30min treatment (n=6). **B-C.** One sample t test (hypothetical value of 1). **D-G.** 1-way ANOVA with Bonferroni's multiple comparison test. * p≤0.05, ** p≤0.01, *** p≤0.001

In cell lysates of U373 cells treated with A-769662 alone, a 2.6 ± 0.5-fold increase in AMPK phosphorylation was observed when compared to the vehicle-treated ($p<0.05$). NA treatment alone had no significant effect on pAMPK. Co-treatment with A-769662 and NA resulted in a 2.2 ± 0.5-fold increase from control (Figure 4.5B; n=5; $p<0.05$). ACC phosphorylation was also increased 10.4 ± 1.6-fold with A-769662 treatment alone ($p<0.01$). NA caused a small (1.4 ± 0.1-fold) but significant increase in ACC phosphorylation ($p<0.05$). Co-application of the two drugs resulted in a 7.7 ± 1.1-fold increase in pACC (Figure 4.5C; n=5; $p<0.01$). A-769662, as observed previously (Figure 4.1) resulted in a significant, 2-fold increase in eATP from 219.3 ± 62.0 nmol/ml to 453.1 ± 99.1 pmol/ml ($p<0.01$). A similar increase in eATP was observed with the co-treatment of cells with both A-769662 and NA (453.7 ± 219.1 pmol/ml; n=9; $p<0.01$). NA treatment alone had no effect on eATP (Figure 4.5D). A-769662 caused a trend for an increase in eLactate in U373 cells (from 243.0 ± 26.6 to 309.7 ± 39.3 nmol/ml); however, this did not reach significance. NA caused a 1.8-fold increase in eLactate to 196.5 ± 14.7 nmol/mg ($p<0.05$) and co-treating with A-769662 and NA enhanced eLactate levels further to 459.8 ± 44.6 nmol/mg (Figure 4.5E; n=6; $p<0.001$).

In CRTAS, A-769662 induced a significant increase in eATP from 39.1 ± 19.2 to 105.0 ± 49.7 pmol/ml ($p<0.05$). A similar increase was observed with the co-treatment of A-769662 and NA (102.7 ± 39.4 pmol/ml; n=6; $p<0.05$). NA treatment on its own had no significant effect on eATP (Figure 4.5F). A-769662 also caused a significant increase in eLactate from 157.2 ± 59.6 to 570.9 ± 87.3 nmol/mg ($p<0.01$). NA resulted in a similar increase in eLactate to 601.5 ± 67.1

nmol/mg ($p<0.01$) and co-application with the two drugs caused a further increase in eLactate to 1076 ± 169.5 nmol/mg (Figure 4.5G; n=6; $p<0.001$).

As previously shown, NA had no effect on eATP, and this study showed that it did not have any effect on A-769662-induced increases on eATP either. However, A-769662 had additive effect on NA-induced eLactate in both U373 and CRTAS.

4.2 Understanding the mechanism of A-769662-mediated ATP release

Introduction

In our studies, A-769662 caused an increase in eATP in astrocytes (Figure 4.1). A-769662 is an AMPK activator commonly used in research to improve our understanding on AMPK activity. It is therefore important to understand the mechanism responsible for the A-769662-mediated increase in eATP, and whether it is a direct result of AMPK activation.

ATP is the universal “danger signal” and acts as a pro-inflammatory mediator, as well as a fast excitatory neurotransmitter, or long-term mediator of proliferation, growth and development (Burnstock, 2006b; Idzko *et al.*, 2014). In astrocytes, ATP has also been shown to be crucial for calcium wave propagation amongst astrocytes (Bowser and Khakh, 2007; Cotrina *et al.*, 1998). Most tissues and cell types express multiple purinergic receptors (P2R), which are activated by ATP and its by-product, ADP, as well as other nucleotides, such as UTP, UDP and UDP-glucose (Idzko *et al.*, 2014), which suggests alterations in ATP release could have significant effects on surrounding cells and tissues.

ATP can be released from cells passively, as a result of damage to the cell walls, or actively in response to a stimulus. Some of the mechanisms behind ATP release suggested in literature are through hemichannels or gap junctions (Cotrina *et al.*, 1998; Garre *et al.*, 2010), P2X7 receptors (Suadicani *et al.*, 2006), large-conductance anion channels (Anderson *et al.*, 2004a), or through vesicles (Bowser and Khakh, 2007; Lalo *et al.*, 2014). Following release, ATP is

rapidly broken down by extracellular ectonucleases into ADP, AMP and adenosine. These can also act as intercellular messengers to elicit a response, for example through activation of P2Y or adenosine receptors, or they can be taken back up into the cell and be recycled (Idzko *et al.*, 2014).

ATP is found at a much higher concentration in the cell, compared to the extracellular compartment. This means that upon damage to the cell membrane, ATP is passively released from the cell following a diffusion gradient. This triggers an inflammatory response, recruiting microglia to the area and causing phagocytosis of the damaged cell (Idzko *et al.*, 2014). This is a non-regulated form of ATP release from cells.

ATP can also be released in a more regulated manner, through hemichannels. Hemichannels are formed by connexins or pannexins organised in a hexamer, embedded in the cell membrane, which allows small molecules, such as ATP, Ca^{2+} and certain dyes to move across the cell membrane. Hemichannels formed by connexins are called connexons, and pannexins called pannexons. Connexons in the cell membrane of adjacent cells can join to form gap junctions that allow intercellular exchange (Bennett *et al.*, 2003; Giaume *et al.*, 2010; Lazarowski *et al.*, 2011). Astrocytes mainly express connexin 43 and connexin 30 (Dermietzel *et al.*, 1991; Giaume *et al.*, 1991) of which connexin 43 in the mediobasal hypothalamus has been shown to play a role in glucosensing and insulin secretion (Allard *et al.*, 2014).

The P2X7 receptor is a purinergic receptor thought to be associated with a variety of pathologies, such as temporal lobe epilepsy, neurodegenerative

disorders such as Alzheimer's disease, neuropathic pain, diabetes, and certain cancers (Burnstock, 2006a). The P2X7 receptor differs from most purinergic receptors in that, once activated by high concentrations of ATP, the P2X7R transitions from a channel to a pore (Surprenant *et al.*, 1996). This allows larger molecules (up to 1kDa) to move through the membrane and results in Ca^{2+} and Na^{+} influx and K^{+} efflux. This pore opening is associated with a variety of physiological and pathophysiological functions, including cell lysis and apoptosis (He *et al.*, 2017; Surprenant *et al.*, 1996), as well as mediating inflammation and immunity (Arulkumaran *et al.*, 2011).

Astrocytes have been shown to release ATP through calcium-induced vesicular exocytosis (Bowser and Khakh, 2007; Lalo *et al.*, 2014), although this is still controversial (Hamilton and Attwell, 2010). ATP release has been shown to be necessary for calcium wave propagation following mechanical stimulation in astrocytes (Bowser and Khakh, 2007).

In this study we aim to examine the underlying mechanism behind the A-769662-mediated increase in eATP.

4.2.1 Blocking gap junctions does not attenuate the A-769662-mediated increase in eATP

To investigate whether the A-769662-mediated increase in eATP is due to increased ATP release through gap junctions, the gap junction inhibitor, carbenoxolone was used. U373 cells and CRTAS, were pretreated with carbenoxolone before being treated with A-769662, and total, intracellular and extracellular ATP (tATP, iATP and eATP respectively) were measured. For eATP measurements, U373 cells and CRTAS were plated at 450,000 cell/dish in round, 6 cm dishes, the day before the experiment. For tATP and iATP measurements, U373 cells were plated at 20,000 cells/well in a black, 96-well plate the day before the experiment.

In U373 cells pre-treated with carbenoxolone (100µM; 30min), followed by a 30 minute treatment with A-769662 (100µM) showed no significant change in tATP or iATP. There was a small, non-significant trend for an increase in tATP and iATP in cells treated with A-769662 (100µM) alone (13% and 11% from control respectively) (Figure 4.6A&B).

U373 cells treated with A-769662 (100µM) showed a 2.6-fold increase in eATP when comparing to vehicle-treated (from 97.6±17.9, to 249.1 ± 34.3 pmol/ml; $p<0.05$). Pre-treating U373 cells with carbenoxolone (100µM) resulted in a further 1.7-fold increase in eATP following a 30 minute A-769662 (100µM) treatment, from 249.1±34.4 to 413.7±55.8pmol/ml, compared to A-769662 treatment alone ($p<0.05$). No significant change in eATP were observed in the cells that received carbenoxolone treatment alone (Figure 4.6C; n=5). CRTAS treated with A-769662 (100µM) alone, showed a 7.8-fold increase in eATP

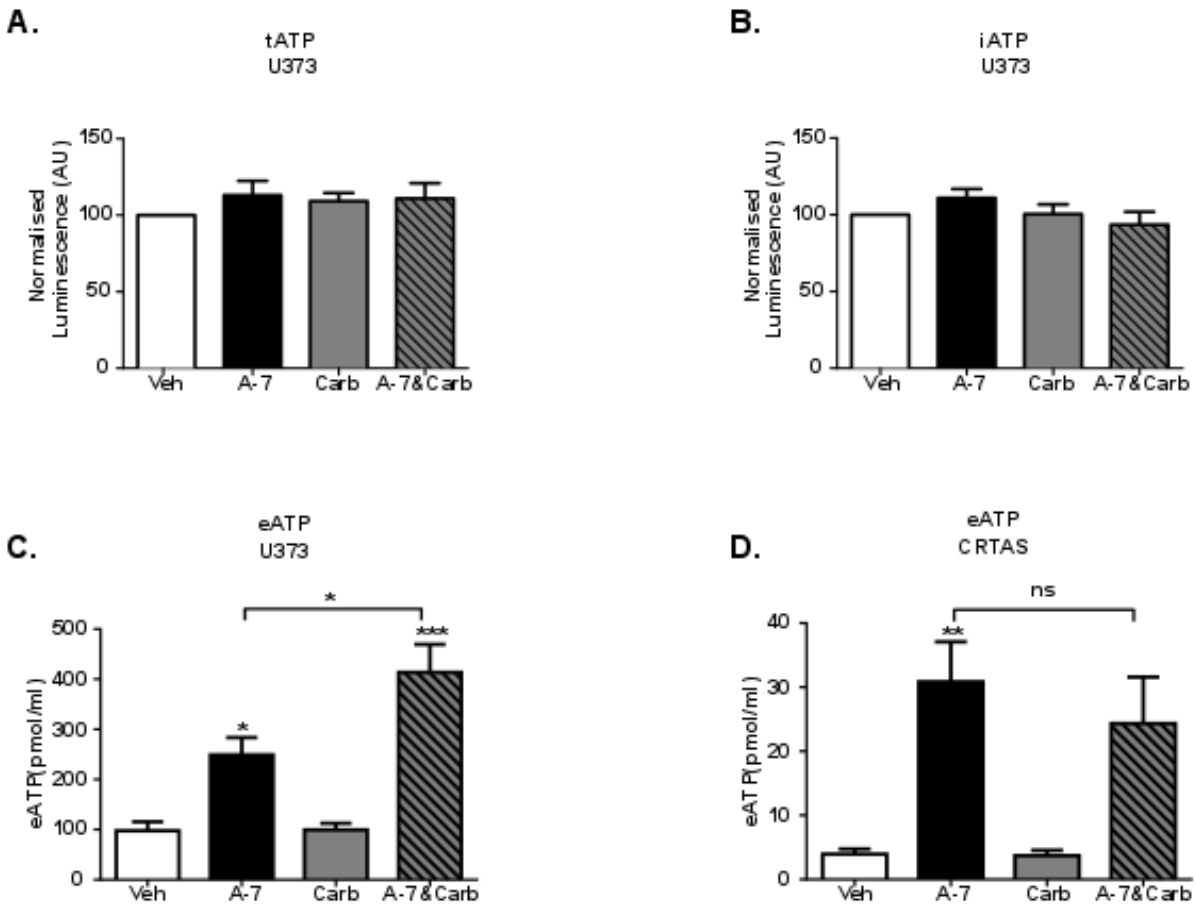

Figure 4.6. Carbenoxolone did not attenuate the A-769662-evoked ATP release. A. Total ATP (normalised to control) at the end of a 30min pre-treatment of U373 cells with A-769662 (100µM), with a 30min carbenoxolone (100µM) pre-incubation (n=3). **B.** Intracellular ATP (normalised to control) at the end the treatment in U373 cells (n=3). **C.** Extracellular ATP at the end the treatment in U373 cells (n=5). **D.** Extracellular ATP at the end of the treatment in CRTAS (n=5). **A-D.** 1-way ANOVA with Bonferroni's multiple comparison test. * p≤0.05, ** p≤0.01, *** p≤0.001

when compared to vehicle-treated, from 4.0 ± 0.8 to 30.8 ± 6.2 pmol/ml (Figure 4.6D; n=5; $p<0.01$). These studies suggest that gap junctions are unlikely to play a role in the A-769662-induced increase in eATP.

4.2.2 Imaging of acidic vesicles in astrocytes using quinacrine

To examine whether the increase in eATP observed following the treatment of astrocytes with A-769662 was mediated through increased vesicular release of ATP, cells were loaded with quinacrine, and changes in fluorescence intensity in individual cells following treatment with A-769662 (100µM) was measured (cells plated at 80,000 cells/dish in round, glass-bottomed, 4 cm dishes for quinacrine imaging, and at 450,000 cells/dish in round, 6 cm dishes for eATP measurements the day before the experiment). Quinacrine is an antimalarial drug that, in live cells, accumulates in acidic vesicles. This is commonly used to image lysosomes or ATP-containing vesicles, it is not, however, a direct measure of ATP release (Akopova *et al.*, 2012; Bodin and Burnstock, 2001; Haanes *et al.*, 2014; Kasymov *et al.*, 2013; Pangrsic *et al.*, 2007; Pierzynska-Mach *et al.*, 2014).

Using Protocol 1 (Chapter 2.2.7), a gradual decrease in fluorescence intensity was observed following addition of vehicle or A-769662. A trend for a decrease in fluorescence was observed in both cells treated with A-769662 (100uM) or vehicle (0.1% DMSO) from the time of drug addition (Figure 4.7A). We were concerned that this decrease in fluorescence from addition of treatment may be the result of cellular stress, and might be masking the effect of A-769662. The protocol was revised, and the experiment was repeated using Protocol 2

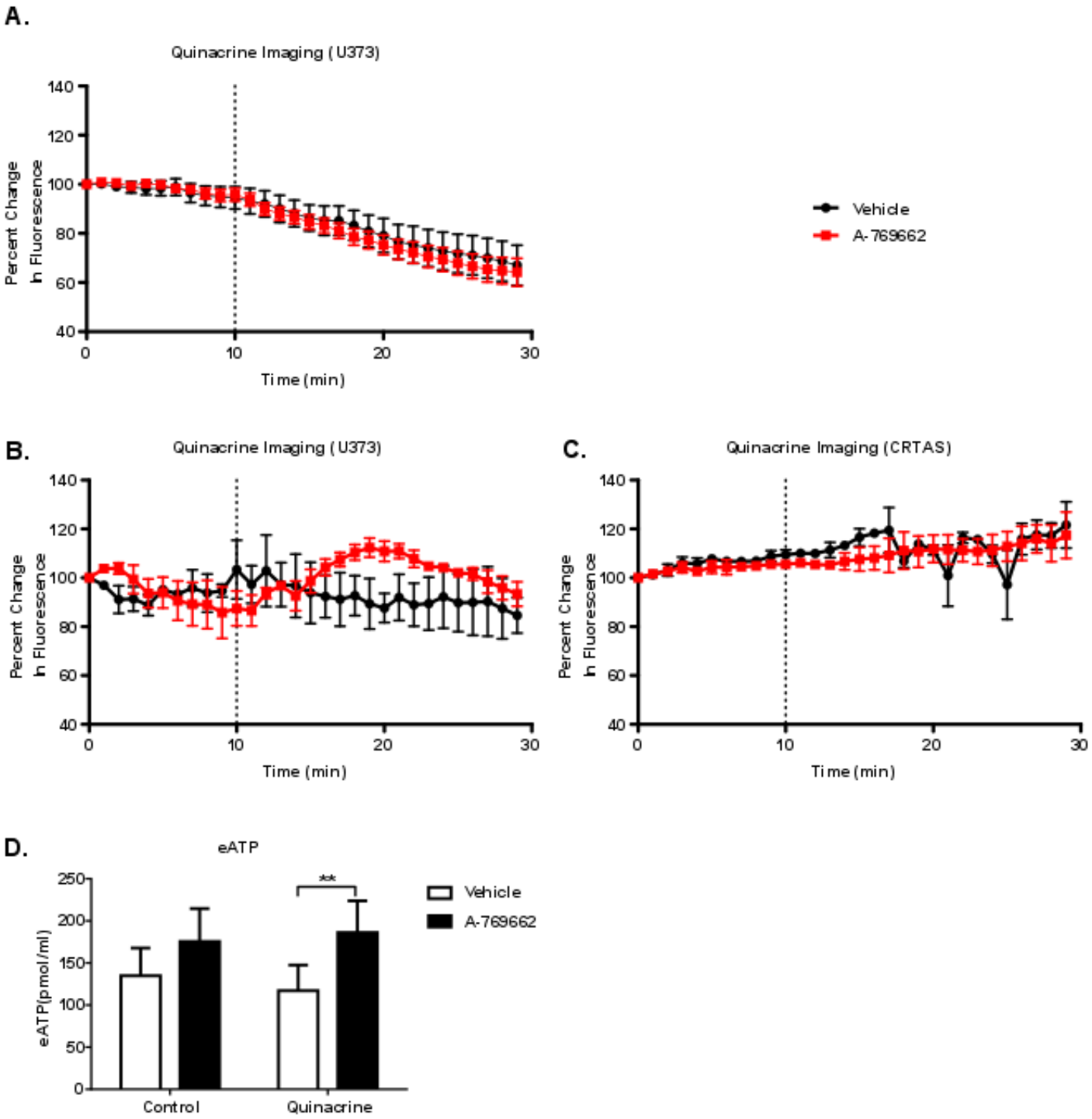

Figure 4.7. No change in fluorescence was observed with A-769662 using Quinacrine. A. Percent change in fluorescence, measured using protocol 1 (see Chapter 2.2.7), in U373 cells pre-incubated with Quinacrine (1µM) measured over 30min, with A-769662 (100µM) or vehicle (0.1% DMSO) added at t=10min (Vehicle n=9, A-769662 n=11). **B.** Percent change in fluorescence, measured using protocol 2 (see Chapter 2.2.7) in U373 cells (Vehicle n=2, A-769662 n=3). **C.** Percent change in fluorescence, measured using protocol 2 (see Chapter 2.2.7) in CRTAS (n=2). **D.** Extracellular ATP in U373 cells at the end of a 30min A-769662 (100µM) after a 15min Quinacrine (1µM) pre-incubation followed by a 15min wash step (n=5). 2-way ANOVA with Bonferroni's multiple comparison test. * p≤0.05, ** p≤0.01, *** p≤0.001

(Chapter 2.2.7). No change in fluorescence was observed using this protocol either (Figure 4.7B&C).

To ensure the experimental conditions did not affect the A-769662-mediated increase in eATP, cells were plated in normal dishes and loaded with Quinacrine for 15 minutes in 2.5mM glucose serum-free, phenol red-free DMEM with 25mM HEPES. The dye was then washed off as in the imaging experiments, and the cells were treated with A-769662 (100µM) for 30min. The CM was collected and eATP measured. As observed previously, A-769662 caused an increase in eATP, but this was a smaller increase than in previous experiments. A-769662 (100µM) for 30 minutes in U373 cells in previous experiments resulted in a 3.6-fold increase in eATP (Figure 4.1G), whereas in U373 cells prepared as for Quinacrine imaging, without loading the cells with dye, only a 1.3-fold increase was observed. Similarly, cells loaded with Quinacrine dye only showed a 1.6-fold increase in eATP after A-769662 treatment (Figure 4.7D).

These experiments were inconclusive, and did not prove or rule out A-769662-mediated vesicular ATP release, they did however suggest that this method may not be suitable for this experiment. Different approaches should be investigated, for example using different reagents such as MANT-ATP for imaging vesicular ATP release, or using a set-up that allows for control of atmospheric conditions, such as CO_2, and thus does not require HEPES for buffering the media.

4.2.3 A-769662 increases intracellular calcium in astrocytes

Vesicular release of ATP from astrocytes is commonly driven by an increase in $[Ca^{2+}]_i$. To investigate whether ATP release is driven by changes in $[Ca^{2+}]_i$, U373 cells and primary astrocytes were loaded with the $[Ca^{2+}]_i$ dye Fluo4 direct, and treated with A-769662 (100µM) whilst recording changes in fluorescence (plated at 20,000 cells/well in a clear 96-well plate the day before the experiment).

Treating U373 cells with A-769662 caused a 1.4-fold increase in $[Ca^{2+}]_i$ (Figure 4.8A). The area under the curve (AUC) increased by 5.1-fold following A-769662 treatment (Figure 4.8B; $p<0.01$; n=3). In CRTAS, the change in $[Ca^{2+}]_i$ was less than that observed in the U373 cells, with a 1.1-fold increase in peak response following A-769662 treatment (Figure 4.8C). However, the increase was sustained during the recording period, giving a 6.4-fold increase in the AUC (Figure 4.8D; $p<0.05$; n=4). In primary hypothalamic astrocytes (HTAS) a 1.3-fold increase in peak response was observed (Figure 4.8E), with a 9.7-fold increase in the area under the curve (Figure 4.8F; $p<0.05$; n=4).

In all three cell types (U373, CRTAS and HTAS), a rapid increase in $[Ca^{2+}]_i$ was observed following application of A-769662 (100µM) . These data suggests that the A-769662-mediated increase in eATP may be by changes in $[Ca^{2+}]_i$.

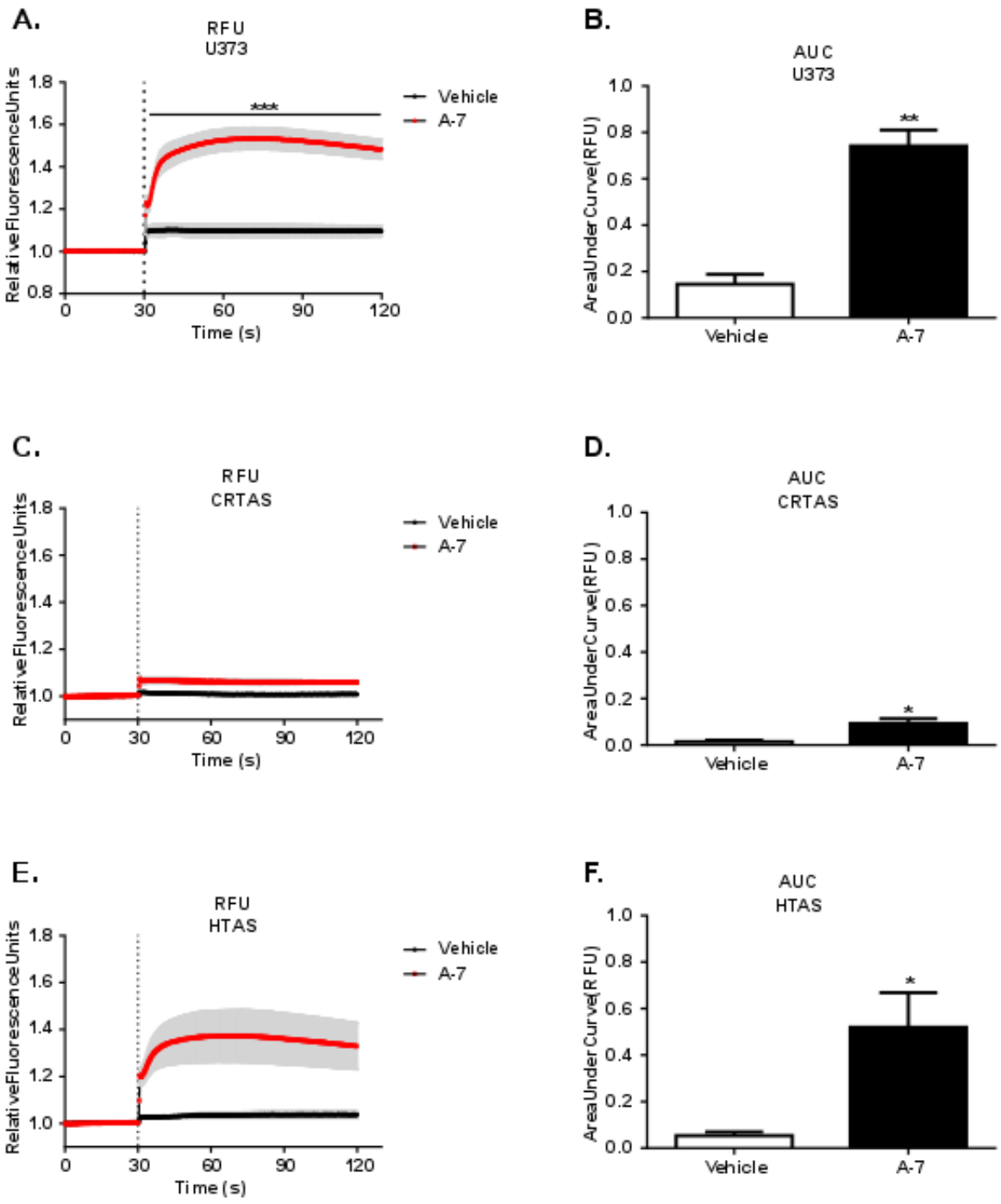

Figure 4.8. A-769662 causes an increase in intracellular calcium. A. Relative fluorescence units from U373 cells treated with vehicle (0.1% DMSO), or A-769662 (100µM) at t=30s (n=3). **B.** Total area under the curve for the two treatment groups generated from figure A. **C**. Relative fluorescence units of the above experiment carried out in CRTAS (n=4). **D.** Total area under the curve for the two treatment groups generated from figure C. **E.** Relative fluorescence units of the above experiment carried out in HTAS (n=4). **F.** Total area under the curve for the two treatment groups generated from figure E**. A, C, E.** 2-way ANOVA with Bonferroni's multiple comparison test. **B, D, F.** Unpaired t test. * p≤0.05, ** p≤0.01, *** p≤0.001

4.2.4 Extracellular calcium is not required for the A-769662-mediated increase in eATP

As shown in the previous experiment, treating astrocytes with A-769662 causes a rapid and persistent increase in $[Ca^{2+}]_i$ (Figure 4.8). To investigate whether the increase in $[Ca^{2+}]_i$ is a result of calcium entry into the cell, U373 cells (plated at 450,000 cells/dish, in round, 6 cm dishes the day bfore the rxperiment), as well as primary mouse astrocytes, were treated with A-769662 in a calcium-free saline buffer (Table 1). U373 cells, CRTAS and HTAS were plated at 450,000 cells/dish in round, 6 cm dishes the day before, the experiment.

In U373 cells, treated with A-769662 (100µM) in normal saline (NS), a 2.3-fold increase in eATP was observed which is comparable to the previously-observed effect of A-769662 (Figure 4.1; $p<0.01$). This indicates that replacing SF DMEM with NS for this experiment has no obvious effects on A-769662-induced ATP release. Treating U373 cells in a calcium-free saline did not have an effect on baseline eATP (112.4 ± 23 in NS and 104.4 ± 18.7 pmol/ml in calcium-free saline), or on the A-769662-mediated eATP response (2.2-fold increase from baseline; Figure 4.9A; $p<0.01$; n=5).

CRTAS treated in calcium-free saline showed a 2-fold increase in baseline eATP from 9.3 ± 2.5 to 19 ± 3.5 pmol/ml when compared to those treated in NS. The eATP from CRTAS treated with A-769662 (100µM) in NS increased by 3.5-fold ($p<0.05$) and those treated in calcium-free saline by 2.5-fold (Figure 4.9B; $p<0.01$; 6). HTAS treated in NS and calcium-free saline showed a similar trend, where baseline eATP was raised by 1.8-fold in those in calcium-free when

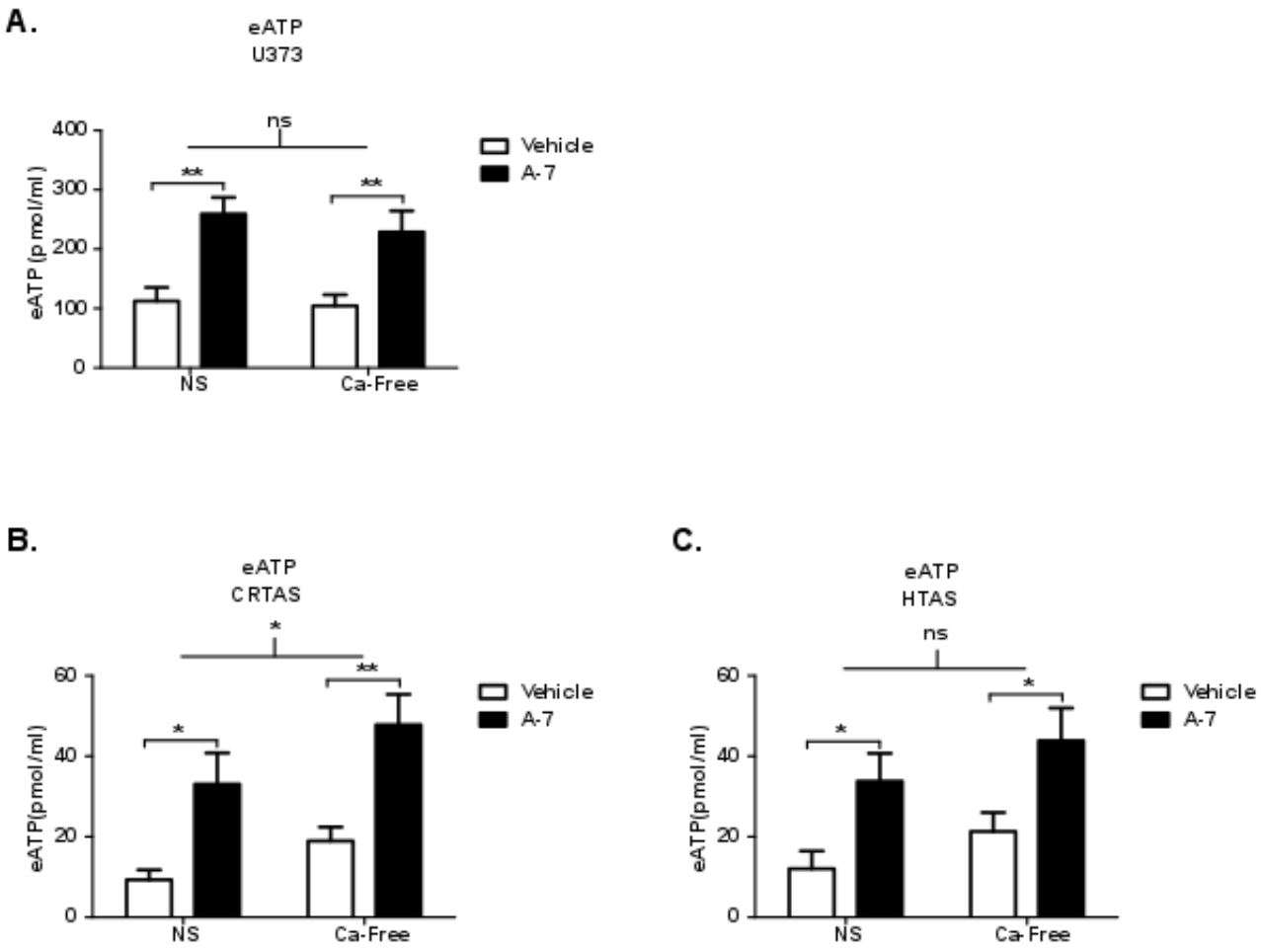

Figure 4.9. Extracellular calcium is not required for the A-769662-mediated increase in eATP. A. Extracellular ATP of samples collected from U373 cells treated with A-769662 (100µM) or vehicle (0.1% DMSO) for 30min in Normal saline or calcium free saline (n=5). **B.** Extracellular ATP from CRTAS treated as above (n=6). **C.** Extracellular ATP from CRTAS at the end of the treatment (n=8). 2-way ANOVA with Bonferroni's multiple comparison test. * $p \leq 0.05$, ** $p \leq 0.01$, *** $p \leq 0.001$

compared to those in NS. In the HTAS treated in NS, a 2.8-fold increase in eATP was observed following the 30 minute treatment with A-769662, which was not significantly different from the 2.1-fold increase observed when the cells were treated in calcium-free saline (Figure 4.9C; $p<0.05$; $n=8$). Primary astrocytes were more sensitive to the removal of extracellular calcium, as, in both CRTAS and HTAS astrocytes, an increase in baseline eATP was observed; However, the A-769662-mediated increase in eATP persisted. Therefore, entry of extracellular calcium is not required for A-769662-mediated increase in eATP.

4.2.5 Chelating intracellular calcium causes a decrease in the A-769662-mediated increase in eATP in primary astrocytes

To investigate whether release of intracellular calcium stores drives the A-769662-mediated increase in eATP, U373 cells, CRTAS and HTAS (plated at 450,000 cells/dish, in round, 6 cm dishes the day before the experiment) were treated with the intracellular calcium chelator, BAPTA-AM (25-50µM), for 30 minutes prior to the A-769662 treatment (100µM). Total ATP, as well as the intracellular ATP/ADP ratio were also measured to determine whether A-769662 and BAPTA-AM affect internal energy status (cells plated at 20,000 cells/well, in black, 96-well plates the day before the experiment).

Treating U373 cells with A-769662 (100µM) following a 30 minute pre-treatment with BAPTA-AM (25µM) resulted in a 2.3-fold increase in eATP, which is comparable to the 2.4-fold increase seen without BAPTA-AM pre-treatment ($n=6$; $p<0.01$). There was no difference in baseline eATP between the vehicle-treated cells (105.0 ± 8 pmol/ml) and the cells treated with BAPTA alone (117.0

± 9.3 pmol/ml; Figure 4.10A). To ensure sufficient $[Ca^{2+}]_i$ chelation, a higher concentration of BAPTA was used. There was no significant effect of BAPTA on baseline eATP (101.6 ± 9.2 vs 97.9 ± 12.5 pmol/ml), nor was there any change in A-769662-induced increase in eATP (Figure 4.10B; n=8). Treating U373 cells with A-769662 or BAPTA had no effect on tATP or ATP/ADP ratio (Figure 4.10C&D; n=6).

CRTAS treated with A-769662 showed a significant 2.7-fold increase in eATP ($p<0.05$). There was no significant difference in the baseline eATP in cells treated with vehicle vs BAPTA-AM (50µM; 27.5 ± 10.8 vs 23 ± 8.5 pmol/ml). There was a trend for an increase in eATP in CRTAS pre-treated with BAPTA followed by A-769662 treatment (1.8-fold), which did not reach significance (Figure 4.10E).

In HTAS, treatment with A-769662 alone caused a 2.9-fold increase in eATP, from 23 ± 5.8 to 65.8 ± 8 pmol/ml. Treating these cells with BAPTA-AM caused a 2.6-fold decrease in eATP from 23.01 ± 5.8 to 8.9 ± 4.7 pmol/ml. The eATP response to A-769662 following BAPTA-AM pre-treatment was reduced significantly by 1.9-fold (34.6 ± 6.2 pmol/ml) when compared to that with A-769662 alone (65.8 ± 8 pmol/ml) (Figure 4.10F; n=5; $p<0.05$).

From this data we see a small attenuation in the A-769662-mediated increase in eATP after BAPTA-AM treatment (50µM) in primary astrocytes, suggesting that release of calcium from intracellular stores may, at least in part, be responsible for A-769662-induced ATP release (Figure 4.10).

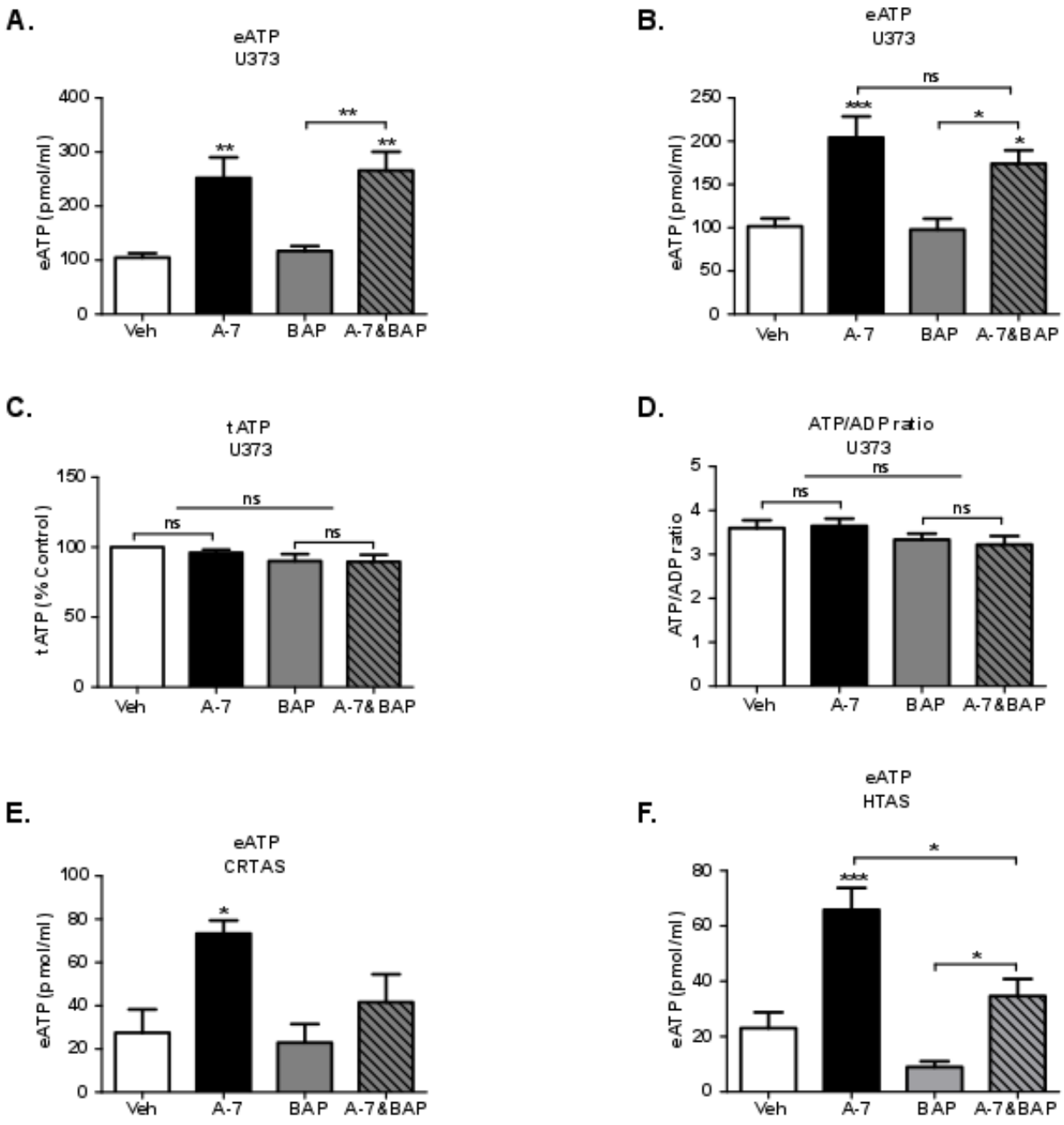

Figure 4.10. Chelating intracellular calcium attenuates the A-769662 mediated ATP release in primary astrocytes. A. Extracellular ATP at the end of a 30min treatment of U373 cells with A-769662 (100µM) or vehicle (0.1% DMSO) +/- 30min pre-treatment with BAPTA (25µM) (n=6). **B.** Extracellular ATP from U373 cells at the end of a 30min treatment with A-769662 (100µM) or vehicle (0.1% DMSO) +/- 30min pre-treatment with BAPTA (50µM) (n=8). **C.** Fold change in total ATP compared to control at the end of the 30min treatment (n=6). **D.** ATP:ADP ratio in U373 cells at the end of the 30min treatment (n=6). **E.** Extracellular ATP at the end of the 30min treatment in CRTAS (n=6). **F.** Extracellular ATP at the end of the 30min treatment in HTAS (n=5). 1-way ANOVA with Bonferroni's multiple comparison test. * p≤0.05, ** p≤0.01, *** p≤0.001

4.2.6 A-769662 causes an increase in eATP and intracellular calcium in AMPK knockout cells

To investigate whether the A-769662 effect on eATP is a result of direct AMPK activation, we used MEF WT and α1/α2 AMPK KO cells. MEF WT and MEF α1/α2 AMPK KO cells were exposed to increasing concentrations of A-769662 for 30 minutes and eATP was measured in both cell types (plated at 450,000 cells/dish in round, 6 cm dishes, plated the day before the experiment). Cells were also plated in 96-well plates to measure tATP (1,000 cells/well in black plates) and $[Ca^{2+}]_I$ (20,000 cells/well in clear plates). Treating MEF WT cells with increasing A-769662 concentrations (10-100μM) for 30 minutes resulted in a concentration-dependent increase in AMPK phosphorylation. This effect was absent in the MEF α1/α2 AMPK KO cells, where no pAMPK was detected (Figure 4.11A).

A concentration-dependent increase in eATP was also observed in the MEF WT cells between A-769662 concentrations of 25 to 100μM. In the MEF WT cells, eATP following a 30 minute treatment with A-769662 concentrations of 25, 50, 75 and 100μM, increased by 1.6, 3.1, 4.6 and 5.1-fold from vehicle respectively, which was significantly different from vehicle-treated at 100μM A-769662. (Figure 4.11B). In the KO cells, eATP increased by 2.2, 6.7, 8.6 and 10-fold when treated with 25, 50, 75 and 100μM A-769662 compared to vehicle, which was significant at 75 and 100μM (Figure 4.11C; n=3; $p<0.05$). Baseline eATP in the MEF α1/α2 AMPK KO cells was 9.1-fold lower than that of the MEF WT cells (69.3 ± 18.9 in WT and 7.6 ± 1.4 pmol/ml in KO). Total ATP in untreated MEF WT cells was 1.9-fold higher than that of MEF α1/α2 AMPK KO cells (Figure 4.11E; n=4; $p<0.05$; Completed by Craig Beall, included here for

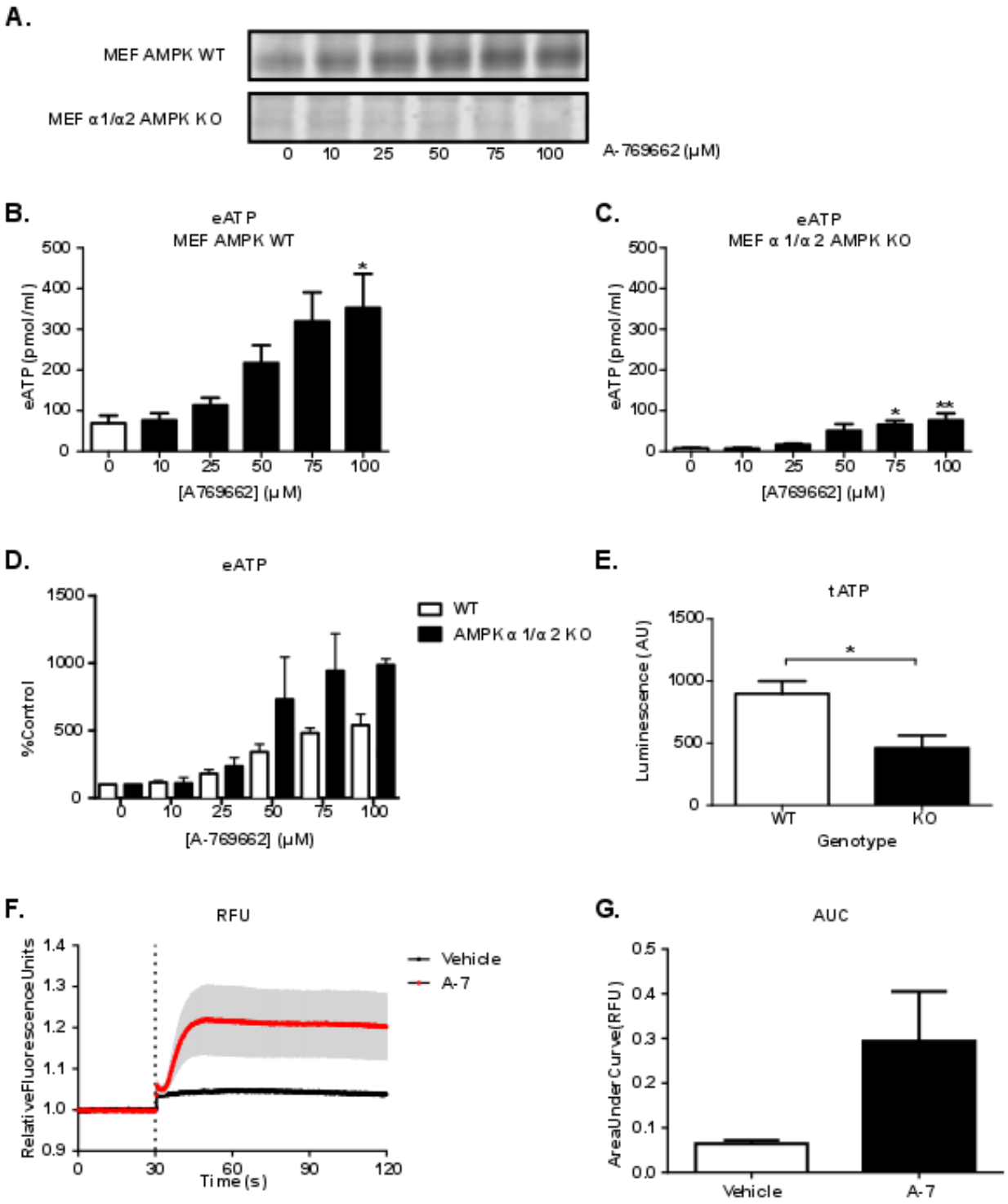

Figure 4.11. A-769662 increases ATP release and intracellular calcium in α1/α2 AMPK KO MEF cells. A. Representative blots of pAMPK in lysates of MEF WT or α1/α2 AMPK KO cells treated with increasing concentrations of A-769662 for 30min. **B.** Extracellular ATP at the end of the experiment above conducted in MEF WT cells (n=3). **C.** Extracellular ATP at the end of the experiment above conducted in MEF α1/α2 AMPK KO cells (n=3). **D.** Graph representing the combined data from figures B and C normalised to 100% using their respective controls (n=3). **E.** Total ATP in MEF WT and α1/α2 AMPK KO cells (n=4). **F.** Relative fluorescence units from MEF α1/ α2 AMPK KO cells treated with vehicle (0.1% DMSO) or A-769662 (100μM) at t=30 (n=3). **G.** Total area under the curve for the two treatment groups generated from figure F. (n=3). **A-B.** 1-way ANOVA with Bonferroni's multiple comparison test. **E&G.** Unpaired t test. **F.** 2-way ANOVA with Bonferroni's multiple comparison test. * p≤0.05, ** p≤0.01, *** p≤0.001

completion). This change in tATP is not sufficient to explain the decrease in baseline eATP observed.

MEF α1/α2 AMPK KO cells exposed to A-769662 (100μM), displayed a trend for an increase in $[Ca^{2+}]_i$ peak response (1.2-fold) and AUC (4.6-fold) when compared to vehicle-treated cells, which was not significant (Figure 4.11F&G; n=3; p=0.1077; Completed by Aman Malhi, included here for completion). This study is underpowered and more data would be needed to complete it.

This study showed that, despite the absence of functional AMPK, A-769662 still induced a concentration-dependent increase in eATP and $[Ca^{2+}]_i$ in MEF α1/α2 AMPK KO cells. This shows that certain aspects of the A-769662 effect on cells may be AMPK-independent.

4.3 Discussion

A-769662, AICAR and Metformin are well used pharmacological agents acting through distinctly different mechanisms (Guigas *et al.*, 2009; Rena *et al.*, 2013). Our first aim was to investigate the actions of these drugs on astrocytes *in vitro*, to identify an appropriate drug to imitate AMPK activation during hypoglycaemia.

A-769662 acts to directly activate AMPK and prevent its dephosphorylation, making it a potent AMPK activator (Cool *et al.*, 2006). AICAR on the other hand enters the cell and is phosphorylated to ZMP which acts as an AMP mimic, directly binding to the γ-subunit to activate AMPK (Day *et al.*, 2007). This difference in AMPK activation mechanism between these two drugs could explain the difference in potency. Metformin has not been shown to directly activate AMPK, and it's mechanism of action is not yet fully understood (Rena *et al.*, 2013).

Our studies show that A-769662 is indeed the most potent AMPK activator out of the three tested, and acts to strongly activate AMPK in a concentration-dependent manner (Figure 4.2.1). AICAR activated AMPK, although to a much lesser degree when compared to A-769662. Both compounds also caused a significant increase in ACC phosphorylation, one of the downstream targets of AMPK, indicating they both increase AMPK activity and not just phosphorylation. Metformin had no significant effect on AMPK or ACC phosphorylation at the concentration and time points used in this study. Previous studies on primary astrocytes have shown effects of metformin on

glycolysis at a concentration of 10mM for 2 hours (Westhaus *et al.*, 2015) and on ketogenesis at a concentration of 1mM for 24 hours (Takahashi *et al.*, 2014). It is possible that a longer incubation or higher concentration was required for sufficient metformin action in our experiments. It is not known if U373 cells express the organic cation transporter 1 (OCT1), one of the most recognised mechanisms for uptake of metformin, which would require a longer incubation time, as seen in other OCT1-deficient cell lines like HEK293, which require a 16 hour incubation (Hawley *et al.*, 2010).

A-769662 also caused a large increase in eATP initially suggesting that AMPK activation may be driving ATP release from these cells. The same effect of A-769662 on eATP was observed in both U373 cells and CRTAS, demonstrating that this effect is not specific to U373 cells. Unlike A-769662, AICAR did not alter eATP. It is possible that AICAR may be acting to prevent increase in ATP release through changes in intracellular ATP or ADP:ATP ratio. Studies disagree on whether AICAR alters intracellular energy stores, and some show no effect on the ADP:ATP ratio (Gadalla *et al.*, 2004; Hawley *et al.*, 2010). Others studies, however, show a decrease in total ATP, which could be responsible for masking changes in eATP (Craig Beall, personal communication, unpublished). Another explanation might be that A-769662 induces ATP release through an AMPK-independent mechanism, as indicated by later experiments.

The eATP in the CM at the end of the 3 hour treatment was lower than that in the 30 minute treatment. The increased volume of media used in the 3 hour treatments alone is not enough to explain the 2.5-fold lower eATP. The smaller

volume in the 30 minute treatments may be leading to an increase in [eATP], which in turn may be driving ATP-induced ATP release. It is possible this effect is lost in the 3 hour experiment, where the higher media volume may be diluting the original [eATP]. We performed a pilot study using Bz-ATP to measure ATP-induced ATP release, however this drug was found to interact with the assay used to measure eATP. Another, non-hydrolysable ATP analogue would need to be used to measure ATP-induced ATP release. Another explanation for the difference between the 30 minute and 3-hour CM eATP could be the action of ecto-nucleotidases. Preliminary studies we performed showed indications of regulated ecto-nucleotidase activity in astrocyte cultures, whereby eATP was greatly increased in euglycaemic compared to hypoglycaemic conditions in the presence of the eATPase inhibitor ARL 67156. This indicates that eATPases are present in our astrocytic cultures, and their activity can be regulated depending on conditions. This means that, following the 3 hour incubation in our experiments, eATPase activity might be upregulated, resulting in a reduced eATP accumulation compared to our 30 minute controls.

A-769662 treatment also caused an increase in eLactate. Extracellular lactate as well as AMPK activity have been shown to play an important role in the CRR. VMH lactate infusion decreases the CRR to hypoglycaemia (Borg *et al.*, 2003) and raises VMH GABA (Zhou *et al.*, 2010). Suppression in VMH GABA signalling is necessary for the release of glucagon and adrenaline, and initiation of the CRR (Zhou *et al.*, 2010), something that is prevented by an increase in VMH lactate. Whilst lactate can be transferred across the brain-blood barrier, it can also be produced by astrocytes in conditions of high energy demand (Pellerin and Magistretti, 2012). Astrocytes are highly glycolytic and are geared

towards lactate production. They highly express glucose transporters, as well as LDH1 and 5, making them highly efficient at glucose uptake and subsequent conversion to lactate which can be exported out of the cell through MCT 1, 2 and 4. Alternatively, GS and GP expression allow for glucose conversion into glycogen for storage which can be broken down when necessary. Energy stress causes AMPK activation, therefore it is plausible that AMPK activation in astrocytes may be driving lactate production and release to support neuronal function. As with the changes observed in eATP, AICAR seemed to have no significant effect on eLactate. If this increase in eLactate is a result of AMPK activation, it is possible that the lack of response with AICAR treatment is due to insufficient AMPK activation. Changes in eLactate are only observed following 100μM A-769662, which also causes a 6.6-fold increase in pAMPK. AICAR (1mM) only caused a 1.5-fold increase in pAMPK, which may not be sufficient to alter lactate production and release (Figure 4.1C&I). It is also possible that this is another AMPK-independent effect of A-769662.

Extracellular lactate is much higher at the end of a 3 hour time point when compared to the 30 minute time point. This is possibly due to lactate accumulating in the media over time. The cells in all treatment groups should have an equivalent amount of glycogen stored and capacity for glycogen and glucose breakdown at the beginning of the experiment, as they come from a homogeneous cell population which has been treated identically up to the point of plating for experiments. This means that by the end of the 3 hour stimulation, all cells might have already produced and released the maximum amount of lactate before running low on glycogen, or before auto-inhibition of lactate production and release. Unpublished data from our lab has shown that following

a 3 hour treatment of primary astrocytes with A-769662 (100μM) causes a decrease in GP and increase in GS activity (Craig Beall, personal communication, unpublished), which would lead to an increase in glucose conversion to glycogen, and decrease in glycogen breakdown. The trend for a decrease in eLactate in the 3 hour A-769662 treatment may be a reflection of this.

Co-treatment of astrocytes with A-769662 and AICAR showed a further enhancement of AMPK phosphorylation. This agrees with previous literature, where small concentrations of A-769662 were shown to significantly enhance AICAR-induced AMPK activation (Ducommun *et al.*, 2014). In agreement to previous findings, this study suggests A-769662 and AICAR activate AMPK through separate mechanisms. It also suggests that the changes in eATP are independent of AMPK activation, as supported later by the MEF α1/α2 AMPK KO experiments (Figure 4.11), as there was no further increase in eATP following co-treatment with both drugs compared to A-769662 alone. This would suggest A-769662 may be targeting a separate, AMPK-independent mechanism to mediate its effect on eATP.

Cells were also treated with A-769662 in euglycaemic and hypoglycaemic conditions, to see whether A-769662 and hypoglycaemia-mediated AMPK activation have an additive effect on eATP. There was no difference in eATP in cells treated with A-769662 at euglycaemic vs hypoglycaemic conditions, suggesting that hypoglycaemia-induced increase in pAMPK, and energy status of the cells do not affect A-769662-mediated ATP release. We also examined eLactate to see whether energy status would limit the A-769662-mediated

increase in lactate release. As observed previously, low glucose caused a decrease in eLactate. Even though eLactate following A-769662 treatment in hypoglycaemic was lower than that in euglycaemic conditions, the A-769662-mediated fold-increase in eLactate was greater in hypoglycaemic (1.5-fold) than euglycaemic conditions (1.2-fold). This indicates that the A-769662-mediated increase in eLactate is not dependant on glucose availability. This increase in eLactate could be the result of A-769662 increasing glucose uptake, glycolysis, glycogenolysis, lactate production or lactate transport. AMPK activation is known to increase glucose uptake and glycolysis (Carling, 2004). Studies have suggested that A-769662 also causes an increase in glucose uptake in certain cell types, including muscle in an AMPK-independent mechanism (Treebak *et al.*, 2009), which may explain the further increase we observed with A-769662 treatment in hypoglycaemia.

We showed that co-treatment of cells with both A-769662 and NA, resulted in an increase in eLactate much greater than either drug alone. NA has not been shown to increase pAMPK in our studies or other published research in astrocytes. This additive effect of the two drugs with the lack of AMPK activation suggests that they are likely to be causing this increase in eLactate through different pathways rather than competing for the same pathway to increase lactate production and export. NA is known to increase glycogenolysis in cells (Gibbs, 2015; Subbarao and Hertz, 1990). AMPK activation is known to increase glucose uptake and processing into glycogen (Carling, 2004) and AMPK ablation in astrocytes has been shown to prevent nitric oxide or oligomycin-induced increases in lactate release (Almeida *et al.*, 2004). We can speculate that A-769662 may be causing this increase in eLactate by increasing

glycolysis through AMPK activation, while NA increases eLactate through an increase in glycogenolysis. Evidence suggests A-769662 causes an increase in glucose uptake in muscle, through an AMPK-independent mechanism involving PI3-kinase (Treebak *et al.*, 2009). If this is also true in astrocytes, this could further increase their capacity for lactate production.

From our studies it was not clear whether A-769662-induced ATP release was through vesicular exocytosis. The data showed no significant difference between fluorescence intensity in vehicle-treated or A-769662-treated cells. However, the eATP using the conditions used in the quinacrine imaging protocol, where phenol red-free DMEM with HEPES was used, was reduced compared to that observed with the protocol used in most of our CM experiments using the phenol red-containing DMEM without HEPES (Figure 4.7). To investigate whether HEPES attenuates the A-769662-mediated increase in eATP, the experiment would need to be repeated using an imaging chamber buffered with CO_2. Another option would be to try a different method of detecting changes in vesicular ATP, such as loading the cells with the fluorescent ATP analogue mant-ATP.

Carbenoxolone did not reduce the A-769662-mediated increase in eATP. In U373 cells, contrary to our predictions, carbenoxolone pre-treatment enhanced the A-769662-mediated increase in eATP (Figure 4.6C), something previously observed in brain slices (Frenguelli *et al.*, 2007). A study on endothelial cells showed that a 6 hour treatment with Carbenoxolone (100µM) caused a marked increase in Cx43 expression at both protein and RNA level, and altered

distribution within cells (Sagar and Larson, 2006). Since the main connexins expressed in astrocytes are Cx43 and Cx30 (Dermietzel *et al.*, 1991; Giaume *et al.*, 1991; Giaume *et al.*, 2010), it is not unreasonable to speculate that carbenoxolone treatment of U373 cells results in a compensatory increase in Cx43 expression. There is a scarcity of data on which gap junctions carbenoxolone may have a higher affinity for, although studies indicate that it has a high affinity for pannexins and much lower affinity for connexins (Bruzzone *et al.*, 2005). Blocking gap junctions in primary astrocytes did not affect A-769662-mediated ATP release (Figure 4.6). Preliminary studies have indicated to a higher expression of Cx43 in U373 cells compared to CRTAS (data not shown), which might explain the differences observed in these two cell lines following A-769662 treatment with a carbenoxolone pre-treatment. This difference in Cx43 expression may also partially explain the lower baseline eATP observed in the CRTAS compared to U373 cells. The lack of an attenuation of the A-769662-mediated increase in eATP in CRTAS would suggest that ATP in this case is not released through gap junctions. Apart from the lower affinity of carbenoxolone for connexins and the evidence suggesting it upregulates Cx43 expression, studies also suggest that it blocks VRAC (Benfenati *et al.*, 2009) and P2X7 receptors (Suadicani *et al.*, 2006). A different gap junction blocker should be used to verify these findings, such as the Cx43-selective blocker, TAT-Gap19. Western blotting could be used to examine differences in Cx43 expression in U373 cells following carbenoxolone treatment.

We have shown that A-769662 (75-100uM) causes a significant increase in eATP in astrocytes (U373 and CRTAS) (Figure 4.2.1D & 4.2.2D). Furthermore,

treating astrocytes with A-769662 (100μM) also resulted in a significant increase in $[Ca^{2+}]_i$ (Figure 4.8). Taken together, this data suggests that this increase in eATP may be driven by an increase in $[Ca^{2+}]_i$ caused by the drug. Increases in $[Ca^{2+}]_i$ have previously been shown to induce vesicular ATP release from astrocytes (Bowser and Khakh, 2007). Data concerning the mechanism behind ATP release from astrocytes is conflicting. Some studies suggest that ATP release is mediated through vesicular exocytosis (Lalo *et al.*, 2014), whereas others suggest not, but that ATP is released through hemichannels (Cotrina *et al.*, 1998; Garre *et al.*, 2010), P2X7 receptors (Suadicani *et al.*, 2006), VRAC (Anderson *et al.*, 2004a), or CFTR (Schwiebert *et al.*, 1995).

Increases in $[Ca^{2+}]_i$ can be through several different mechanisms. Intracellular calcium can increase through more influx from the extracellular media. In order to investigate whether this was the source of $[Ca^{2+}]_i$ observed after A-769662 stimulation, the experiment was repeated in calcium-free media. This had effect on the U373 cell line, but lack of extracellular calcium raised baseline eATP in CRTAS (Figure 4.9). Removal of extracellular calcium is a stressful stimulus, and since ATP is a universal danger signal it is possible that it evokes a response in astrocytes. Reduction in extracellular calcium has been shown to cause an increase in $[Ca^{2+}]_I$ in astrocytes in culture, in a phospholipase C-dependant mechanism, involving inositol triphosphate (IP_3) and the release of ATP (Stout and Charles, 2003; Zanotti and Charles, 1997). This could explain the effect we observed in the CRTAS. One main difference between the CRTAS and U373 is that the latter is a transformed cell line, which means they may be

lacking one or more constituents required for this mechanism, which would explain the difference observed between the two cell types. Increased mTOR and S6K1 have been implicated in the tumorigenesis of U373 cells (Nakamura *et al.*, 2008). Our lab has also shown a constitutively active PKB in U373 cells (unpublished data, Craig Beall, personal communication). This suggests there may be a mutation upstream of PKB, such as phosphoinositide 3-kinase (PI3K), which could explain the differences observed. In fact, it has been shown that a hallmark of astrogliomas is a deregulation of the PI3K pathway (Cancer Genome Atlas Research, 2008). Regarding A-769662 stimulation; there was no significant attenuation of the increase in the extracellular ATP in either cell types, suggesting that extracellular calcium is not involved in the drug's effect on ATP release.

Another mechanism by which intracellular calcium can be increased is through release of intracellular calcium stores. To investigate that, we used the intracellular calcium chelator, BAPTA-AM. Chelating intracellular calcium caused a small decrease in ATP release following treatment with A-769662 in the U373 cells and a much larger decrease in CRTAS. This had the biggest effect in HTAS, where there was a significant decrease in ATP release following A-769662 treatment, however, BAPTA-AM seems to also have an effect on extracellular ATP at baseline in these cells (Figure 4.10). In our studies, primary astrocyte eATP was decreased with treatment of BAPTA-AM alone. This contradicts other studies which have shown an increase in ATP release following BAPTA-AM treatment in CRTAS (Anderson *et al.*, 2004a). This observed result could be the result of differences in methodology. BAPTA-AM

was also shown to decrease intracellular ATP in CRTAS (Anderson *et al.*, 2004a). In our studies, tATP and ATP:ADP ratio were only measured in U373 cells, where BAPTA-AM had no effect on baseline eATP, tATP or ATP:ADP. This may be different in the CRTAS; However it was not measured in the current study. Most astroglioma cells show overactivation of the PI3K pathway, which is involved in $[Ca^{2+}]_i$ mobilisation (Cancer Genome Atlas Research, 2008), which may be responsible for the differences we observe between U373 cells and primary astrocytes regarding $[Ca^{2+}]_i$ chelation. This could also be the result of the comparably higher (~4 times higher) baseline eATP of U373 cells compared to the primary astrocytes masking the effect of chelating intracellular or removing extracellular calcium.

To investigate whether the effect observed of A-769662 treatment on astrocytes is a result of AMPK activation, the studies were repeated in MEF α1/α2 AMPK KO cells. The increase in intracellular calcium as well as the increase in extracellular ATP was preserved in the MEF α1/α2 AMPK KO cells following stimulation with A-769662 (Figure 4.11). This indicates that whether the increase in intracellular calcium and eATP are related or not, neither are a result of AMPK activity. It is possible that A-769662 targets an AMPK-independent pathway which results in the release of intracellular calcium stores, driving ATP release from the cell. This is an effect of A-769662 that has not previously been reported. Whilst some studies have previously indicated A-769662 may have AMPK-independent effects, none of them looked at eATP. Moreno et al showed an increase in 26S proteasome activity in MEF cells and an increase in toxicity and apoptosis following a treatment with A-769662, both of which were AMPK-independent (Moreno *et al.*, 2008). Treeback et al reported PI3K-dependent

increase in glucose uptake in muscle that was AMPK-independent (Treebak *et al.*, 2009). This suggests A-769662 may have AMPK-independent effects on cellular function. It is important to note that in these experiments high concentrations of A-769662 were used. During the original identification and characterisation of A-769662, the EC_{50} was determined to be in the low µM range for the tissues examined (<10µM), and any cross-reactivity was studied at 10µM (Cool *et al.*, 2006). In our experiments the effects of A-769662 on eATP and $[Ca^{2+}]_i$ were observed at concentrations from 50µM and above, which would suggest that A-769662 has off-target effects at higher concentrations. Many studies use A-769662 at concentrations above 100µM, which raises the question of whether the effects they are observing are a result of AMPK activation as suggested. It is important to report this off-target effect of high concentrations of A-769662 on eATP, as eATP is an inflammatory mediator, which can then act on purinergic receptors to induce cytokine release and immune responses. Some of the effects of A-769662 observed in studies using high concentrations may not be the result of AMPK activation, but of inflammatory and immune responses mediated by this increase in eATP, therefore, care must be taken when interpreting data obtained using this drug.

Chapter 5: Conclusions

Whole body energy homeostasis is regulated through both peripheral as well as central organs, with the hypothalamus being one of the most important central regulators of energy homeostasis. The central response to hypoglycaemia undergoes maladaptive changes following RH which result in impaired CRR to hypoglycaemia (Arbelaez *et al.*, 2008; LaGamma *et al.*, 2014; McCrimmon *et al.*, 2006; Segel *et al.*, 2002). Whilst both glucosensing neurones, and astrocytes are in part involved in the hormonal response to hypoglycaemia, the majority of studies only focus on glucosensing neurones, or whole brain areas, with little work on astrocytes specifically. The aim of this study was to investigate whether astrocytes can intrinsically detect and respond to hypoglycaemia, and whether RH results in adaptive responses in astrocytic gliotransmission.

AMPK activity in the VMH has been implicated in the development of impaired CRR to hypoglycaemia, where inhibition results in blunted counter regulation of hypoglycaemia (Han *et al.*, 2005; McCrimmon *et al.*, 2008), and activation can reverse RH-induced impairment in the CRR to hypoglycaemia (McCrimmon *et al.*, 2006; McCrimmon *et al.*, 2004). The role of AMPK in neurones, particularly glucosensing neurones in the VMH, has been well-characterised (Beall *et al.*, 2012b; Taib *et al.*, 2013); However the role of AMPK in astrocytes has not been extensively studied. In this study hypoglycaemia caused an increase in astrocytic pAMPK. This response is common across most cells and acts on

downstream targets to decrease anabolic and increase catabolic processes, thus conserving energy (Taib *et al.*, 2013).

During exposure to hypoglycaemic conditions, astrocytes maintained eLactate levels for at least 15min. At the later time points (30, 180min), eLactate decreased; However, this decrease did not reflect the decrease in glucose availability, even following 180min. This suggests that astrocytes can maintain lactate production and export even in prolonged hypoglycaemic conditions. This is likely mediated through increased glucose uptake and glycolysis, both of which can be a direct result of AMPK activation (Carling, 2004), as well as through increased glycogenolysis. It is important to bear in mind that in this study there is no lactate demand from neurones, which could potentially drive astrocytic lactate production and release *in* vivo or in a co-culture set-up.

During hypoglycaemia, astrocytes are likely to be exposed to a variety of hormones, in addition to a decrease in glucose availability. For example, during hypoglycaemia, NA is released from the hindbrain directly to the hypothalamus (Palkovits *et al.*, 1980). Our study showed that exposing astrocytes to NA in euglycaemic and hypoglycaemic conditions causes a large increase in eLactate, indicating that astrocytic lactate production and export can be further stimulated by NA during a hypoglycaemic stimulus. Although not directly addressed in the current study, this increased lactate production may be a result of increased glycogenolysis by NA, in conjunction with increased glucose uptake and/or glycolysis as a result of increased AMPK activity during hypoglycaemic conditions.

Our study showed that astrocytes intrinsically respond to hypoglycaemic conditions. The next step was to investigate whether these responses change following exposure to RH. Following RH, there was a blunted pAMPK response to further hypoglycaemia although this did not translate to changes in lactate release following RH. In other tissues, AMPK activation increases glucose uptake and glycolysis (Carling, 2004), therefore a decrease in eLactate would be expected if AMPK activation is blunted. It is possible that the attenuated pAMPK response to hypoglycaemia is not sufficient to cause a significant change in eLactate. Another potential explanation is that, according to the glycogen supercompensation hypothesis, cells exposed to RH may have a larger glycogen store (Canada *et al.*, 2011; Oz *et al.*, 2009), allowing increased lactate production through glycogenolysis. An important additional study would be to measure glycogen content following RH. If there are no changes in glycogen storage in astrocytes following RH, a co-culture of astrocytes with neurones may prove a more representative model, as it would account for any substances released by neurones, and would provide astrocytes with a lactate demand from the neurones during hypoglycaemic conditions.

Despite there not being a significant change in eATP during a single hypoglycaemic stimulus, there was a trend for an increase. This small increase was significantly attenuated following RH. Accurately measuring eATP is challenging, as eATPases can rapidly break down eATP (Zimmermann *et al.*, 2012). This means that taking measurements at specific time points can result in a high variability in the resulting eATP measurements, masking small

changes. A more effective way of measuring eATP during a hypoglycaemic stimulus, is using biosensors (Llaudet *et al.*, 2005), which can take a real-time measure of eATP. This can be used in cultured cells, or in brain slices. Using ATP biosensors in brain slices would also take into account neuronal signalling onto astrocytes, which may enhance or blunt the changes in eATP observed during hypoglycaemic stimulus. Astrocytes respond to changes in their environment, as well as neuronal and other glial transmission. Glucosensing neurones respond to hypoglycaemic stimulus by releasing a variety of neurotransmitters and hormones, such as NA, ACTH and glucocorticoid (Palkovits *et al.*, 1980; Watts and Donovan, 2010). The exposure of astrocytes to these at the same time as the hypoglycaemic stimulus could alter the eATP response to hypoglycaemia. Extracellular ATP is a universal danger signal and neuromodulator (Idzko *et al.*, 2014) through activation of purinergic receptors. This leads to increases in $[Ca^{2+}]_I$ and can cause calcium wave propagation amongst astrocytes (Bowser and Khakh, 2007; Cotrina *et al.*, 1998). ATP can also lead to cytokine release and recruitment of microglia (Idzko *et al.*, 2014). Therefore, the blunted eATP response to hypoglycaemia could result in blunted ATP-induced ATP release and diminished calcium wave propagation. The next step in this study could be the investigation of calcium wave propagation following RH. Astrocytic cytokine release following RH could also be studied, as well as microglial recruitment.

To investigate whether the blunted eATP response following RH was a result of the attenuated pAMPK response, a variety of AMPK activating drugs were used and pAMPK and eATP were measured. Of the three AMPK activators tested,

only A-769662 resulted in an increase in eATP in a concentration-dependent manner. Co-application of A-769662 and AICAR enhanced AMPK activation as shown previously (Ducommun *et al.*, 2014), but it had no further effect on eATP, suggesting the changes in eATP observed are not a result of AMPK activation, as later confirmed using MEF α1/α2 AMPK KO model. Similarly, exposing astrocytes to a hypoglycaemic stimulus in the presence of A-769662 had no further effect on the A-769662-mediated increase in eATP. Treating MEF α1/α2 AMPK KO cells to A-769662 also resulted in a concentration-dependent increase in eATP, further supporting the hypothesis that changes in eATP observed during drug treatment or low glucose are not a result of AMPK activation.

It is important to point out that in our experiments, A-769662 resulted in AMPK-independent changes in eATP as well as $[Ca^{2+}]_i$. Whilst A-769662 has been thought of as one of the most potent and specific AMPK activators, our studies suggest that it may have AMPK-independent effects, which could result in inflammatory signalling as a result of the increased eATP (Idzko *et al.*, 2014). This may lead to incorrect conclusions from studies using this drug at concentrations of 50 μM and higher, if the assumption is that all results obtained are due to direct AMPK activation. There have been a several studies the past few years suggesting that A-769662 may mediate some of its effects through AMPK-independent mechanisms, specifically on glucose uptake (Treebak *et al.*, 2009) and proteosomal activity (Moreno *et al.*, 2008); However this mechanism has not yet been identified. Our studies suggest that the changes observed in eATP were not a result of ATP release through gap junctions, and were not

driven by the influx of calcium from the extracellular space. There was some inhibition following chelation of intracellular calcium stores, suggesting that A-769662 may be triggering the release of intracellular stores, resulting in ATP release.

In conclusion, we have shown that astrocytes intrinsically detect and respond to a hypoglycaemic stimulus, measured through an increase in AMPK activation. The resulting increase in pAMPK and eATP, are moderately blunted following RH. We have further shown that the changes in pAMPK and eATP following a hypoglycaemic or pharmacological stimulus are two independent processes. This led us to the discovery that the well-known AMPK activating drug A-769662, has an AMPK-independent effect on eATP and $[Ca^{2+}]_i$, which may influence the interpretation of data obtained using this drug. The mechanism behind A-769662-induced increase in eATP is still unknown, but may involve release of calcium from intracellular stores.

This is the first study to report on the effects of RH on human as well as primary mouse astrocytes. Further studies on glycogen storage, cytokine release, calcium wave propagation and microglial recruitment would allow us to determine what impact these changes may have on cell-to-cell interactions. Investigating the effect of RH in astrocyte-neuron co-cultures would allow us to study this further and determine the molecular adaptations in both, and how these interact. Further studies would also be required to determine what target A-769662 mediates its effects on eATP and $[Ca^{2+}]_i$ through, to enable better interpretation of results using this drug.

Supplementary figures

S1

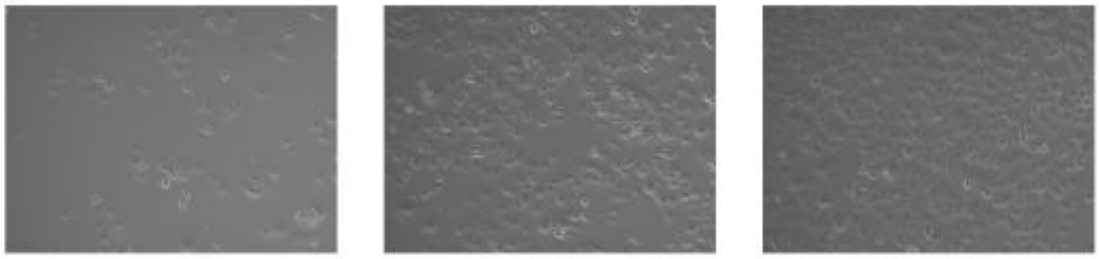

150,000 450,000 1,000,000

S2

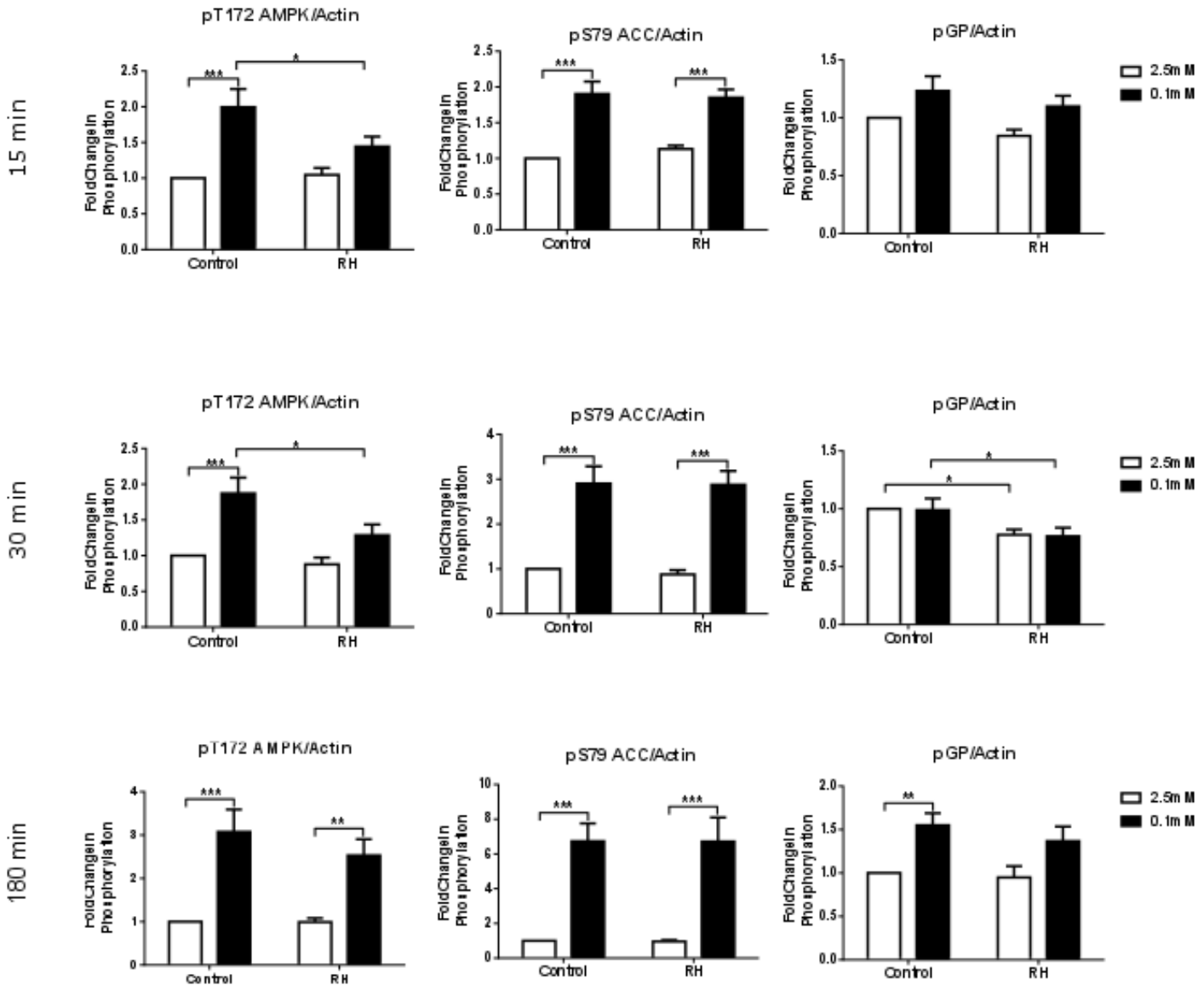
15 min
30 min
180 min
pT172 AMPK/Actin
pS79 ACC/Actin
pGP/Actin
Fold Change in Phosphorylation
Control
RH
2.5m M
0.1m M

S3

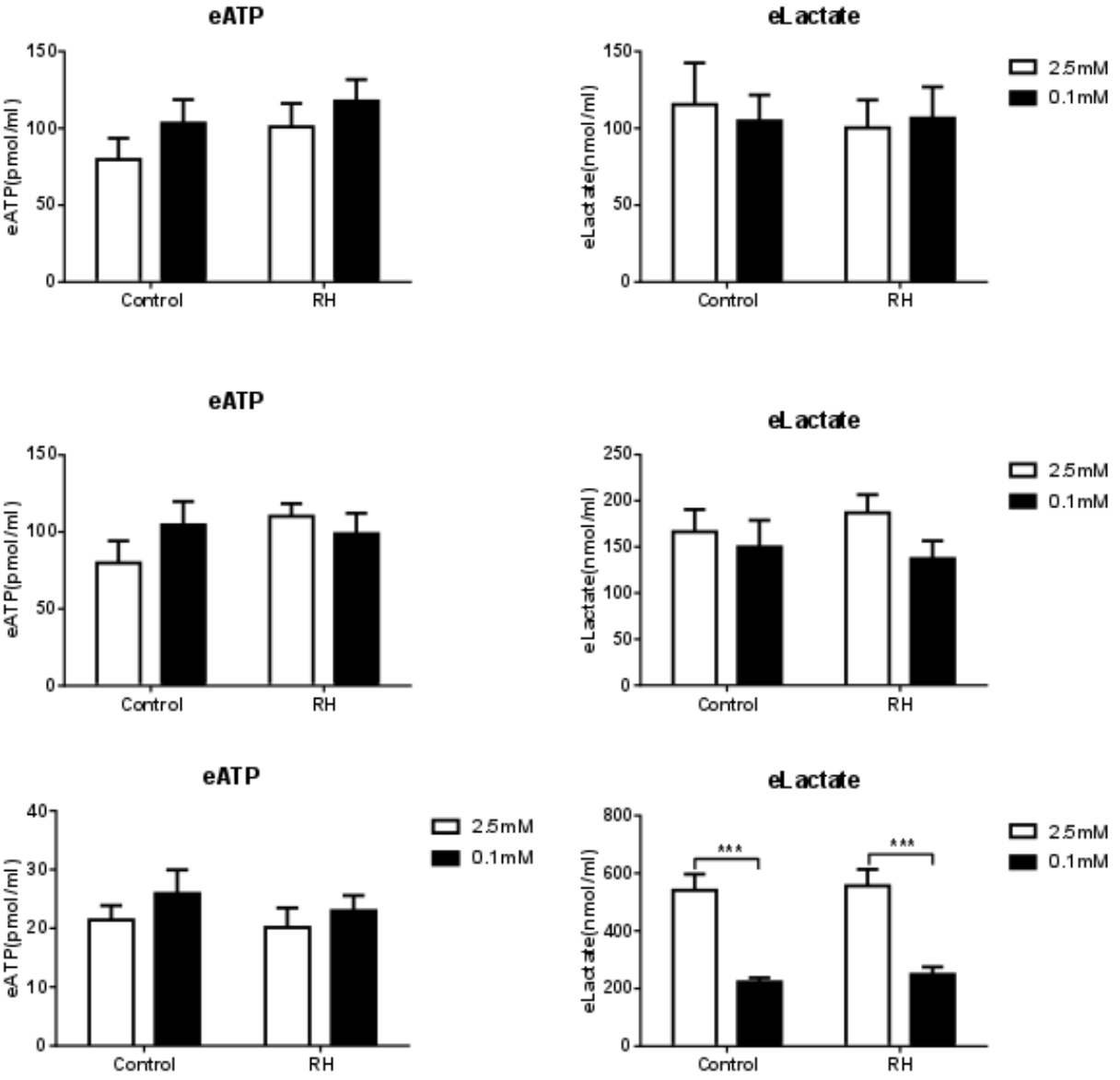
eATP
eATP(pmol/ml)
150
100
50
0
Control
RH
eLactate
eLactate(nmol/ml)
250
200
150
100
50
0
2.5mM
0.1mM
40
30
20
10
800
600
400
200
***

S3

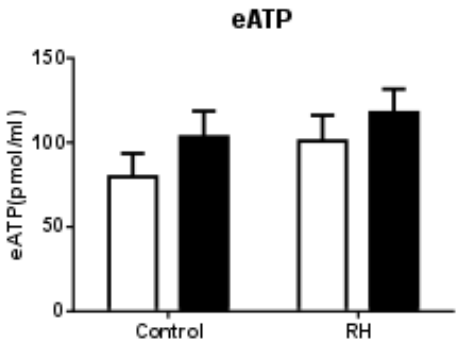
eATP
eATP(pmol/ml)
150
100
50
0
Control
RH

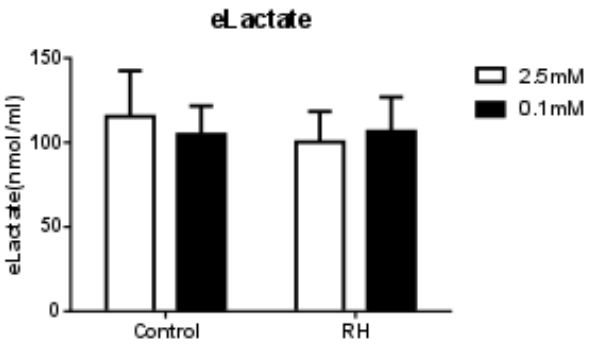
eLactate
eLactate(nmol/ml)
150
100
50
0
Control
RH
2.5mM
0.1mM

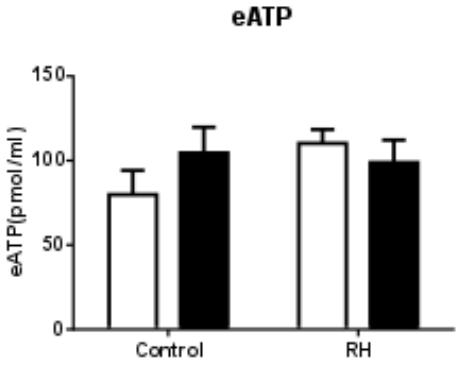
eATP
eATP(pmol/ml)
150
100
50
0
Control
RH

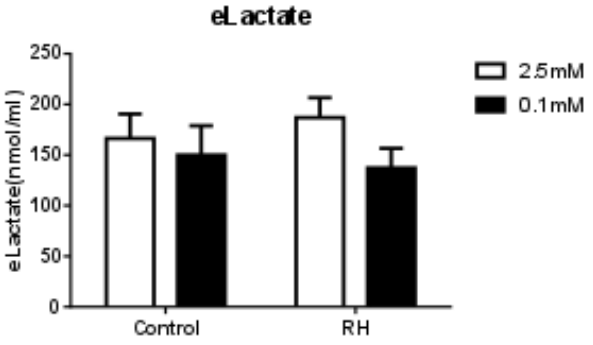
eLactate
eLactate(nmol/ml)
250
200
150
100
50
0
Control
RH
2.5mM
0.1mM

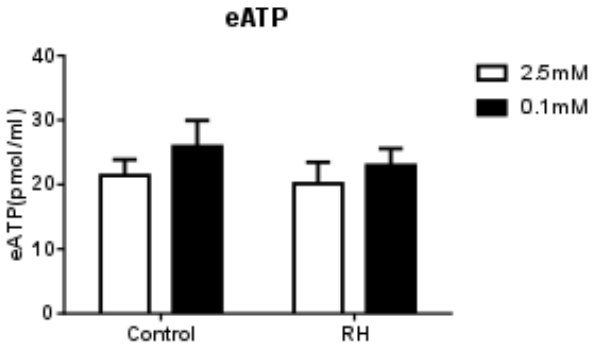
eATP
eATP(pmol/ml)
40
30
20
10
0
Control
RH
2.5mM
0.1mM

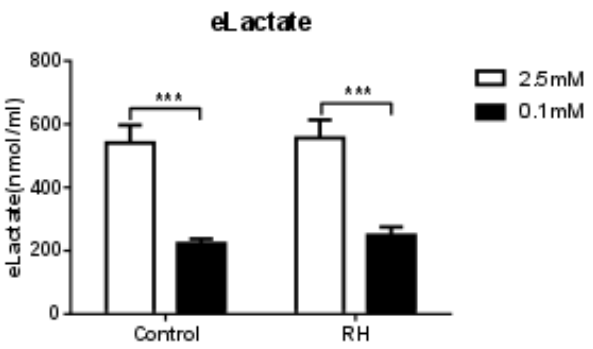
eLactate
eLactate(nmol/ml)
800
600
400
200
0
***
***
Control
RH
2.5mM
0.1mM

S4

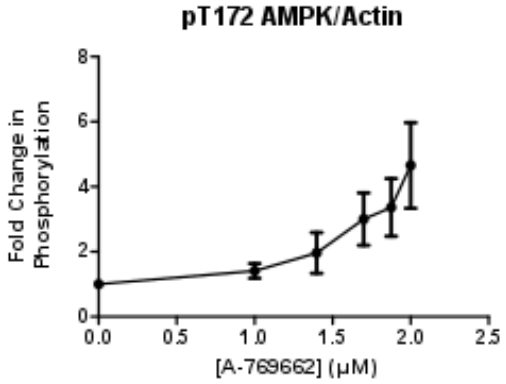
pT172 AMPK/Actin
Fold Change in Phosphorylation
0
2
4
6
8
0.0
0.5
1.0
1.5
2.0
2.5
[A-769662] (µM)

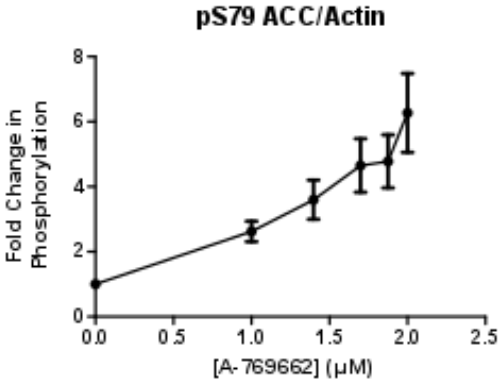
pS79 ACC/Actin
Fold Change in Phosphorylation
0
2
4
6
8
0.0
0.5
1.0
1.5
2.0
2.5
[A-769662] (µM)

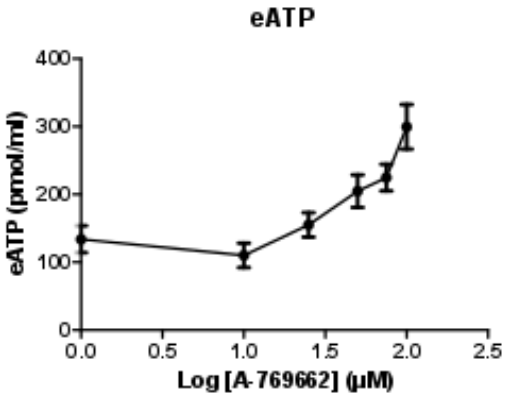
eATP
eATP (pmol/ml)
0
100
200
300
400
0.0
0.5
1.0
1.5
2.0
2.5
Log [A-769662] (µM)

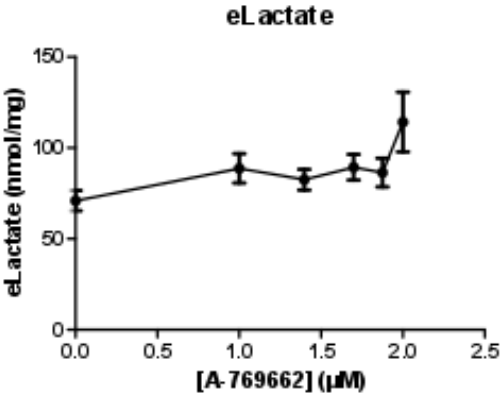
eLactate
eLactate (nmol/mg)
0
50
100
150
0.0
0.5
1.0
1.5
2.0
2.5
[A-769662] (µM)

S5

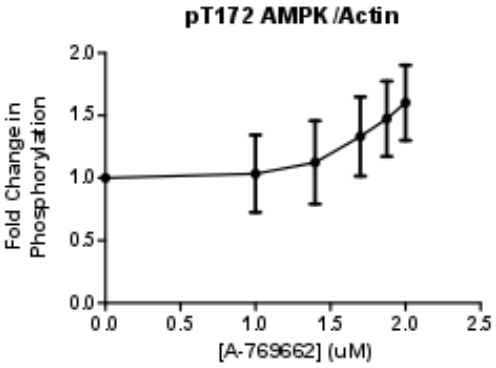
pT172 AMPK /Actin
Fold Change in Phosphorylation
2.0
1.5
1.0
0.5
0.0
0.0
0.5
1.0
1.5
2.0
2.5
[A-769662] (uM)

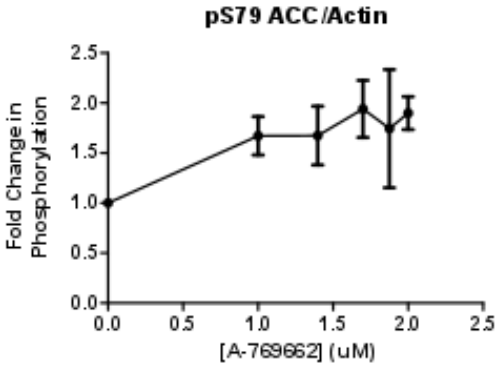
pS79 ACC /Actin
Fold Change in Phosphorylation
2.5
2.0
1.5
1.0
0.5
0.0
0.0
0.5
1.0
1.5
2.0
2.5
[A-769662] (uM)

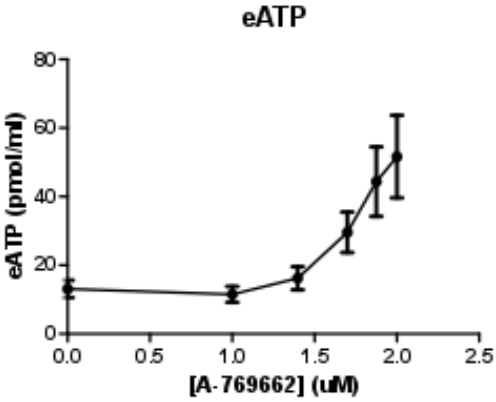
eATP
eATP (pmol/ml)
80
60
40
20
0
0.0
0.5
1.0
1.5
2.0
2.5
[A-769662] (uM)

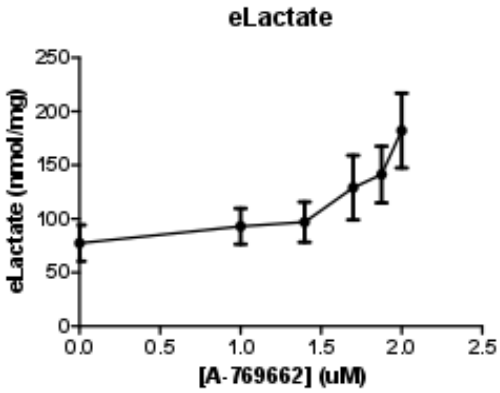
eLactate
eLactate (nmol/mg)
250
200
150
100
50
0
0.0
0.5
1.0
1.5
2.0
2.5
[A-769662] (uM)

S6

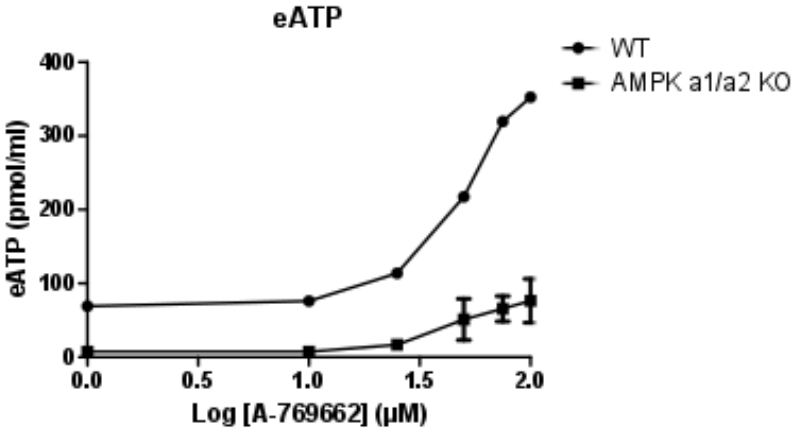
eATP
WT
AMPK a1/a2 KO
eATP (pmol/ml)
400
300
200
100
0
0.0
0.5
1.0
1.5
2.0
Log [A-769662] (µM)

References

Akopova, I., Tatur, S., Grygorczyk, M., Luchowski, R., Gryczynski, I., Gryczynski, Z., Borejdo, J., and Grygorczyk, R. (2012). Imaging exocytosis of ATP-containing vesicles with TIRF microscopy in lung epithelial A549 cells. Purinergic Signal 8, 59-70.

Alberti, K.G., and Zimmet, P.Z. (1998). Definition, diagnosis and classification of diabetes mellitus and its complications. Part 1: diagnosis and classification of diabetes mellitus provisional report of a WHO consultation. Diabet Med 15, 539-553.

Allard, C., Carneiro, L., Collins, S.C., Chretien, C., Grall, S., Penicaud, L., and Leloup, C. (2013). Alteration of hypothalamic glucose and lactate sensing in 48h hyperglycemic rats. Neurosci Lett 534, 75-79.

Allard, C., Carneiro, L., Grall, S., Cline, B.H., Fioramonti, X., Chretien, C., Baba-Aissa, F., Giaume, C., Penicaud, L., and Leloup, C. (2014). Hypothalamic astroglial connexins are required for brain glucose sensing-induced insulin secretion. J Cereb Blood Flow Metab 34, 339-346.

Almeida, A., Moncada, S., and Bolanos, J.P. (2004). Nitric oxide switches on glycolysis through the AMP protein kinase and 6-phosphofructo-2-kinase pathway. Nat Cell Biol 6, 45-51.

Alquier, T., Kawashima, J., Tsuji, Y., and Kahn, B.B. (2007). Role of hypothalamic adenosine 5'-monophosphate-activated protein kinase in the impaired counterregulatory response induced by repetitive neuroglucopenia. Endocrinology 148, 1367-1375.

Anderson, C.M., Bergher, J.P., and Swanson, R.A. (2004a). ATP-induced ATP release from astrocytes. J Neurochem 88, 246-256.

Anderson, S.N., Cool, B.L., Kifle, L., Chiou, W., Egan, D.A., Barrett, L.W., Richardson, P.L., Frevert, E.U., Warrior, U., Kofron, J.L., and Burns, D.J. (2004b). Microarrayed compound screening (microARCS) to identify activators and inhibitors of AMP-activated protein kinase. J Biomol Screen 9, 112-121.

Araque, A., Carmignoto, G., Haydon, P.G., Oliet, S.H., Robitaille, R., and Volterra, A. (2014). Gliotransmitters travel in time and space. Neuron 81, 728-739.

Araque, A., Parpura, V., Sanzgiri, R.P., and Haydon, P.G. (1999). Tripartite synapses: glia, the unacknowledged partner. Trends Neurosci 22, 208-215.

Arbelaez, A.M., Powers, W.J., Videen, T.O., Price, J.L., and Cryer, P.E. (2008). Attenuation of counterregulatory responses to recurrent hypoglycemia by active thalamic inhibition: a mechanism for hypoglycemia-associated autonomic failure. Diabetes 57, 470-475.

Arulkumaran, N., Unwin, R.J., and Tam, F.W. (2011). A potential therapeutic role for P2X7 receptor (P2X7R) antagonists in the treatment of inflammatory diseases. Expert Opin Investig Drugs 20, 897-915.

Ashcroft, F.M., and Rorsman, P. (1990). ATP-sensitive K+ channels: a link between B-cell metabolism and insulin secretion. Biochem Soc Trans 18, 109-111.

Ashford, M.L., Boden, P.R., and Treherne, J.M. (1990). Glucose-induced excitation of hypothalamic neurones is mediated by ATP-sensitive K+ channels. Pflugers Arch 415, 479-483.

Avogaro, A., Gnudi, L., Valerio, A., Maran, A., Miola, M., Opportuno, A., Tiengo, A., and Bier, D.M. (1993). Effects of different plasma glucose concentrations on lipolytic and ketogenic responsiveness to epinephrine in type I (insulin-dependent) diabetic subjects. J Clin Endocrinol Metab 76, 845-850.

Balfour, R.H., Hansen, A.M., and Trapp, S. (2006). Neuronal responses to transient hypoglycaemia in the dorsal vagal complex of the rat brainstem. J Physiol 570, 469-484.

Banarer, S., and Cryer, P.E. (2003). Sleep-related hypoglycemia-associated autonomic failure in type 1 diabetes: reduced awakening from sleep during hypoglycemia. Diabetes 52, 1195-1203.

Banting, F.G., Best, C.H., Collip, J.B., Campbell, W.R., and Fletcher, A.A. (1922). Pancreatic Extracts in the Treatment of Diabetes Mellitus. Can Med Assoc J 12, 141-146.

Banting, F.G., Campbell, W.R., and Fletcher, A.A. (1923). Further Clinical Experience with Insulin (Pancreatic Extracts) in the Treatment of Diabetes Mellitus. Br Med J 1, 8-12.

Beall, C., Ashford, M.L., and McCrimmon, R.J. (2012a). The physiology and pathophysiology of the neural control of the counterregulatory response. Am J Physiol Regul Integr Comp Physiol 302, R215-223.
Beall, C., Hamilton, D.L., Gallagher, J., Logie, L., Wright, K., Soutar, M.P., Dadak, S., Ashford, F.B., Haythorne, E., Du, Q*., et al.* (2012b). Mouse hypothalamic GT1-7 cells demonstrate AMPK-dependent intrinsic glucose-sensing behaviour. Diabetologia 55, 2432-2444.
Beall, C., Piipari, K., Al-Qassab, H., Smith, M.A., Parker, N., Carling, D., Viollet, B., Withers, D.J., and Ashford, M.L. (2010). Loss of AMP-activated protein kinase alpha2 subunit in mouse beta-cells impairs glucose-stimulated insulin secretion and inhibits their sensitivity to hypoglycaemia. Biochem J 429, 323-333.
Beall, C., Watterson, K.R., McCrimmon, R.J., and Ashford, M.L. (2013). AMPK modulates glucose-sensing in insulin-secreting cells by altered phosphotransfer to KATP channels. J Bioenerg Biomembr 45, 229-241.
Beg, Z.H., Allmann, D.W., and Gibson, D.M. (1973). Modulation of 3-hydroxy-3-methylglutaryl coenzyme A reductase activity with cAMP and with protein fractions of rat liver cytosol. Biochem Biophys Res Commun 54, 1362-1369.
Benfenati, V., Caprini, M., Nicchia, G.P., Rossi, A., Dovizio, M., Cervetto, C., Nobile, M., and Ferroni, S. (2009). Carbenoxolone inhibits volume-regulated anion conductance in cultured rat cortical astroglia. Channels (Austin) 3, 323-336.
Bennett, M.V., Contreras, J.E., Bukauskas, F.F., and Saez, J.C. (2003). New roles for astrocytes: gap junction hemichannels have something to communicate. Trends Neurosci 26, 610-617.
Bergeron, R., Previs, S.F., Cline, G.W., Perret, P., Russell, R.R., 3rd, Young, L.H., and Shulman, G.I. (2001). Effect of 5-aminoimidazole-4-carboxamide-1-beta-D-ribofuranoside infusion on in vivo glucose and lipid metabolism in lean and obese Zucker rats. Diabetes 50, 1076-1082.
Bezzi, P., and Volterra, A. (2001). A neuron-glia signalling network in the active brain. Curr Opin Neurobiol 11, 387-394.
Blomstrand, F., Venance, L., Siren, A.L., Ezan, P., Hanse, E., Glowinski, J., Ehrenreich, H., and Giaume, C. (2004). Endothelins regulate astrocyte gap junctions in rat hippocampal slices. Eur J Neurosci 19, 1005-1015.
Bloomgarden, Z. (2016). Fear of Hypoglycemia. J Diabetes.
Bodin, P., and Burnstock, G. (2001). Evidence that release of adenosine triphosphate from endothelial cells during increased shear stress is vesicular. J Cardiovasc Pharmacol 38, 900-908.
Borg, M.A., Tamborlane, W.V., Shulman, G.I., and Sherwin, R.S. (2003). Local lactate perfusion of the ventromedial hypothalamus suppresses hypoglycemic counterregulation. Diabetes 52, 663-666.
Borg, W.P., Sherwin, R.S., During, M.J., Borg, M.A., and Shulman, G.I. (1995). Local ventromedial hypothalamus glucopenia triggers counterregulatory hormone release. Diabetes 44, 180-184.
Bowser, D.N., and Khakh, B.S. (2004). ATP excites interneurons and astrocytes to increase synaptic inhibition in neuronal networks. J Neurosci 24, 8606-8620.
Bowser, D.N., and Khakh, B.S. (2007). Vesicular ATP is the predominant cause of intercellular calcium waves in astrocytes. J Gen Physiol 129, 485-491.
Bradford, M.M. (1976). A rapid and sensitive method for the quantitation of microgram quantities of protein utilizing the principle of protein-dye binding. Anal Biochem 72, 248-254.
Broer, S., and Brookes, N. (2001). Transfer of glutamine between astrocytes and neurons. J Neurochem 77, 705-719.
Brown, A.M., Tekkok, S.B., and Ransom, B.R. (2003). Glycogen regulation and functional role in mouse white matter. J Physiol 549, 501-512.
Bruzzone, R., Barbe, M.T., Jakob, N.J., and Monyer, H. (2005). Pharmacological properties of homomeric and heteromeric pannexin hemichannels expressed in Xenopus oocytes. J Neurochem 92, 1033-1043.
Burnstock, G. (1972). Purinergic nerves. Pharmacol Rev 24, 509-581.

Burnstock, G. (2006a). Pathophysiology and therapeutic potential of purinergic signaling. Pharmacol Rev 58, 58-86.
Burnstock, G. (2006b). Purinergic signalling--an overview. Novartis Found Symp 276, 26-48; discussion 48-57, 275-281.
Burnstock, G., and Novak, I. (2013). Purinergic signalling and diabetes. Purinergic Signal 9, 307-324.
Bushong, E.A., Martone, M.E., Jones, Y.Z., and Ellisman, M.H. (2002). Protoplasmic astrocytes in CA1 stratum radiatum occupy separate anatomical domains. J Neurosci 22, 183-192.
Canada, S.E., Weaver, S.A., Sharpe, S.N., and Pederson, B.A. (2011). Brain glycogen supercompensation in the mouse after recovery from insulin-induced hypoglycemia. J Neurosci Res 89, 585-591.
Cancer Genome Atlas Research, N. (2008). Comprehensive genomic characterization defines human glioblastoma genes and core pathways. Nature 455, 1061-1068.
Carling, D. (2004). The AMP-activated protein kinase cascade--a unifying system for energy control. Trends Biochem Sci 29, 18-24.
Carling, D., Zammit, V.A., and Hardie, D.G. (1987). A common bicyclic protein kinase cascade inactivates the regulatory enzymes of fatty acid and cholesterol biosynthesis. FEBS Lett 223, 217-222.
Carlson, C.A., and Kim, K.H. (1973). Regulation of hepatic acetyl coenzyme A carboxylase by phosphorylation and dephosphorylation. The Journal of biological chemistry 248, 378-380.
Cavaliere, F., Amadio, S., Angelini, D.F., Sancesario, G., Bernardi, G., and Volonte, C. (2004). Role of the metabotropic P2Y(4) receptor during hypoglycemia: cross talk with the ionotropic NMDAR1 receptor. Exp Cell Res 300, 149-158.
Chan, O., Cheng, H., Herzog, R., Czyzyk, D., Zhu, W., Wang, A., McCrimmon, R.J., Seashore, M.R., and Sherwin, R.S. (2008). Increased GABAergic tone in the ventromedial hypothalamus contributes to suppression of counterregulatory responses after antecedent hypoglycemia. Diabetes 57, 1363-1370.
Chan, O., Paranjape, S.A., Horblitt, A., Zhu, W., and Sherwin, R.S. (2013). Lactate-induced release of GABA in the ventromedial hypothalamus contributes to counterregulatory failure in recurrent hypoglycemia and diabetes. Diabetes 62, 4239-4246.
Chari, M., Yang, C.S., Lam, C.K., Lee, K., Mighiu, P., Kokorovic, A., Cheung, G.W., Lai, T.Y., Wang, P.Y., and Lam, T.K. (2011). Glucose transporter-1 in the hypothalamic glial cells mediates glucose sensing to regulate glucose production in vivo. Diabetes 60, 1901-1906.
Choi, I.Y., Seaquist, E.R., and Gruetter, R. (2003). Effect of hypoglycemia on brain glycogen metabolism in vivo. J Neurosci Res 72, 25-32.
Chow, E., Bernjak, A., Williams, S., Fawdry, R.A., Hibbert, S., Freeman, J., Sheridan, P.J., and Heller, S.R. (2014). Risk of cardiac arrhythmias during hypoglycemia in patients with type 2 diabetes and cardiovascular risk. Diabetes 63, 1738-1747.
Clark, A.L., Best, C.J., and Fisher, S.J. (2014). Even silent hypoglycemia induces cardiac arrhythmias. Diabetes 63, 1457-1459.
Cool, B., Zinker, B., Chiou, W., Kifle, L., Cao, N., Perham, M., Dickinson, R., Adler, A., Gagne, G., Iyengar, R*., et al.* (2006). Identification and characterization of a small molecule AMPK activator that treats key components of type 2 diabetes and the metabolic syndrome. Cell Metab 3, 403-416.
Corton, J.M., Gillespie, J.G., and Hardie, D.G. (1994). Role of the AMP-activated protein kinase in the cellular stress response. Curr Biol 4, 315-324.
Cotrina, M.L., Lin, J.H., Alves-Rodrigues, A., Liu, S., Li, J., Azmi-Ghadimi, H., Kang, J., Naus, C.C., and Nedergaard, M. (1998). Connexins regulate calcium signaling by controlling ATP release. Proc Natl Acad Sci U S A 95, 15735-15740.
Cryer, P.E. (2002). Hypoglycaemia: the limiting factor in the glycaemic management of Type I and Type II diabetes. Diabetologia 45, 937-948.
Cryer, P.E. (2011). Death during intensive glycemic therapy of diabetes: mechanisms and implications. Am J Med 124, 993-996.

Cummins, C.J., Lust, W.D., and Passonneau, J.V. (1983). Regulation of glycogenolysis in transformed astrocytes in vitro. J Neurochem 40, 137-144.
da Silva Xavier, G., Leclerc, I., Varadi, A., Tsuboi, T., Moule, S.K., and Rutter, G.A. (2003). Role for AMP-activated protein kinase in glucose-stimulated insulin secretion and preproinsulin gene expression. Biochem J 371, 761-774.
Day, P., Sharff, A., Parra, L., Cleasby, A., Williams, M., Horer, S., Nar, H., Redemann, N., Tickle, I., and Yon, J. (2007). Structure of a CBS-domain pair from the regulatory gamma1 subunit of human AMPK in complex with AMP and ZMP. Acta Crystallogr D Biol Crystallogr 63, 587-596.
Dermietzel, R., Hertberg, E.L., Kessler, J.A., and Spray, D.C. (1991). Gap junctions between cultured astrocytes: immunocytochemical, molecular, and electrophysiological analysis. J Neurosci 11, 1421-1432.
Donnelly, L.A., Morris, A.D., Frier, B.M., Ellis, J.D., Donnan, P.T., Durrant, R., Band, M.M., Reekie, G., Leese, G.P., and Collaboration, D.M. (2005). Frequency and predictors of hypoglycaemia in Type 1 and insulin-treated Type 2 diabetes: a population-based study. Diabet Med 22, 749-755.
Duarte, J.M., Oses, J.P., Rodrigues, R.J., and Cunha, R.A. (2007). Modification of purinergic signaling in the hippocampus of streptozotocin-induced diabetic rats. Neuroscience 149, 382-391.
Ducommun, S., Ford, R.J., Bultot, L., Deak, M., Bertrand, L., Kemp, B.E., Steinberg, G.R., and Sakamoto, K. (2014). Enhanced activation of cellular AMPK by dual-small molecule treatment: AICAR and A769662. Am J Physiol Endocrinol Metab 306, E688-696.
Dunn-Meynell, A.A., Routh, V.H., Kang, L., Gaspers, L., and Levin, B.E. (2002). Glucokinase is the likely mediator of glucosensing in both glucose-excited and glucose-inhibited central neurons. Diabetes 51, 2056-2065.
El-Mir, M.Y., Nogueira, V., Fontaine, E., Averet, N., Rigoulet, M., and Leverve, X. (2000). Dimethylbiguanide inhibits cell respiration via an indirect effect targeted on the respiratory chain complex I. The Journal of biological chemistry 275, 223-228.
Fanelli, C., Pampanelli, S., Epifano, L., Rambotti, A.M., Ciofetta, M., Modarelli, F., Di Vincenzo, A., Annibale, B., Lepore, M., Lalli, C., and et al. (1994). Relative roles of insulin and hypoglycaemia on induction of neuroendocrine responses to, symptoms of, and deterioration of cognitive function in hypoglycaemia in male and female humans. Diabetologia 37, 797-807.
Fanelli, C.G., Epifano, L., Rambotti, A.M., Pampanelli, S., Di Vincenzo, A., Modarelli, F., Lepore, M., Annibale, B., Ciofetta, M., Bottini, P., and et al. (1993). Meticulous prevention of hypoglycemia normalizes the glycemic thresholds and magnitude of most of neuroendocrine responses to, symptoms of, and cognitive function during hypoglycemia in intensively treated patients with short-term IDDM. Diabetes 42, 1683-1689.
Foretz, M., Hebrard, S., Leclerc, J., Zarrinpashneh, E., Soty, M., Mithieux, G., Sakamoto, K., Andreelli, F., and Viollet, B. (2010). Metformin inhibits hepatic gluconeogenesis in mice independently of the LKB1/AMPK pathway via a decrease in hepatic energy state. J Clin Invest 120, 2355-2369.
Frayling, C., Britton, R., and Dale, N. (2011). ATP-mediated glucosensing by hypothalamic tanycytes. J Physiol 589, 2275-2286.
Frenguelli, B.G., Wigmore, G., Llaudet, E., and Dale, N. (2007). Temporal and mechanistic dissociation of ATP and adenosine release during ischaemia in the mammalian hippocampus. J Neurochem 101, 1400-1413.
Gadalla, A.E., Pearson, T., Currie, A.J., Dale, N., Hawley, S.A., Sheehan, M., Hirst, W., Michel, A.D., Randall, A., Hardie, D.G., and Frenguelli, B.G. (2004). AICA riboside both activates AMP-activated protein kinase and competes with adenosine for the nucleoside transporter in the CA1 region of the rat hippocampus. J Neurochem 88, 1272-1282.
Gandhi, G.K., Ball, K.K., Cruz, N.F., and Dienel, G.A. (2010). Hyperglycaemia and diabetes impair gap junctional communication among astrocytes. ASN Neuro 2, e00030.

Garre, J.M., Retamal, M.A., Cassina, P., Barbeito, L., Bukauskas, F.F., Saez, J.C., Bennett, M.V., and Abudara, V. (2010). FGF-1 induces ATP release from spinal astrocytes in culture and opens pannexin and connexin hemichannels. Proc Natl Acad Sci U S A 107, 22659-22664.
Geddes, J., Schopman, J.E., Zammitt, N.N., and Frier, B.M. (2008). Prevalence of impaired awareness of hypoglycaemia in adults with Type 1 diabetes. Diabet Med 25, 501-504.
Giaume, C., Fromaget, C., el Aoumari, A., Cordier, J., Glowinski, J., and Gros, D. (1991). Gap junctions in cultured astrocytes: single-channel currents and characterization of channel-forming protein. Neuron 6, 133-143.
Giaume, C., Koulakoff, A., Roux, L., Holcman, D., and Rouach, N. (2010). Astroglial networks: a step further in neuroglial and gliovascular interactions. Nat Rev Neurosci 11, 87-99.
Gibbs, M.E. (2015). Role of Glycogenolysis in Memory and Learning: Regulation by Noradrenaline, Serotonin and ATP. Front Integr Neurosci 9, 70.
Gill, G.V., Woodward, A., Casson, I.F., and Weston, P.J. (2009). Cardiac arrhythmia and nocturnal hypoglycaemia in type 1 diabetes--the 'dead in bed' syndrome revisited. Diabetologia 52, 42-45.
Glas, R., Sauter, N.S., Schulthess, F.T., Shu, L., Oberholzer, J., and Maedler, K. (2009). Purinergic P2X7 receptors regulate secretion of interleukin-1 receptor antagonist and beta cell function and survival. Diabetologia 52, 1579-1588.
Gourine, A.V., Kasymov, V., Marina, N., Tang, F., Figueiredo, M.F., Lane, S., Teschemacher, A.G., Spyer, K.M., Deisseroth, K., and Kasparov, S. (2010). Astrocytes control breathing through pH-dependent release of ATP. Science 329, 571-575.
Gowans, G.J., Hawley, S.A., Ross, F.A., and Hardie, D.G. (2013). AMP is a true physiological regulator of AMP-activated protein kinase by both allosteric activation and enhancing net phosphorylation. Cell Metab 18, 556-566.
Guigas, B., Sakamoto, K., Taleux, N., Reyna, S.M., Musi, N., Viollet, B., and Hue, L. (2009). Beyond AICA riboside: in search of new specific AMP-activated protein kinase activators. IUBMB Life 61, 18-26.
Guillod-Maximin, E., Lorsignol, A., Alquier, T., and Penicaud, L. (2004). Acute intracarotid glucose injection towards the brain induces specific c-fos activation in hypothalamic nuclei: involvement of astrocytes in cerebral glucose-sensing in rats. J Neuroendocrinol 16, 464-471.
Gundersen, V., Storm-Mathisen, J., and Bergersen, L.H. (2015). Neuroglial Transmission. Physiol Rev 95, 695-726.
Haanes, K.A., Kowal, J.M., Arpino, G., Lange, S.C., Moriyama, Y., Pedersen, P.A., and Novak, I. (2014). Role of vesicular nucleotide transporter VNUT (SLC17A9) in release of ATP from AR42J cells and mouse pancreatic acinar cells. Purinergic Signal 10, 431-440.
Hamilton, N.B., and Attwell, D. (2010). Do astrocytes really exocytose neurotransmitters? Nat Rev Neurosci 11, 227-238.
Han, S.M., Namkoong, C., Jang, P.G., Park, I.S., Hong, S.W., Katakami, H., Chun, S., Kim, S.W., Park, J.Y., Lee, K.U., and Kim, M.S. (2005). Hypothalamic AMP-activated protein kinase mediates counter-regulatory responses to hypoglycaemia in rats. Diabetologia 48, 2170-2178.
Hawley, S.A., Boudeau, J., Reid, J.L., Mustard, K.J., Udd, L., Makela, T.P., Alessi, D.R., and Hardie, D.G. (2003). Complexes between the LKB1 tumor suppressor, STRAD alpha/beta and MO25 alpha/beta are upstream kinases in the AMP-activated protein kinase cascade. J Biol 2, 28.
Hawley, S.A., Pan, D.A., Mustard, K.J., Ross, L., Bain, J., Edelman, A.M., Frenguelli, B.G., and Hardie, D.G. (2005). Calmodulin-dependent protein kinase kinase-beta is an alternative upstream kinase for AMP-activated protein kinase. Cell Metab 2, 9-19.
Hawley, S.A., Ross, F.A., Chevtzoff, C., Green, K.A., Evans, A., Fogarty, S., Towler, M.C., Brown, L.J., Ogunbayo, O.A., Evans, A.M., and Hardie, D.G. (2010). Use of cells expressing gamma subunit variants to identify diverse mechanisms of AMPK activation. Cell Metab 11, 554-565.
He, Y., Taylor, N., Fourgeaud, L., and Bhattacharya, A. (2017). The role of microglial P2X7: modulation of cell death and cytokine release. J Neuroinflammation 14, 135.

Herrero-Martin, G., Hoyer-Hansen, M., Garcia-Garcia, C., Fumarola, C., Farkas, T., Lopez-Rivas, A., and Jaattela, M. (2009). TAK1 activates AMPK-dependent cytoprotective autophagy in TRAIL-treated epithelial cells. EMBO J 28, 677-685.
Herzog, R.I., Chan, O., Yu, S., Dziura, J., McNay, E.C., and Sherwin, R.S. (2008). Effect of acute and recurrent hypoglycemia on changes in brain glycogen concentration. Endocrinology 149, 1499-1504.
Herzog, R.I., Jiang, L., Herman, P., Zhao, C., Sanganahalli, B.G., Mason, G.F., Hyder, F., Rothman, D.L., Sherwin, R.S., and Behar, K.L. (2013). Lactate preserves neuronal metabolism and function following antecedent recurrent hypoglycemia. J Clin Invest 123, 1988-1998.
Hurley, R.L., Anderson, K.A., Franzone, J.M., Kemp, B.E., Means, A.R., and Witters, L.A. (2005). The Ca2+/calmodulin-dependent protein kinase kinases are AMP-activated protein kinase kinases. The Journal of biological chemistry 280, 29060-29066.
Idzko, M., Ferrari, D., and Eltzschig, H.K. (2014). Nucleotide signalling during inflammation. Nature 509, 310-317.
Inokuma, K., Ogura-Okamatsu, Y., Toda, C., Kimura, K., Yamashita, H., and Saito, M. (2005). Uncoupling protein 1 is necessary for norepinephrine-induced glucose utilization in brown adipose tissue. Diabetes 54, 1385-1391.
Ishihara, H., Maechler, P., Gjinovci, A., Herrera, P.L., and Wollheim, C.B. (2003). Islet beta-cell secretion determines glucagon release from neighbouring alpha-cells. Nat Cell Biol 5, 330-335.
Iwabuchi, S., Kawahara, K., and Harata, N.C. (2014). Effects of pharmacological inhibition of AMP-activated protein kinase on GLUT3 expression and the development of ischemic tolerance in astrocytes. Neurosci Res 84, 68-71.
Joy, N.G., Tate, D.B., Younk, L.M., and Davis, S.N. (2015). Effects of Acute and Antecedent Hypoglycemia on Endothelial Function and Markers of Atherothrombotic Balance in Healthy Humans. Diabetes 64, 2571-2580.
Kacem, K., Lacombe, P., Seylaz, J., and Bonvento, G. (1998). Structural organization of the perivascular astrocyte endfeet and their relationship with the endothelial glucose transporter: a confocal microscopy study. Glia 23, 1-10.
Karnani, M., and Burdakov, D. (2011). Multiple hypothalamic circuits sense and regulate glucose levels. Am J Physiol Regul Integr Comp Physiol 300, R47-55.
Kasymov, V., Larina, O., Castaldo, C., Marina, N., Patrushev, M., Kasparov, S., and Gourine, A.V. (2013). Differential sensitivity of brainstem versus cortical astrocytes to changes in pH reveals functional regional specialization of astroglia. J Neurosci 33, 435-441.
Koizumi, S., Fujishita, K., Tsuda, M., Shigemoto-Mogami, Y., and Inoue, K. (2003). Dynamic inhibition of excitatory synaptic transmission by astrocyte-derived ATP in hippocampal cultures. Proc Natl Acad Sci U S A 100, 11023-11028.
Koltin, D., and Daneman, D. (2008). Dead-in-bed syndrome - a diabetes nightmare. Pediatr Diabetes 9, 504-507.
LaGamma, E.F., Kirtok, N., Chan, O., and Nankova, B.B. (2014). Partial blockade of nicotinic acetylcholine receptors improves the counterregulatory response to hypoglycemia in recurrently hypoglycemic rats. Am J Physiol Endocrinol Metab 307, E580-588.
Lalo, U., Palygin, O., Rasooli-Nejad, S., Andrew, J., Haydon, P.G., and Pankratov, Y. (2014). Exocytosis of ATP from astrocytes modulates phasic and tonic inhibition in the neocortex. PLoS Biol 12, e1001747.
Lam, T.K., Gutierrez-Juarez, R., Pocai, A., and Rossetti, L. (2005). Regulation of blood glucose by hypothalamic pyruvate metabolism. Science 309, 943-947.
Laughton, J.D., Bittar, P., Charnay, Y., Pellerin, L., Kovari, E., Magistretti, P.J., and Bouras, C. (2007). Metabolic compartmentalization in the human cortex and hippocampus: evidence for a cell- and region-specific localization of lactate dehydrogenase 5 and pyruvate dehydrogenase. BMC Neurosci 8, 35.
Lazarowski, E.R., Sesma, J.I., Seminario-Vidal, L., and Kreda, S.M. (2011). Molecular mechanisms of purine and pyrimidine nucleotide release. Adv Pharmacol 61, 221-261.

Lengacher, S., Magistretti, P.J., and Pellerin, L. (2004). Quantitative rt-PCR analysis of uncoupling protein isoforms in mouse brain cortex: methodological optimization and comparison of expression with brown adipose tissue and skeletal muscle. J Cereb Blood Flow Metab 24, 780-788.
Llaudet, E., Hatz, S., Droniou, M., and Dale, N. (2005). Microelectrode biosensor for real-time measurement of ATP in biological tissue. Anal Chem 77, 3267-3273.
Longnus, S.L., Wambolt, R.B., Parsons, H.L., Brownsey, R.W., and Allard, M.F. (2003). 5-Aminoimidazole-4-carboxamide 1-beta -D-ribofuranoside (AICAR) stimulates myocardial glycogenolysis by allosteric mechanisms. Am J Physiol Regul Integr Comp Physiol 284, R936-944.
Marty, N., Dallaporta, M., Foretz, M., Emery, M., Tarussio, D., Bady, I., Binnert, C., Beermann, F., and Thorens, B. (2005). Regulation of glucagon secretion by glucose transporter type 2 (glut2) and astrocyte-dependent glucose sensors. J Clin Invest 115, 3545-3553.
Mason, G.F., Petersen, K.F., Lebon, V., Rothman, D.L., and Shulman, G.I. (2006). Increased brain monocarboxylic acid transport and utilization in type 1 diabetes. Diabetes 55, 929-934.
Matsui, T., Soya, S., Kawanaka, K., and Soya, H. (2015). Brain Glycogen Decreases During Intense Exercise Without Hypoglycemia: The Possible Involvement of Serotonin. Neurochem Res.
McCrimmon, R.J., Fan, X., Cheng, H., McNay, E., Chan, O., Shaw, M., Ding, Y., Zhu, W., and Sherwin, R.S. (2006). Activation of AMP-activated protein kinase within the ventromedial hypothalamus amplifies counterregulatory hormone responses in rats with defective counterregulation. Diabetes 55, 1755-1760.
McCrimmon, R.J., Fan, X., Ding, Y., Zhu, W., Jacob, R.J., and Sherwin, R.S. (2004). Potential role for AMP-activated protein kinase in hypoglycemia sensing in the ventromedial hypothalamus. Diabetes 53, 1953-1958.
McCrimmon, R.J., Shaw, M., Fan, X., Cheng, H., Ding, Y., Vella, M.C., Zhou, L., McNay, E.C., and Sherwin, R.S. (2008). Key role for AMP-activated protein kinase in the ventromedial hypothalamus in regulating counterregulatory hormone responses to acute hypoglycemia. Diabetes 57, 444-450.
Mitrakou, A., Ryan, C., Veneman, T., Mokan, M., Jenssen, T., Kiss, I., Durrant, J., Cryer, P., and Gerich, J. (1991). Hierarchy of glycemic thresholds for counterregulatory hormone secretion, symptoms, and cerebral dysfunction. Am J Physiol 260, E67-74.
Moreno, D., Knecht, E., Viollet, B., and Sanz, P. (2008). A769662, a novel activator of AMP-activated protein kinase, inhibits non-proteolytic components of the 26S proteasome by an AMPK-independent mechanism. FEBS Lett 582, 2650-2654.
Nakamura, J.L., Garcia, E., and Pieper, R.O. (2008). S6K1 plays a key role in glial transformation. Cancer Res 68, 6516-6523.
Naylor, R.N., Greeley, S.A., Bell, G.I., and Philipson, L.H. (2011). Genetics and pathophysiology of neonatal diabetes mellitus. J Diabetes Investig 2, 158-169.
Nelson, S.R., Schulz, D.W., Passonneau, J.V., and Lowry, O.H. (1968). Control of glycogen levels in brain. J Neurochem 15, 1271-1279.
Newman, L.A., Korol, D.L., and Gold, P.E. (2011). Lactate produced by glycogenolysis in astrocytes regulates memory processing. PLoS One 6, e28427.
Ogden, C.L., Yanovski, S.Z., Carroll, M.D., and Flegal, K.M. (2007). The epidemiology of obesity. Gastroenterology 132, 2087-2102.
Oomura, Y., Ono, T., Ooyama, H., and Wayner, M.J. (1969). Glucose and osmosensitive neurones of the rat hypothalamus. Nature 222, 282-284.
Owen, M.R., Doran, E., and Halestrap, A.P. (2000). Evidence that metformin exerts its anti-diabetic effects through inhibition of complex 1 of the mitochondrial respiratory chain. Biochem J 348 Pt 3, 607-614.
Oya, M., Kitaguchi, T., Yanagihara, Y., Numano, R., Kakeyama, M., Ikematsu, K., and Tsuboi, T. (2013). Vesicular nucleotide transporter is involved in ATP storage of secretory lysosomes in astrocytes. Biochem Biophys Res Commun 438, 145-151.

Oz, G., Kumar, A., Rao, J.P., Kodl, C.T., Chow, L., Eberly, L.E., and Seaquist, E.R. (2009). Human brain glycogen metabolism during and after hypoglycemia. Diabetes 58, 1978-1985.
Oz, G., Tesfaye, N., Kumar, A., Deelchand, D.K., Eberly, L.E., and Seaquist, E.R. (2012). Brain glycogen content and metabolism in subjects with type 1 diabetes and hypoglycemia unawareness. J Cereb Blood Flow Metab 32, 256-263.
Palkovits, M., Zaborszky, L., Feminger, A., Mezey, E., Fekete, M.I., Herman, J.P., Kanyicska, B., and Szabo, D. (1980). Noradrenergic innervation of the rat hypothalamus:experimental biochemical and electron microscopic studies. Brain Res 191, 161-171.
Pangrsic, T., Potokar, M., Stenovec, M., Kreft, M., Fabbretti, E., Nistri, A., Pryazhnikov, E., Khiroug, L., Giniatullin, R., and Zorec, R. (2007). Exocytotic release of ATP from cultured astrocytes. The Journal of biological chemistry 282, 28749-28758.
Pascual, O., Ben Achour, S., Rostaing, P., Triller, A., and Bessis, A. (2012). Microglia activation triggers astrocyte-mediated modulation of excitatory neurotransmission. Proc Natl Acad Sci U S A 109, E197-205.
Pellerin, L., Bergersen, L.H., Halestrap, A.P., and Pierre, K. (2005). Cellular and subcellular distribution of monocarboxylate transporters in cultured brain cells and in the adult brain. J Neurosci Res 79, 55-64.
Pellerin, L., and Magistretti, P.J. (1994). Glutamate uptake into astrocytes stimulates aerobic glycolysis: a mechanism coupling neuronal activity to glucose utilization. Proc Natl Acad Sci U S A 91, 10625-10629.
Pellerin, L., and Magistretti, P.J. (2012). Sweet sixteen for ANLS. J Cereb Blood Flow Metab 32, 1152-1166.
Perreten Lambert, H., Zenger, M., Azarias, G., Chatton, J.Y., Magistretti, P.J., and Lengacher, S. (2014). Control of mitochondrial pH by uncoupling protein 4 in astrocytes promotes neuronal survival. The Journal of biological chemistry 289, 31014-31028.
Pierzynska-Mach, A., Janowski, P.A., and Dobrucki, J.W. (2014). Evaluation of acridine orange, LysoTracker Red, and quinacrine as fluorescent probes for long-term tracking of acidic vesicles. Cytometry A 85, 729-737.
Polekhina, G., Gupta, A., Michell, B.J., van Denderen, B., Murthy, S., Feil, S.C., Jennings, I.G., Campbell, D.J., Witters, L.A., Parker, M.W.*, et al.* (2003). AMPK beta subunit targets metabolic stress sensing to glycogen. Curr Biol 13, 867-871.
Rena, G., Pearson, E.R., and Sakamoto, K. (2013). Molecular mechanism of action of metformin: old or new insights? Diabetologia 56, 1898-1906.
Richardson, S.J., Willcox, A., Bone, A.J., Morgan, N.G., and Foulis, A.K. (2011). Immunopathology of the human pancreas in type-I diabetes. Semin Immunopathol 33, 9-21.
Routh, V.H., Hao, L., Santiago, A.M., Sheng, Z., and Zhou, C. (2014). Hypothalamic glucose sensing: making ends meet. Front Syst Neurosci 8, 236.
Sagar, G.D., and Larson, D.M. (2006). Carbenoxolone inhibits junctional transfer and upregulates Connexin43 expression by a protein kinase A-dependent pathway. J Cell Biochem 98, 1543-1551.
Schultes, B., Jauch-Chara, K., Gais, S., Hallschmid, M., Reiprich, E., Kern, W., Oltmanns, K.M., Peters, A., Fehm, H.L., and Born, J. (2007). Defective awakening response to nocturnal hypoglycemia in patients with type 1 diabetes mellitus. PLoS Med 4, e69.
Schwartz, N.S., Clutter, W.E., Shah, S.D., and Cryer, P.E. (1987). Glycemic thresholds for activation of glucose counterregulatory systems are higher than the threshold for symptoms. J Clin Invest 79, 777-781.
Schwiebert, E.M., Egan, M.E., Hwang, T.H., Fulmer, S.B., Allen, S.S., Cutting, G.R., and Guggino, W.B. (1995). CFTR regulates outwardly rectifying chloride channels through an autocrine mechanism involving ATP. Cell 81, 1063-1073.
Scott, J.W., Hawley, S.A., Green, K.A., Anis, M., Stewart, G., Scullion, G.A., Norman, D.G., and Hardie, D.G. (2004). CBS domains form energy-sensing modules whose binding of adenosine ligands is disrupted by disease mutations. J Clin Invest 113, 274-284.

Scott, J.W., Ling, N., Issa, S.M., Dite, T.A., O'Brien, M.T., Chen, Z.P., Galic, S., Langendorf, C.G., Steinberg, G.R., Kemp, B.E., and Oakhill, J.S. (2014). Small molecule drug A-769662 and AMP synergistically activate naive AMPK independent of upstream kinase signaling. Chem Biol 21, 619-627.
Segel, S.A., Paramore, D.S., and Cryer, P.E. (2002). Hypoglycemia-associated autonomic failure in advanced type 2 diabetes. Diabetes 51, 724-733.
Silver, I.A., and Erecinska, M. (1994). Extracellular glucose concentration in mammalian brain: continuous monitoring of changes during increased neuronal activity and upon limitation in oxygen supply in normo-, hypo-, and hyperglycemic animals. J Neurosci 14, 5068-5076.
Sim, A.T., and Hardie, D.G. (1988). The low activity of acetyl-CoA carboxylase in basal and glucagon-stimulated hepatocytes is due to phosphorylation by the AMP-activated protein kinase and not cyclic AMP-dependent protein kinase. FEBS Lett 233, 294-298.
Solini, A., Chiozzi, P., Falzoni, S., Morelli, A., Fellin, R., and Di Virgilio, F. (2000). High glucose modulates P2X7 receptor-mediated function in human primary fibroblasts. Diabetologia 43, 1248-1256.
Solini, A., Chiozzi, P., Morelli, A., Adinolfi, E., Rizzo, R., Baricordi, O.R., and Di Virgilio, F. (2004). Enhanced P2X7 activity in human fibroblasts from diabetic patients: a possible pathogenetic mechanism for vascular damage in diabetes. Arterioscler Thromb Vasc Biol 24, 1240-1245.
Song, Z., and Routh, V.H. (2005). Differential effects of glucose and lactate on glucosensing neurons in the ventromedial hypothalamic nucleus. Diabetes 54, 15-22.
Stout, C., and Charles, A. (2003). Modulation of intercellular calcium signaling in astrocytes by extracellular calcium and magnesium. Glia 43, 265-273.
Suadicani, S.O., Brosnan, C.F., and Scemes, E. (2006). P2X7 receptors mediate ATP release and amplification of astrocytic intercellular Ca2+ signaling. J Neurosci 26, 1378-1385.
Subbarao, K.V., and Hertz, L. (1990). Effect of adrenergic agonists on glycogenolysis in primary cultures of astrocytes. Brain Res 536, 220-226.
Suh, S.W., Bergher, J.P., Anderson, C.M., Treadway, J.L., Fosgerau, K., and Swanson, R.A. (2007). Astrocyte glycogen sustains neuronal activity during hypoglycemia: studies with the glycogen phosphorylase inhibitor CP-316,819 ([R-R*,S*]-5-chloro-N-[2-hydroxy-3-(methoxymethylamino)-3-oxo-1-(phenylmethyl)pro pyl]-1H-indole-2-carboxamide). J Pharmacol Exp Ther 321, 45-50.
Surprenant, A., Rassendren, F., Kawashima, E., North, R.A., and Buell, G. (1996). The cytolytic P2Z receptor for extracellular ATP identified as a P2X receptor (P2X7). Science 272, 735-738.
Swanson, R.A., and Choi, D.W. (1993). Glial glycogen stores affect neuronal survival during glucose deprivation in vitro. J Cereb Blood Flow Metab 13, 162-169.
Taib, B., Bouyakdan, K., Hryhorczuk, C., Rodaros, D., Fulton, S., and Alquier, T. (2013). Glucose regulates hypothalamic long-chain fatty acid metabolism via AMP-activated kinase (AMPK) in neurons and astrocytes. The Journal of biological chemistry 288, 37216-37229.
Takahashi, S., Iizumi, T., Mashima, K., Abe, T., and Suzuki, N. (2014). Roles and regulation of ketogenesis in cultured astroglia and neurons under hypoxia and hypoglycemia. ASN Neuro 6.
Tanenberg, R.J., Newton, C.A., and Drake, A.J. (2010). Confirmation of hypoglycemia in the "dead-in-bed" syndrome, as captured by a retrospective continuous glucose monitoring system. Endocr Pract 16, 244-248.
Tattersall, R.B., and Gill, G.V. (1991). Unexplained deaths of type 1 diabetic patients. Diabet Med 8, 49-58.
Towler, D.A., Havlin, C.E., Craft, S., and Cryer, P. (1993). Mechanism of awareness of hypoglycemia. Perception of neurogenic (predominantly cholinergic) rather than neuroglycopenic symptoms. Diabetes 42, 1791-1798.
Treebak, J.T., Birk, J.B., Hansen, B.F., Olsen, G.S., and Wojtaszewski, J.F. (2009). A-769662 activates AMPK beta1-containing complexes but induces glucose uptake through a PI3-kinase-dependent pathway in mouse skeletal muscle. Am J Physiol Cell Physiol 297, C1041-1052.
Unoki, H., Takahashi, A., Kawaguchi, T., Hara, K., Horikoshi, M., Andersen, G., Ng, D.P., Holmkvist, J., Borch-Johnsen, K., Jorgensen, T.*, et al.* (2008). SNPs in KCNQ1 are associated with

susceptibility to type 2 diabetes in East Asian and European populations. Nat Genet 40, 1098-1102.
Vincent, M.F., Bontemps, F., and Van den Berghe, G. (1996). Substrate cycling between 5-amino-4-imidazolecarboxamide riboside and its monophosphate in isolated rat hepatocytes. Biochem Pharmacol 52, 999-1006.
Viollet, B., Andreelli, F., Jorgensen, S.B., Perrin, C., Geloen, A., Flamez, D., Mu, J., Lenzner, C., Baud, O., Bennoun, M.*, et al.* (2003). The AMP-activated protein kinase alpha2 catalytic subunit controls whole-body insulin sensitivity. J Clin Invest 111, 91-98.
Voight, B.F., Scott, L.J., Steinthorsdottir, V., Morris, A.P., Dina, C., Welch, R.P., Zeggini, E., Huth, C., Aulchenko, Y.S., Thorleifsson, G.*, et al.* (2010). Twelve type 2 diabetes susceptibility loci identified through large-scale association analysis. Nat Genet 42, 579-589.
Walls, A.B., Sickmann, H.M., Brown, A., Bouman, S.D., Ransom, B., Schousboe, A., and Waagepetersen, H.S. (2008). Characterization of 1,4-dideoxy-1,4-imino-d-arabinitol (DAB) as an inhibitor of brain glycogen shunt activity. J Neurochem 105, 1462-1470.
Walz, W., and Mukerji, S. (1988). Lactate release from cultured astrocytes and neurons: a comparison. Glia 1, 366-370.
Watts, A.G., and Donovan, C.M. (2010). Sweet talk in the brain: glucosensing, neural networks, and hypoglycemic counterregulation. Front Neuroendocrinol 31, 32-43.
Wendt, A., Birnir, B., Buschard, K., Gromada, J., Salehi, A., Sewing, S., Rorsman, P., and Braun, M. (2004). Glucose inhibition of glucagon secretion from rat alpha-cells is mediated by GABA released from neighboring beta-cells. Diabetes 53, 1038-1045.
Westhaus, A., Blumrich, E.M., and Dringen, R. (2015). The Antidiabetic Drug Metformin Stimulates Glycolytic Lactate Production in Cultured Primary Rat Astrocytes. Neurochem Res.
Wiesinger, H., Hamprecht, B., and Dringen, R. (1997). Metabolic pathways for glucose in astrocytes. Glia 21, 22-34.
Willcox, A., Richardson, S.J., Bone, A.J., Foulis, A.K., and Morgan, N.G. (2011). Immunohistochemical analysis of the relationship between islet cell proliferation and the production of the enteroviral capsid protein, VP1, in the islets of patients with recent-onset type 1 diabetes. Diabetologia 54, 2417-2420.
Wink, M.R., Braganhol, E., Tamajusuku, A.S., Lenz, G., Zerbini, L.F., Libermann, T.A., Sevigny, J., Battastini, A.M., and Robson, S.C. (2006). Nucleoside triphosphate diphosphohydrolase-2 (NTPDase2/CD39L1) is the dominant ectonucleotidase expressed by rat astrocytes. Neuroscience 138, 421-432.
Woods, A., Dickerson, K., Heath, R., Hong, S.P., Momcilovic, M., Johnstone, S.R., Carlson, M., and Carling, D. (2005). Ca2+/calmodulin-dependent protein kinase kinase-beta acts upstream of AMP-activated protein kinase in mammalian cells. Cell Metab 2, 21-33.
Xiao, B., Sanders, M.J., Underwood, E., Heath, R., Mayer, F.V., Carmena, D., Jing, C., Walker, P.A., Eccleston, J.F., Haire, L.F.*, et al.* (2011). Structure of mammalian AMPK and its regulation by ADP. Nature 472, 230-233.
Yasuda, K., Miyake, K., Horikawa, Y., Hara, K., Osawa, H., Furuta, H., Hirota, Y., Mori, H., Jonsson, A., Sato, Y.*, et al.* (2008). Variants in KCNQ1 are associated with susceptibility to type 2 diabetes mellitus. Nat Genet 40, 1092-1097.
Yegutkin, G.G. (2008). Nucleotide- and nucleoside-converting ectoenzymes: Important modulators of purinergic signalling cascade. Biochim Biophys Acta 1783, 673-694.
Zanotti, S., and Charles, A. (1997). Extracellular calcium sensing by glial cells: low extracellular calcium induces intracellular calcium release and intercellular signaling. J Neurochem 69, 594-602.
Zhou, H., Zhang, T., Harmon, J.S., Bryan, J., and Robertson, R.P. (2007). Zinc, not insulin, regulates the rat alpha-cell response to hypoglycemia in vivo. Diabetes 56, 1107-1112.
Zhou, L., Podolsky, N., Sang, Z., Ding, Y., Fan, X., Tong, Q., Levin, B.E., and McCrimmon, R.J. (2010). The medial amygdalar nucleus: a novel glucose-sensing region that modulates the counterregulatory response to hypoglycemia. Diabetes 59, 2646-2652.

Zimmermann, H., Zebisch, M., and Strater, N. (2012). Cellular function and molecular structure of ecto-nucleotidases. Purinergic Signal 8, 437-502.